Highlights of 5-th International Symposium of Semiconductor Tracking Detectors

14-17 June 2004, Hiroshima

Series of symposia dedicated to large tracking systems

- History of tracking semiconductor detectors
- High Energy Physics Experiments LHC (ATLAS, CMS), B-factories (BABAR, BELLE), NLC ?
- NASA Projects AMS, GLAST

Semiconductor Tracking Detectors

historical overview

M. Turala

Pre-history

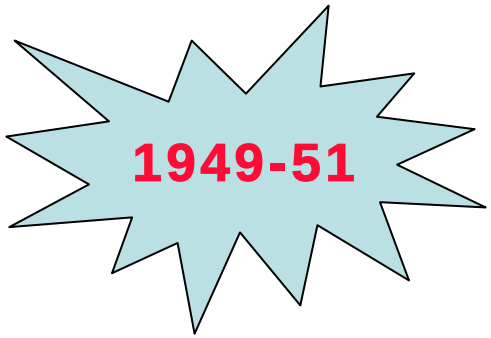

K.G. McKay, A Germanium Counter, Phys Rev 76 (1949), 1537

P.J. van Heerden et al., The Crystal Counter, Physica 16, (1950), 505

G.K. McKay, Electron-Hole Production in Germanium by Alpha-Particles, Phys.Rev. 84 (1951), 829

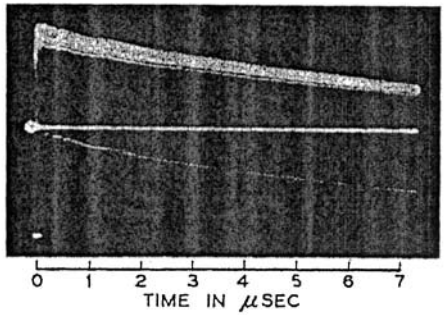

FIG. 3. Photograph of pulses from sixteen alpha-particles striking the $n-p$ barrier.

Pre-history

1960-80

Si detectors in particle physics

- Cross-section measurements, JINR Dubna (V. Nikitin et al.)
- Active targets, CERN (G. Bellini et al.)
- Neutrino/ muon flux monitoring, CERN (E. Heijne et al.)
- BOL experiment at the Synchrocyclotron in Amsterdam

Si strip detectors technology

1980-81

J. Kemmer et al., Development of 10-micrometer Resolution Silicon Counters for Charm Signature Observation with the ACCMOR Spectrometer, Nucl. Instr. Meth., 169 (1980), Batavia 1981, Proc. Silicon Detectors for High Energy Physics

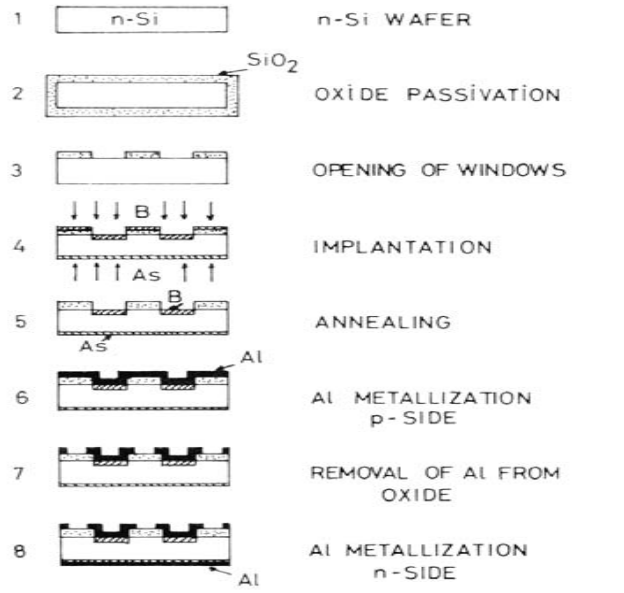

Fig. 1 : Successive steps of the manufacturing process of passivated ion-implanted silicon detectors

First HEP experiments

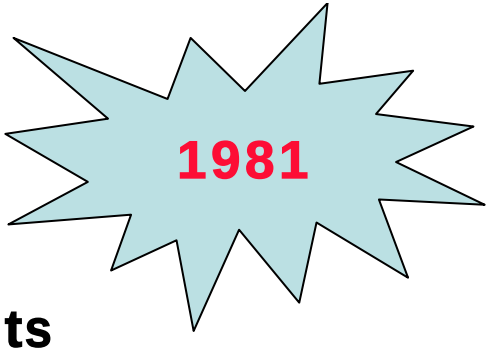

Identification (tagging) and measurements of particles with short lifetimes:

- charm lifetime: longer for mesons, e.g. $D^{\pm}$ $(10.51\pm0.13) \times 10^{-13}$s
  shorter for baryons, e.g. Λ_c $(2.06\pm0.12) \times 10^{-13}$s
- average beauty hadron lifetime: $(15.64\pm0.14) \times 10^{-13}$s
- τ lepton lifetime: $(2.906\pm0.011) \times 10^{-13}$s

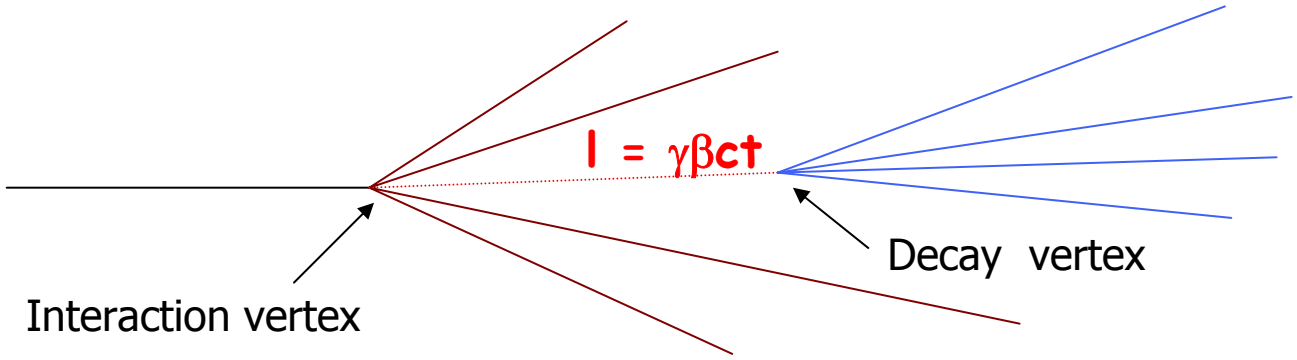

decay length $l = \gamma\beta ct$, so typically the decay vertex is at a distance of single millimeters from the interaction vertex

First HEP experiments

1981

NA11 experiment at CERN

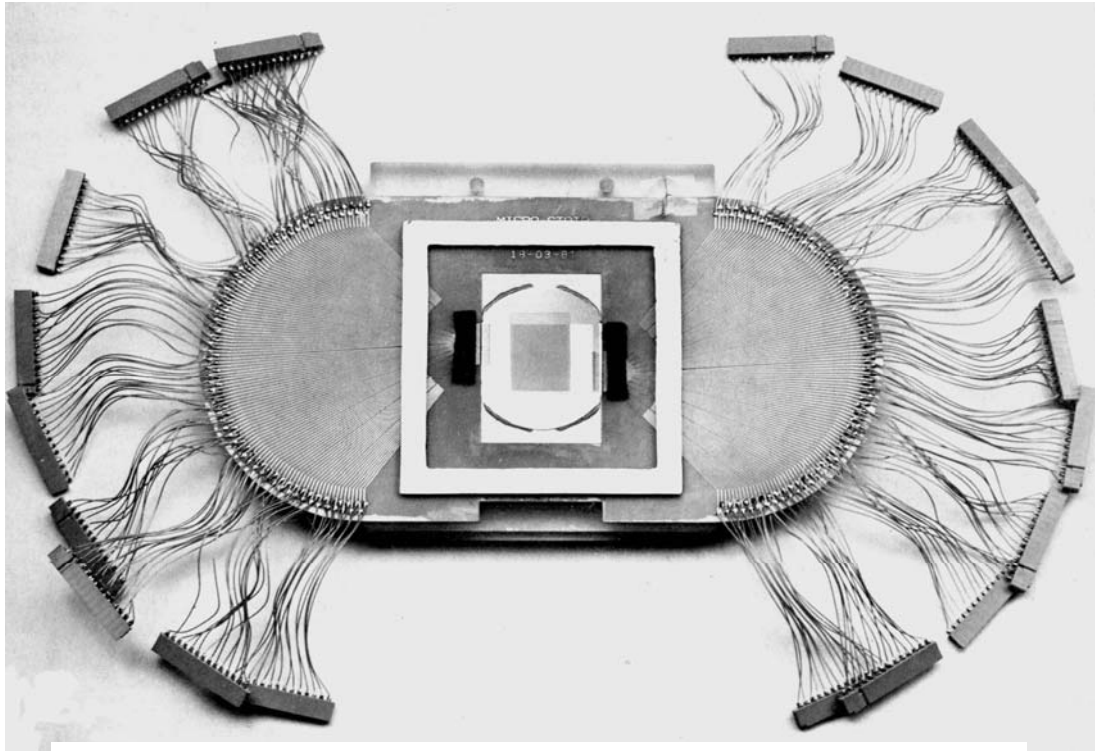

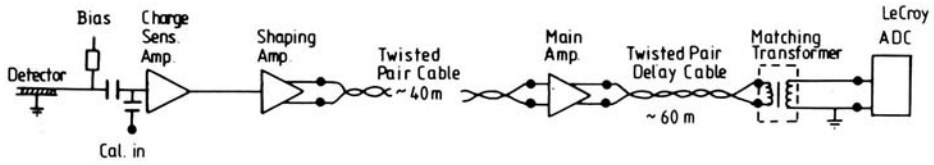

Fig. 5. Block diagram of the readout electronics.

First CCDs for HEP

1982

R. Bailey et al., First Measurement of Efficiency and Precision of CCD Detectors for High Energy Physics, Nucl. Instr. Meth. 213 (1983)

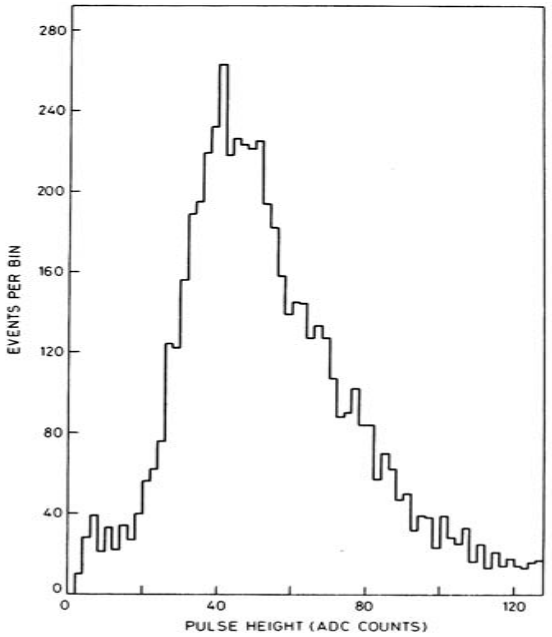

Fig. 15. Pulse height distribution for clusters due to beam tracks in CCD1.

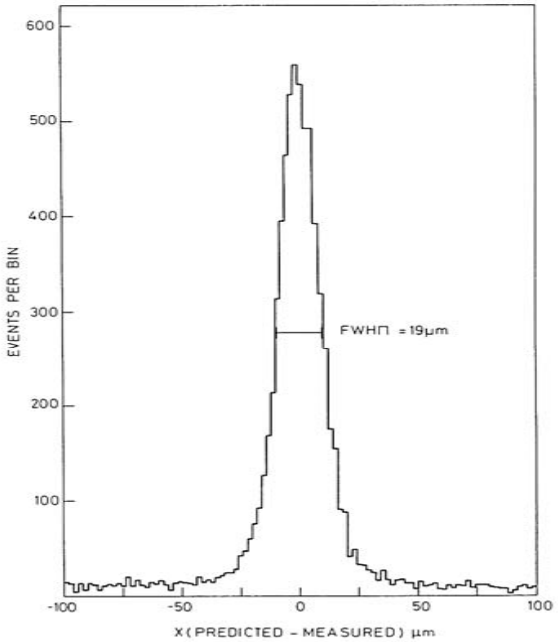

Fig. 23. Deviations in cluster positions in CCD2 from predicted positions from CCD1 and 3 (x).

Silicon drift chambers

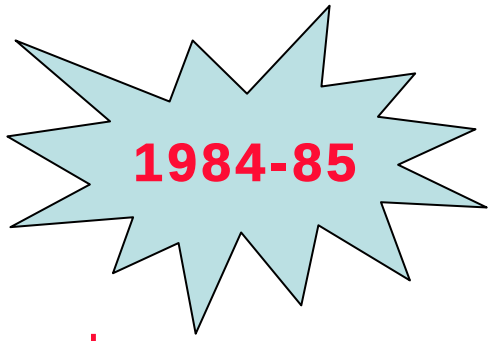

E. Gatti and P. Rehak, Semiconductor Drift Chamber – an Application of a Novel Charge Transport Scheme, Nucl. Instr. Meth. A226 (1984)

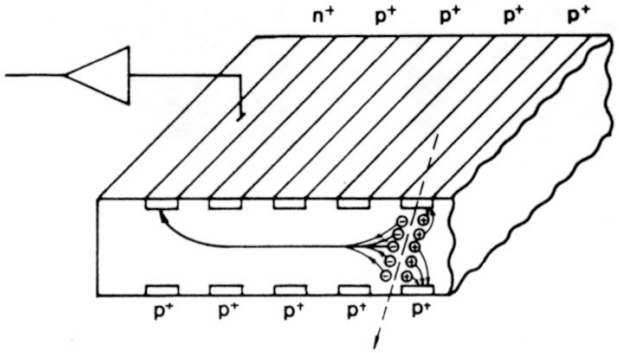

Fig. 1

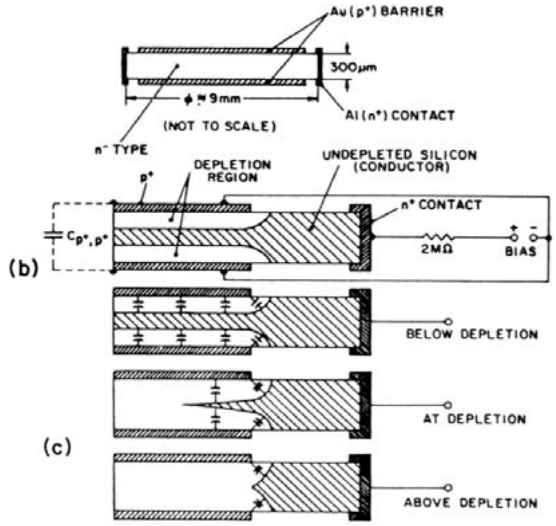

VLSI readout

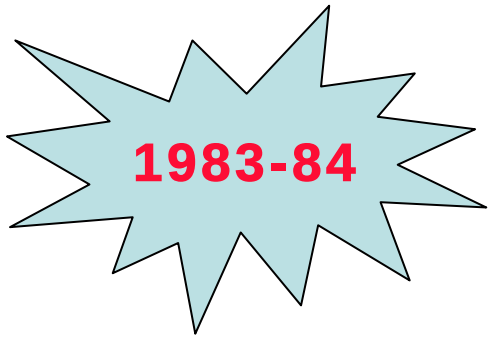

R. Hofmann et al., High Resolution Silicon Detectors – Status and Future Developments of the MPI/ TU Munich Group, Nucl. Instr. Meth. A225 (1984)

R. Hofmann et al., Development of Readout Electronics for Monolithic Integration with Diode Strip Readout, 3rd European Symposium on Semiconductor Detectors, Munich, 14-16 Nov. 1983, Nucl. Instr. Meth. A226 (1984)

J.T. Walker et al., Development of High Density Readout for Silicon Strip Detectors, Nucl. Instr. Meth. A226 (1984)

1985-86

VLSI readout

Next generation of VLSI readout chips

S.A. Kleinfelder et al., A Flexible 128 Channel Silicon Strip Detector Instrumentation Integrated Circuit with Sparse Data Readout, IEEE Trans. NS-35 (1988)

D. Joyce et al., Silicon detector tests with the RAL Microplex Readout Chip, Nucl. Instr. Meth, A279 (1989)

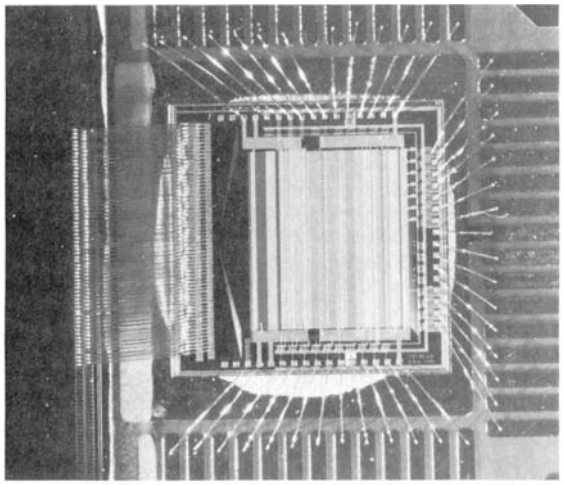

8. Close up photo of SVX I.C. bonded to CDF detector. Note two level wire bonding with $\approx 50\mu m$ pitch.

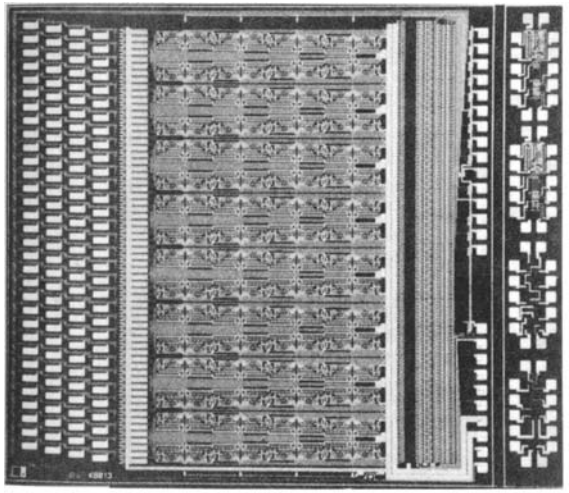

Figure 1. The MX1 Chip 6.4mm by 6.4mm.

Si vertex detectors for e+e-

1986-1987

First vertex detector for Mark II experiment at SLC

A. Litke et al., A Silicon Strip Vertex Detector for the Mark-II Experiment at the SLAS Linear Collider, Nucl. Instr. Meth., A265 (1988)

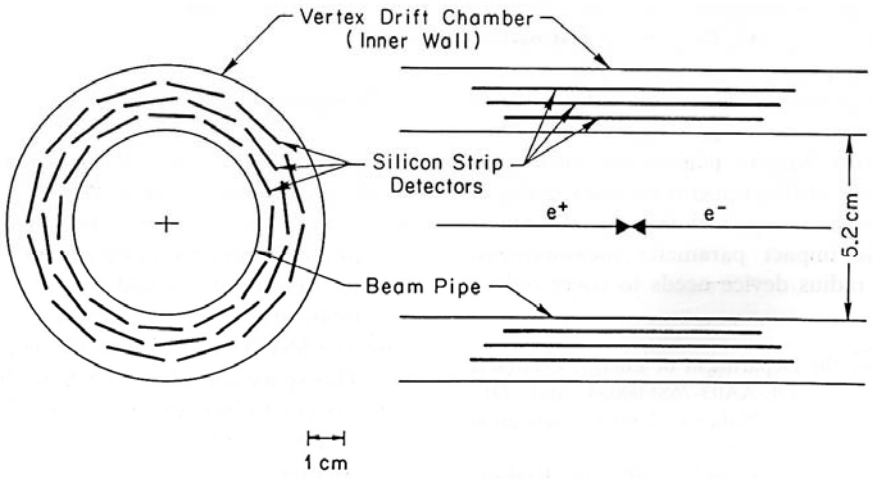

Fig. 1. Layout of the silicon strip vertex detector.

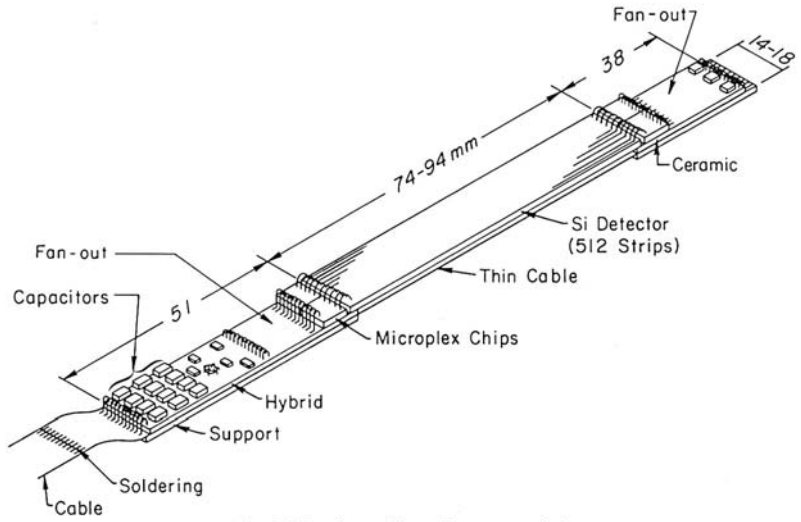

Fig. 2. Plan for a silicon detector module.

Microvertex DELPHI

1986-2000

N. Bingefors et al., NIM A328 (1993), V. Chabaud et al.,NIM A368 (1996), P. Chochula et al., NIM A412 (1998)

1989-1990

192 detectors (all s-s)
55296 readout channels

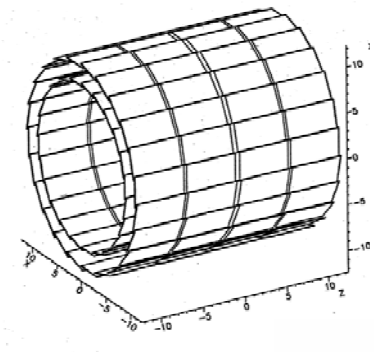

1991-1993

288 detectors (all s-s)
73728 readout channels

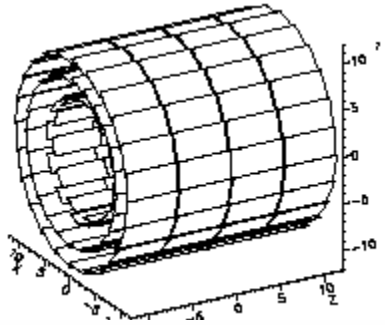

1994-1995

288 detectors (96 s-s, 192 d-s)
125952 readout channels

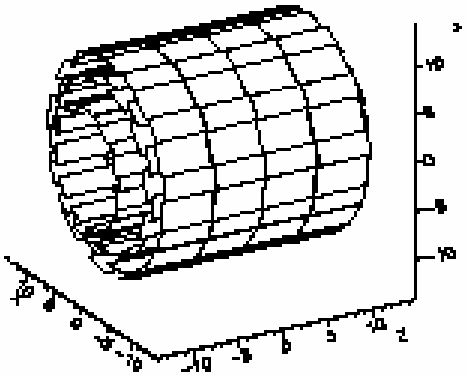

1996-2000

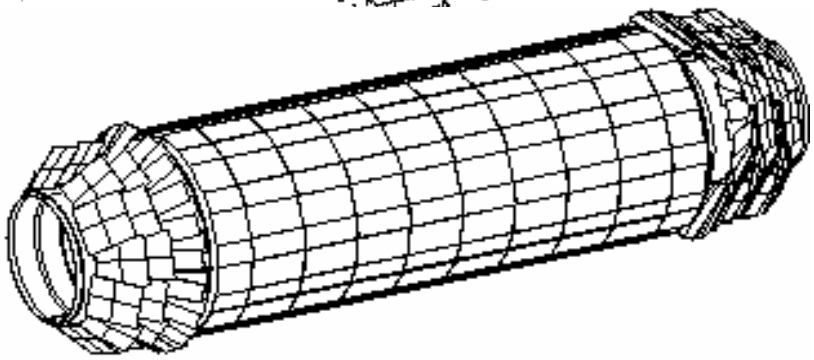

888 detectors,
1399808 readout channels:

736 strip detectors with
174080 readout channels

1225728 pixels

From A. Zalewska

Si vertex detectors at LEP

1986-2000

K.Österberg, Performance of the vertex detectors at LEP2, NIM A435 (1999)

ALEPH
VDETII

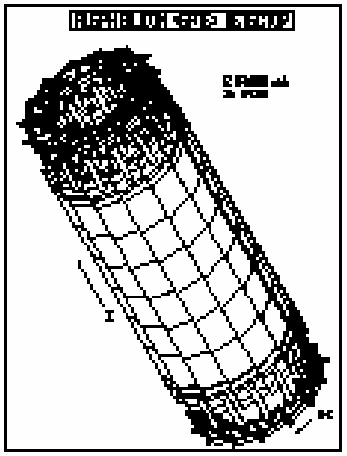

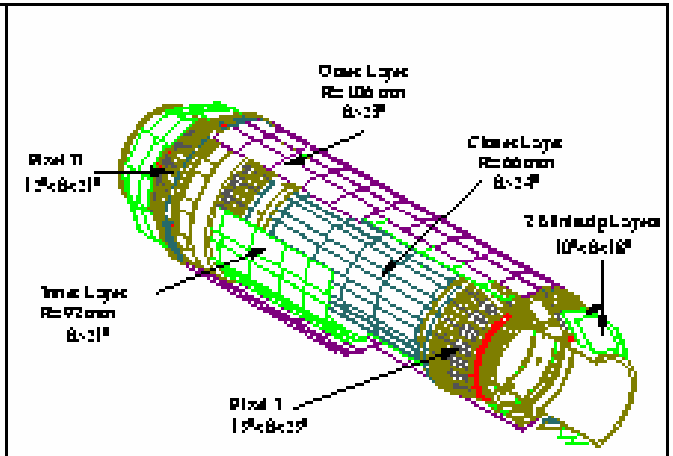

DELPHI
Si Tracker

OPAL
µVTX3

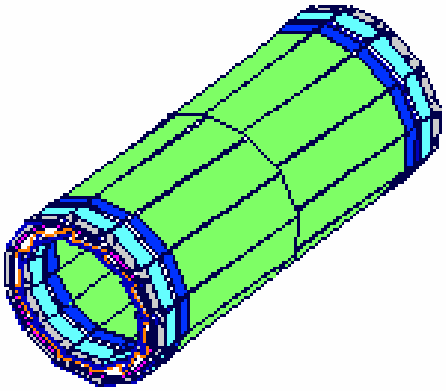

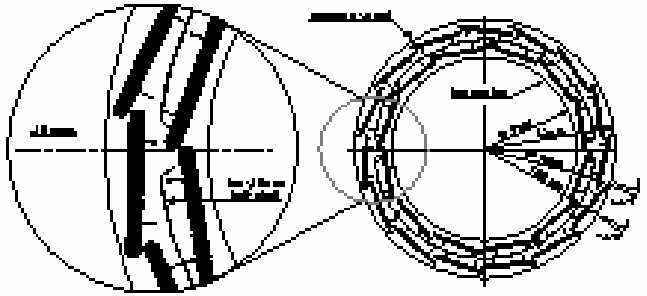

L3
SMD

1986-1995

SLD vertex detector

Vertex detectors for SLD spectrometer at SLC

K. Abe et al.., Design and Performance of the SLD Vertex Detector: a 307 Mpixel Tracking System, Nucl. Instr. Meth A400 (1997)

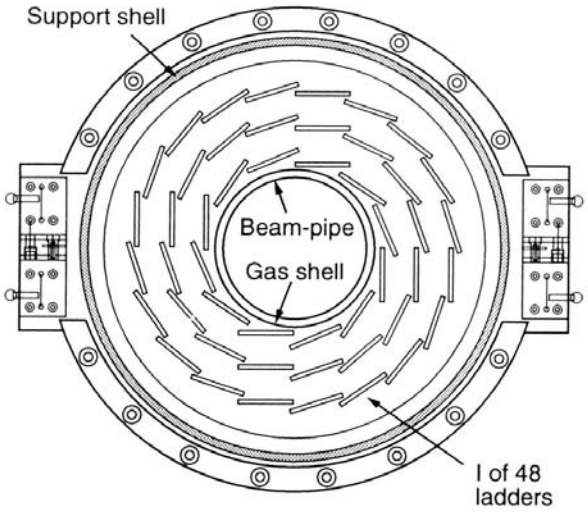

Fig. 47 Cross-section (XY view) of SLD upgrade vertex detector.

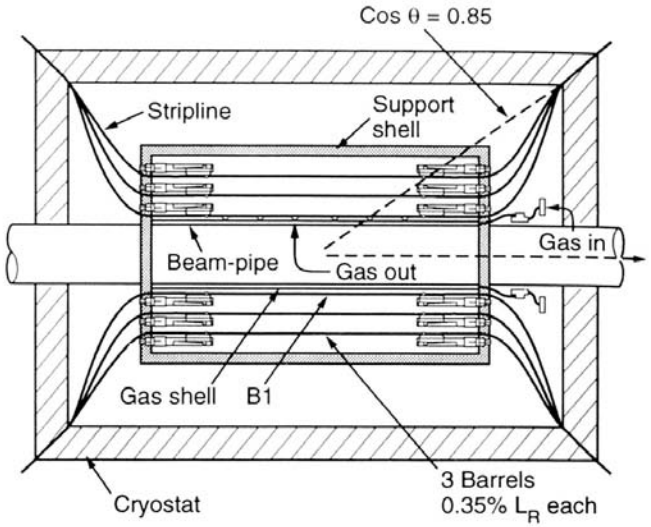

Fig. 48 Cross-section (RZ view) of SLD upgrade vertex detector.

Vertex detectors of BaBar

1995-…..

B. Aubert et al., The BaBar detector, Nucl. Instr. Meth A479 (2002)

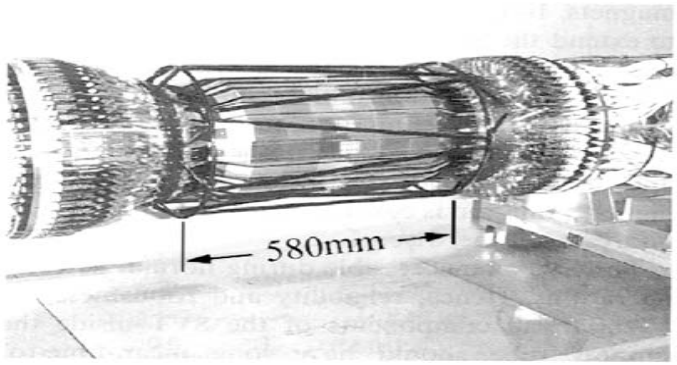

Fig. 16. Fully assembled SVT. The silicon sensors of the outer layer are visible, as is the carbon–fiber space frame (black structure) that surrounds the silicon.

B. Aubert et al. / Nuclear Instruments and Methods in Physics Research A 479 (2002) 1–116

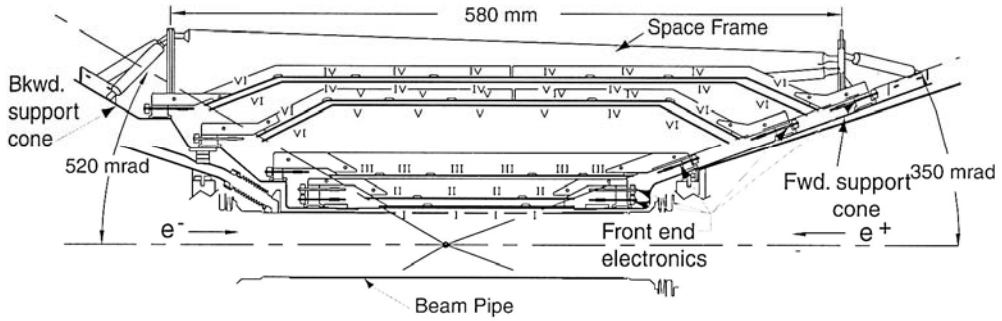

Fig. 17. Schematic view of SVT: longitudinal section. The roman numerals label the six different types of sensors.

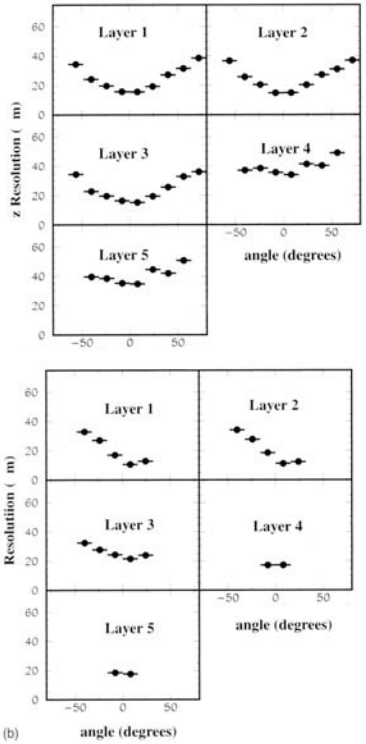

Fig. 27. SVT hit resolution in the (a) z and (b) ϕ coordinate in μm, plotted as a function of track incident angle in degrees. Each plot shows a different layer of the SVT. The plots in the ϕ coordinate for layers 1–3 are asymmetric around $\phi = 0$ because of the "pinwheel" design of the inner layers. There are fewer points in the ϕ resolution plots for the outer layers as they subtend smaller angles than the inner layers.

Vertex detector of Belle

1995-….

A. Abashian et al., The Belle Detector, Nucl. Instr. Meth A479 (2002)

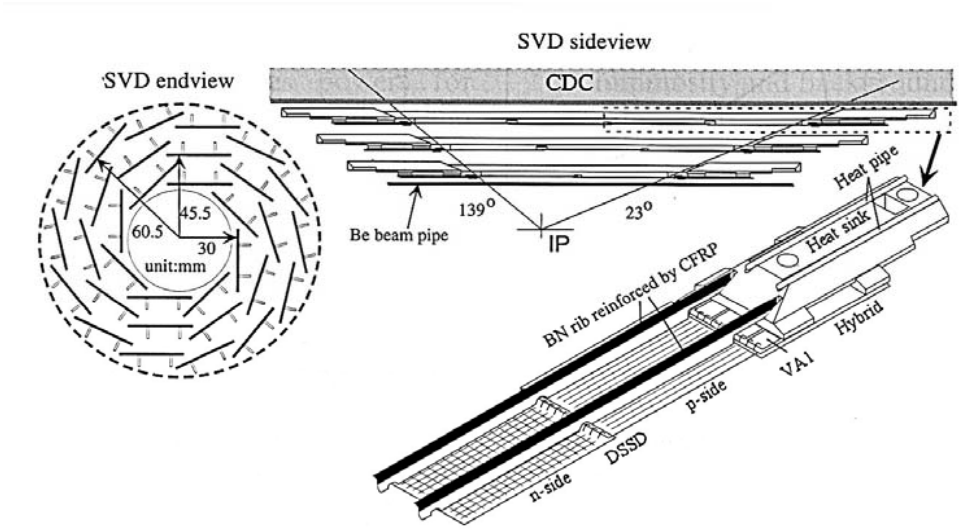

Fig. 13. Detector configuration of SVD.

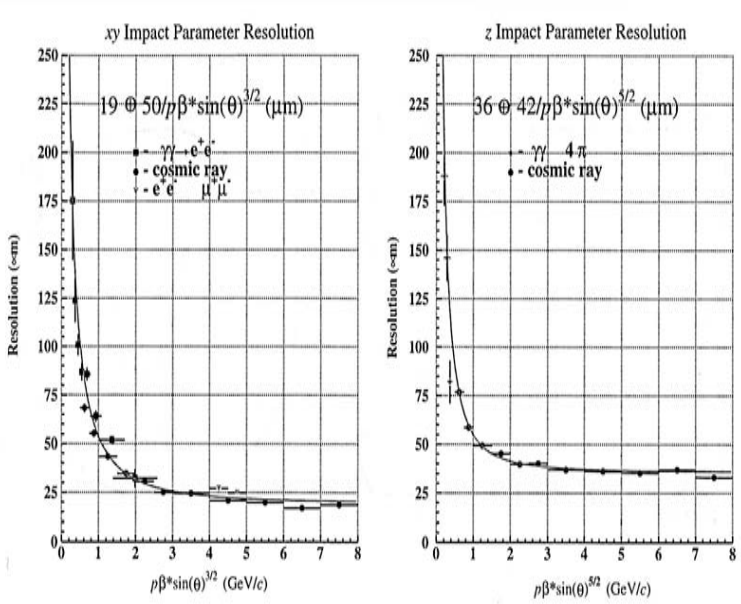

Fig. 21. Impact parameter resolution.

SVD used in the Level 1.5 Trigger for rejection of beam gas background

Pixel detectors

1987-1988

First Pixel Detectors

S.L. Shapiro et al.., Silicon PIN Diode Array Hybrids for Charged Particle Detection, Nucl. Instr. Meth., A275 (1989)

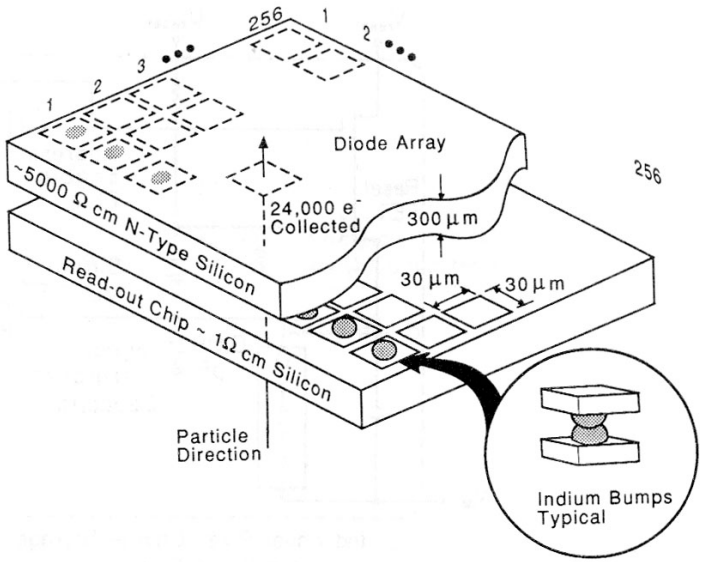

Fig. 1. Schematic representation of a hybrid detector.

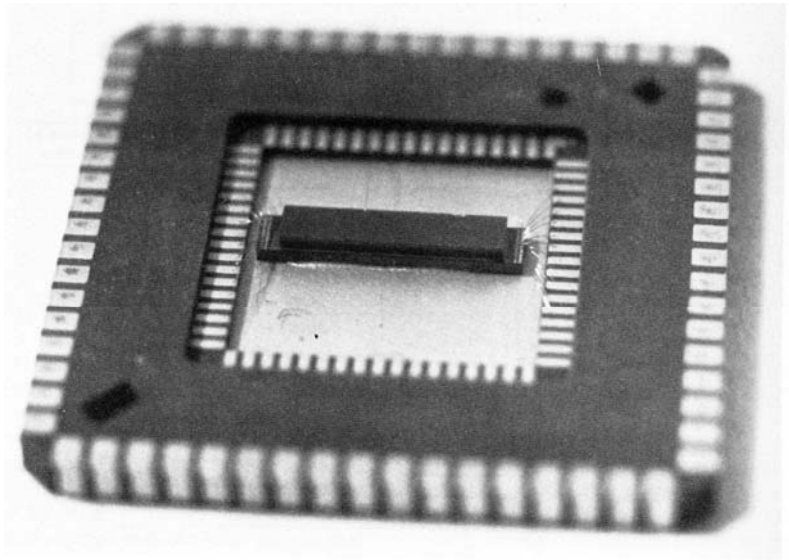

Fig. 6. A photograph of a 10×64 readout chip bump bonded to a germanium PIN diode array.

Pixel detectors

Monolithic Active Pixel Sensors (MAPS)

G. Deptuch et al., Monolithic Active Pixel Sensors with On-Pixel Amplification and Double Sampling Operation, Nucl. Instr. Meth., A512 (2003)

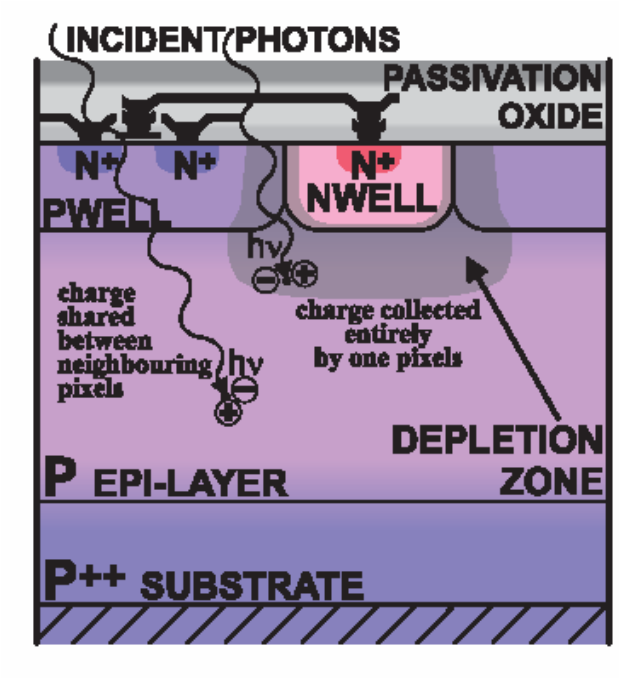

-The active volume (epi-layer, ~10 µm thick) is underneath the readout electronics, providing 100% fill factor

-The charge generated by ionization is collected by the n-well/p-epi diode

-Charge collection is achieved through the thermal diffusion

The device can be fabricated using a standard, cost effective and easily available twin-tub CMOS process on epi substrate. No post-processing (e.g. bump-bonding)!

System-on a chip approach possible

From W. Dulinski

Pixel detectors

Monolithic Active Pixel Sensors (MAPS)

Yu. Gomushkin et al., Tracking Performance and Radiation Tolerance of Monolithic Active Pixel Sensor, Nucl. Instr. Meth., A512 (2003), A513 (2003)

Measured CMOS MAPS tracking performance (20 µm pitch)

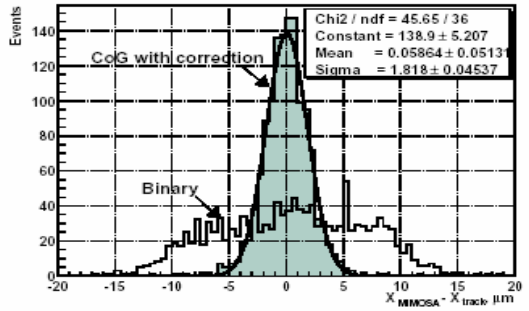

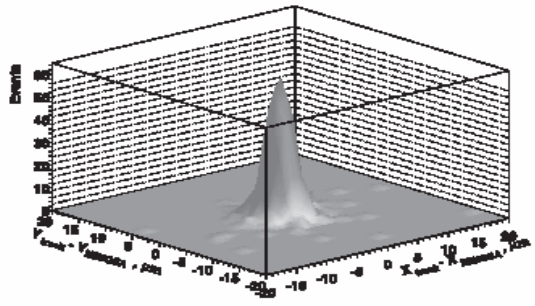

ENC: 10–20 e^-, $S/N_{seed,\ mean\ Landau}$:20-30
Efficiency (5σ seed cut): $\varepsilon_{MIP} > 99\ \%$
Spatial resolution: $\sigma = 1.4 - 2.4\ \mu m$

Demonstrated on several devices in various submicron CMOS processes:

AMS 0.6 µm, 14 µm epi
Alcatel 0.35 µm, 4 µm api
AMS 0.35 µm, no(!) epi
…
TSMC 0.25 µm, 8 µm epi
(LBL team)

From W. Dulinski

1990-94-...

Towards high luminosities

R&D programme for LHC

- RD2 Proposal to Study a Tracking/ Preshower Detector for LHC
- RD8 Proposal to Develop GaAs Detectors for Physics at the LHC
- RD19 Development of Hybrid and Monolithic Silicon Micropattern Detectors
- RD20 Development of High Resolution Si Strip Detectors for High Luminosity at LHC
- RD29 A Mixed Analog-Digital Radiation Hard Technology for High Energy Physics Applications
- RD39 Development of Superconducting Strip Detectors
- RD41 Development of Diamond Tracking Detectors for High Luminosity Experiments at the LHC
- RD48 (Radiation Hardening of Silicon Detectors - *ROSE*)
- RD49 (Studying Radiation Tolerant ICs for LHC - *RADTOL*)

1958 – 1982 - .....

Radiation damage

First observations in 1958

W. H. Fonger, J.J. Loferski and P. Rappaport, Radiation Induced Noise in p-n Junction, Journal Applied Physics, v 29, nr. 1 (1958)

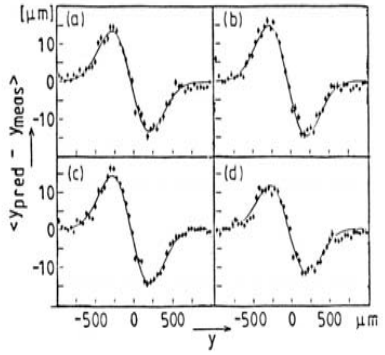

Fig. 34 Measured coordinate distortions from radiation damage in a 14° detector. (a) -3 mm < x < +3 mm; (b) -3 mm < x < -1 mm; (c) -1 mm < x < +1 mm; (d) +1 mm < x < +3 mm. x and y see Fig. 33. The curves are fits to a model with a potential equation where the change in donor concentration due to radiation damage is parametrized by a Gaussian following the beam profile [18].

First observations in HEP

H. Dietl et al., Radiation Damage in Silicon Strip Detectors, In *Bari 1985, Proceedings, High Energy Physics*, Nucl. Inst. Meth. A253 (1987)

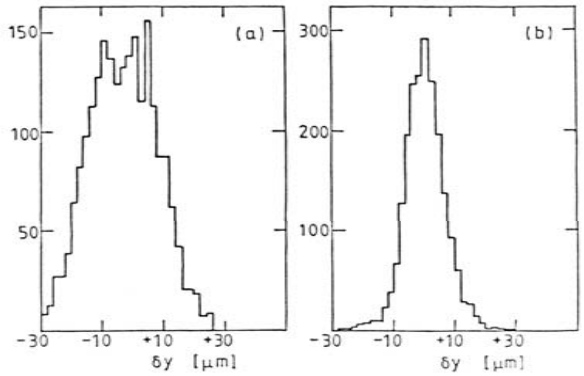

Fig. 37. Measured impact parameter of beam tracks (y projection) at primary vertex. (a) Before radiation damage correction; (b) after correction.

1988 - 1992

Radiation damage

Beginning of systematic studies

E. Beuville et al., Measurements of Degradation of Silicon Detectors and Electronics in Various Radiation Environments, Nucl. Instrum. Meth. A288 (1990), 68-75

D. Pitzl, et al., Type Inversion in Silicon Detectors, Nucl. Instr. Meth., A311 (1992), 98-1004

- Donor removal and acceptor creation $N_{eff}(\Phi) = N_o e^{-c\Phi} - \beta\Phi$
- Type inversion @ fluences 0.4 – 3 x 10^{13} cm^{-2} depending on the resistivity
- Anti-annealing →increase of the depletion voltage by ~ 30% in 2 years

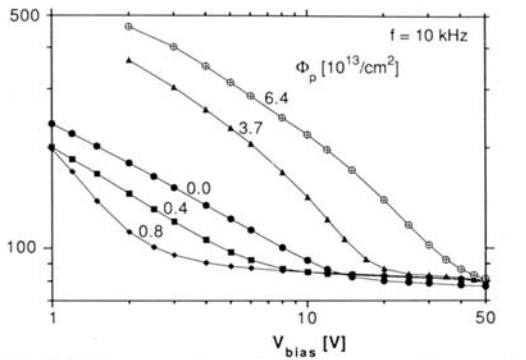

Fig. 2. C–V curves of one photodiode measured at several intermediate proton fluences.

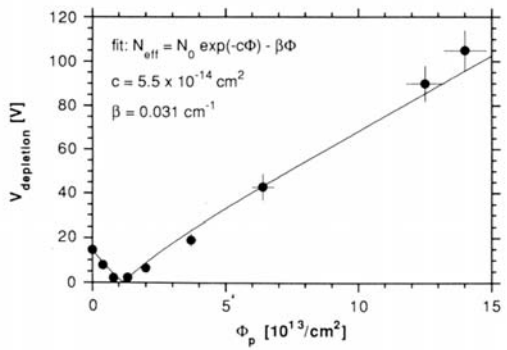

Fig. 3. Depletion voltage for photodiodes during proton irradiation. The line is the best fit according to eqs. (1) and (2). Type inversion occurs at $\Phi = 1.1 \times 10^{13}$ cm^{-2}.

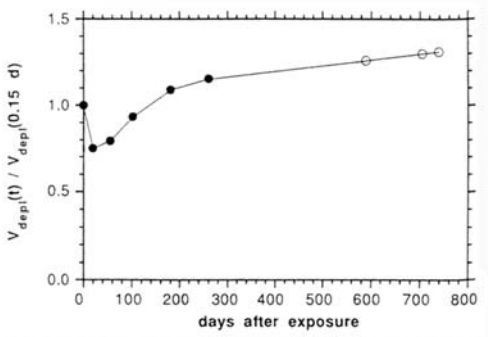

Fig. 10. Post-irradiation behaviour of the depletion voltage for photodiodes. The diodes were irradiated in 1990 (full symbols) and 1989 (open symbols).

Radiation damage

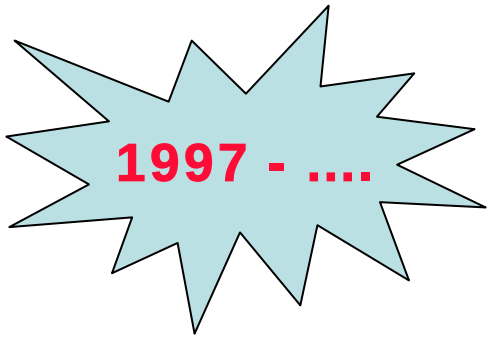

Submicron CMOS process

N. S. Saks et al., IEEE Trans NS-31 (1984), 1249

A. Marchioro, Deep Submicron Technologies for HEP, Proc. 4th Workshop on LHC Electronics, Report CERN/LHCC/98-36 (1998), 40-46

P. Jarron et al., Deep Submicron CMOS Technologies for the LHC Experiments, Nucl. Phys. Proc. Suppl.78 (1999), 625-634

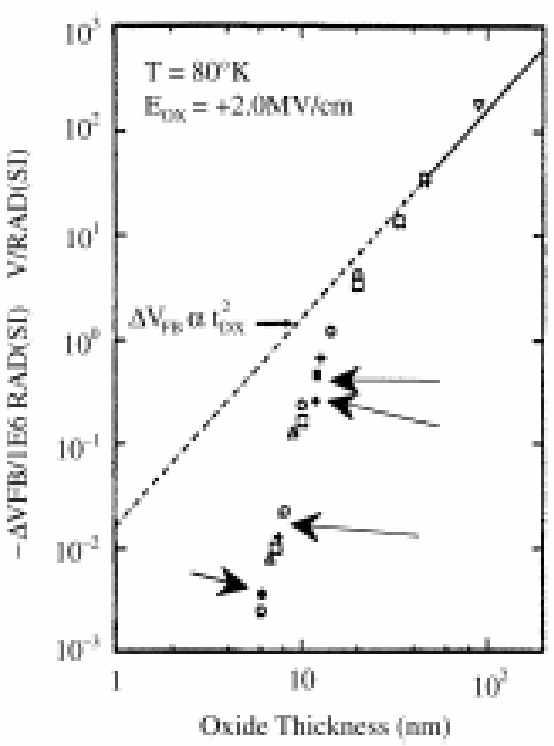

Fig. 8. Flat band voltage shifts measured as a function of gate oxide thickness after irradiation dose of 1 Mrad [14].

1995-...

Si vertex-trackers for LHC

CMS – 210 m² of silicon sensors !

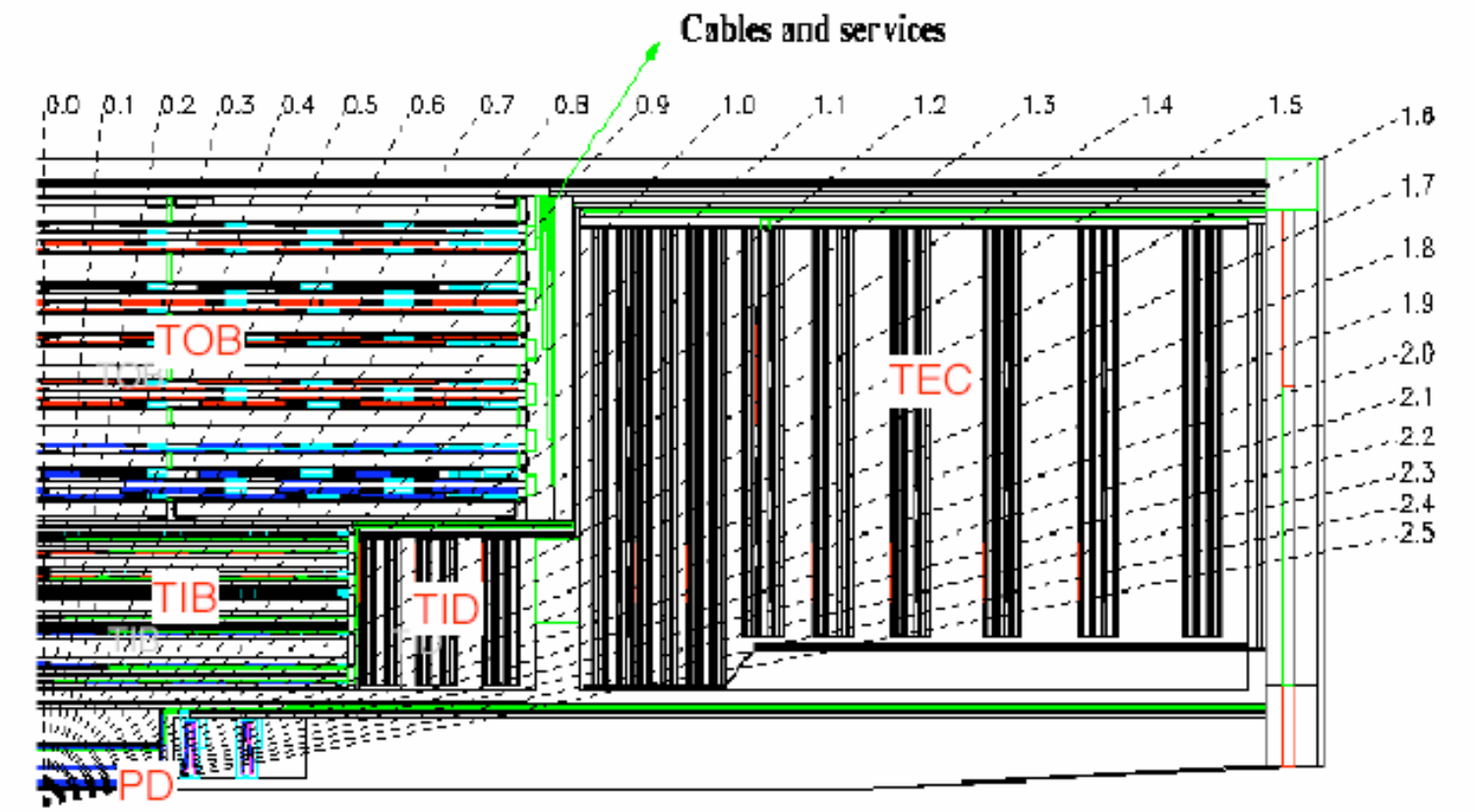

Full Silicon Tracker

210 m² of silicon sensors, 10^7 strips, 6.7 10^7 pixels

1995-...

Si vertex-trackers for LHC

CMS – Si strip detector modules / pixel electronics

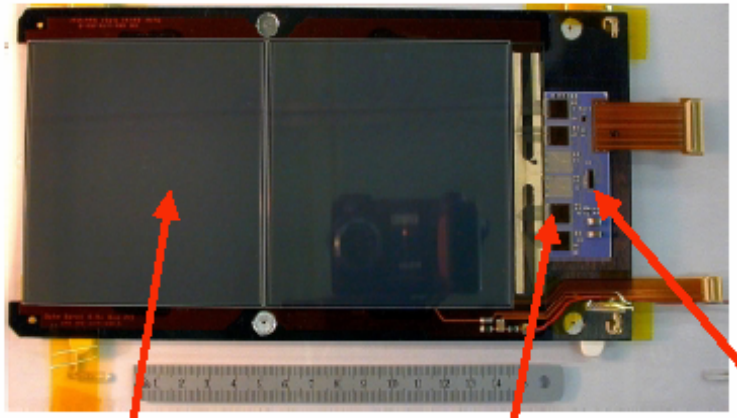

15'000 modules

15'000 hybrids

Reliable, high yield
Industrial hybrid
Fabrication and assembly

25,000,000 Bonds

Automated module assembly

0.25µm ROC, IBM_PSI146

Sensors: Production batches received from Hamamatsu (excellent quality) and ST (improvement needed)

Problems solved: packaging of ASICs, bondability of pitch adaptors, ordering CF frames

Hybrids: latest batch good, 4700 ordered, awaiting bulk order (delivery in Oct 03)

Readout Chip: 0.25µm ROC received Aug-03. Works very well (first iteration!). Performance superior to DMILL chip.
Chip irradiated to 25 Mrad works fine.

Tracking in space

1994 -2007 - ....

AMS (ALPHA Magnetic Spectrometer)

Y-H. Chang, The AMS Silicon Tracker
Nucl. Instr. Meth., A466 (2001), 282

- Rigidity ($dR/R \approx 2\%$ for 1 GeV Protons) with Magnet
- Signed Charge (dE/dx)
- 8 Planes, ~6m2
- Pitch (Bending): 27.5μm
- Pitch (Non-Bending): 104μm

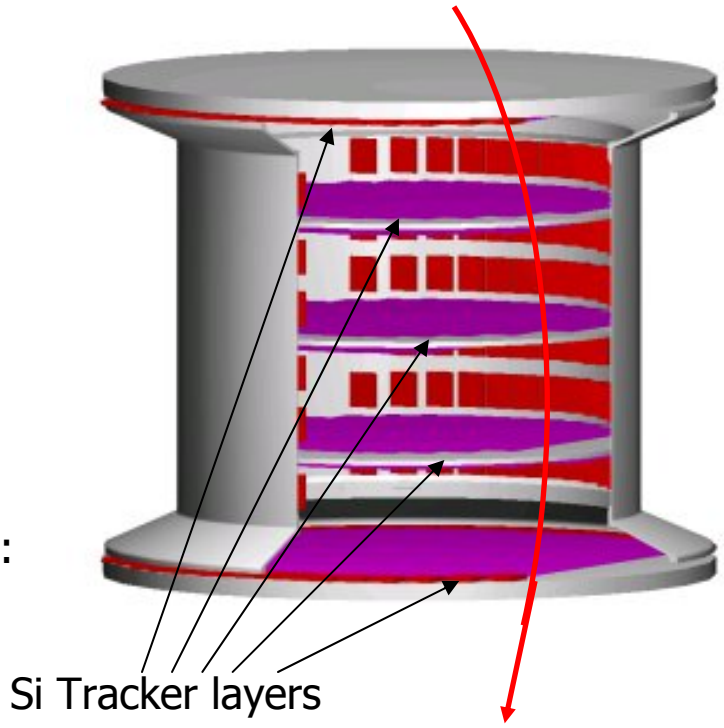

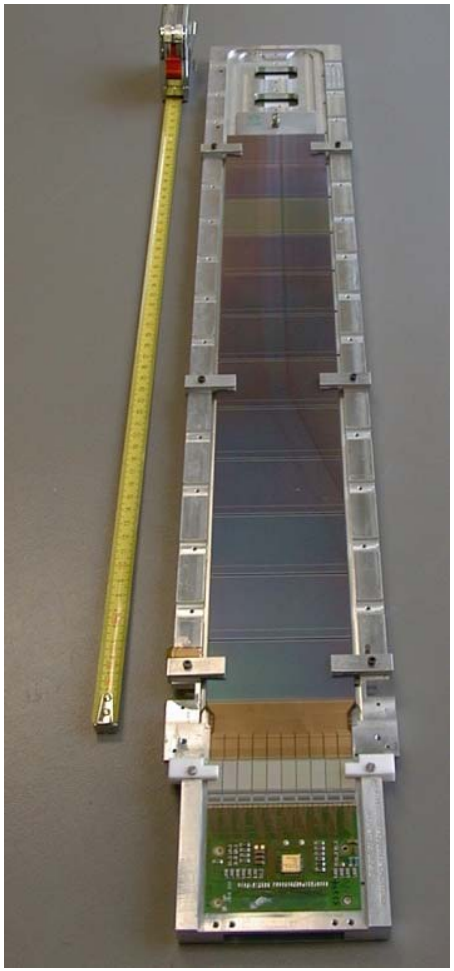

1997-2006- ...

Tracking in space

GLAST Si tracker (1999 beam tests)

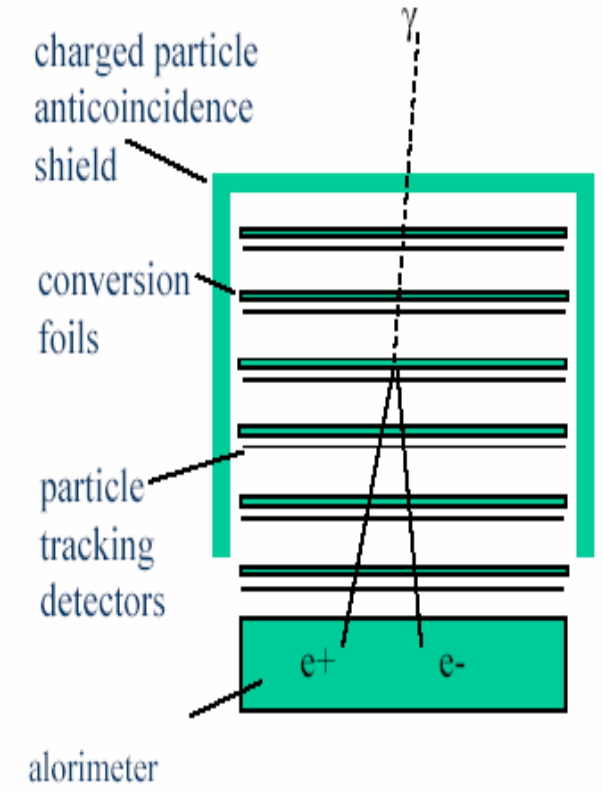

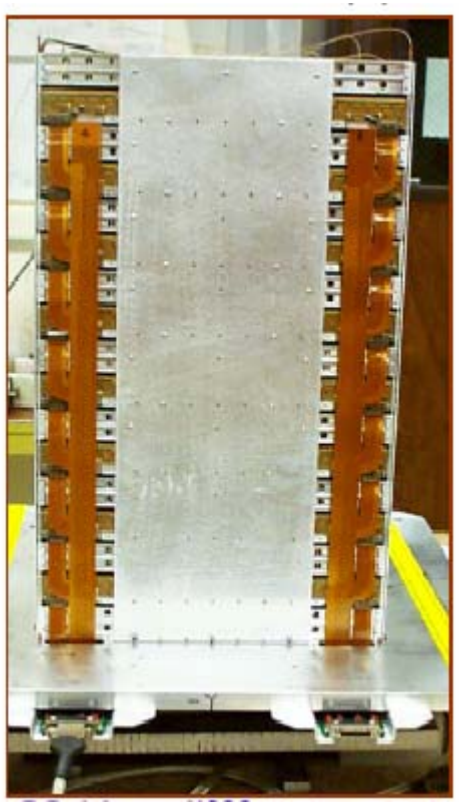

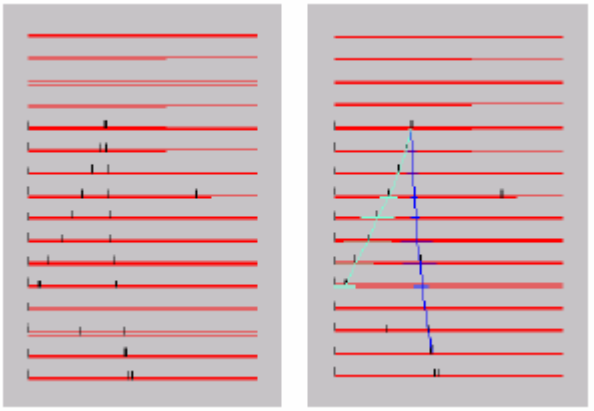

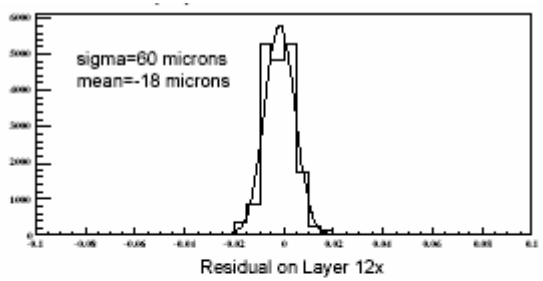

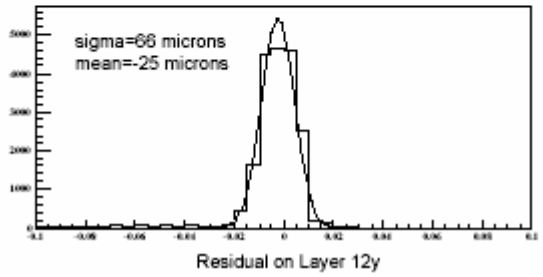

From R. Johnson

Production at HAMAMATSU

- 75% to 90% of the market (my estimate)
- 4 inch line since 1986
- 6 inch line since 1998
- Excellent quality control & feedback
- 6 inch line for Single Sided Strips only
- 0.6μm process O.K.

- FUTURE “PLANS”
- No large scale production for HEP
- Pixel & Drift Detectors
- Extend the Detector thickness up to 2 mm for higher energy X-rays

Position sensing in high energy heavy ion experiments

- NA45 (CERES) Experiment at SPS at CERN a) 3’’ cylindrical drift detector and b) 4’’ cylindrical detector (past)
- STAR Experiment at RHIC at BNL (present)
- ALICE Experiment at LHC at CERN (future)

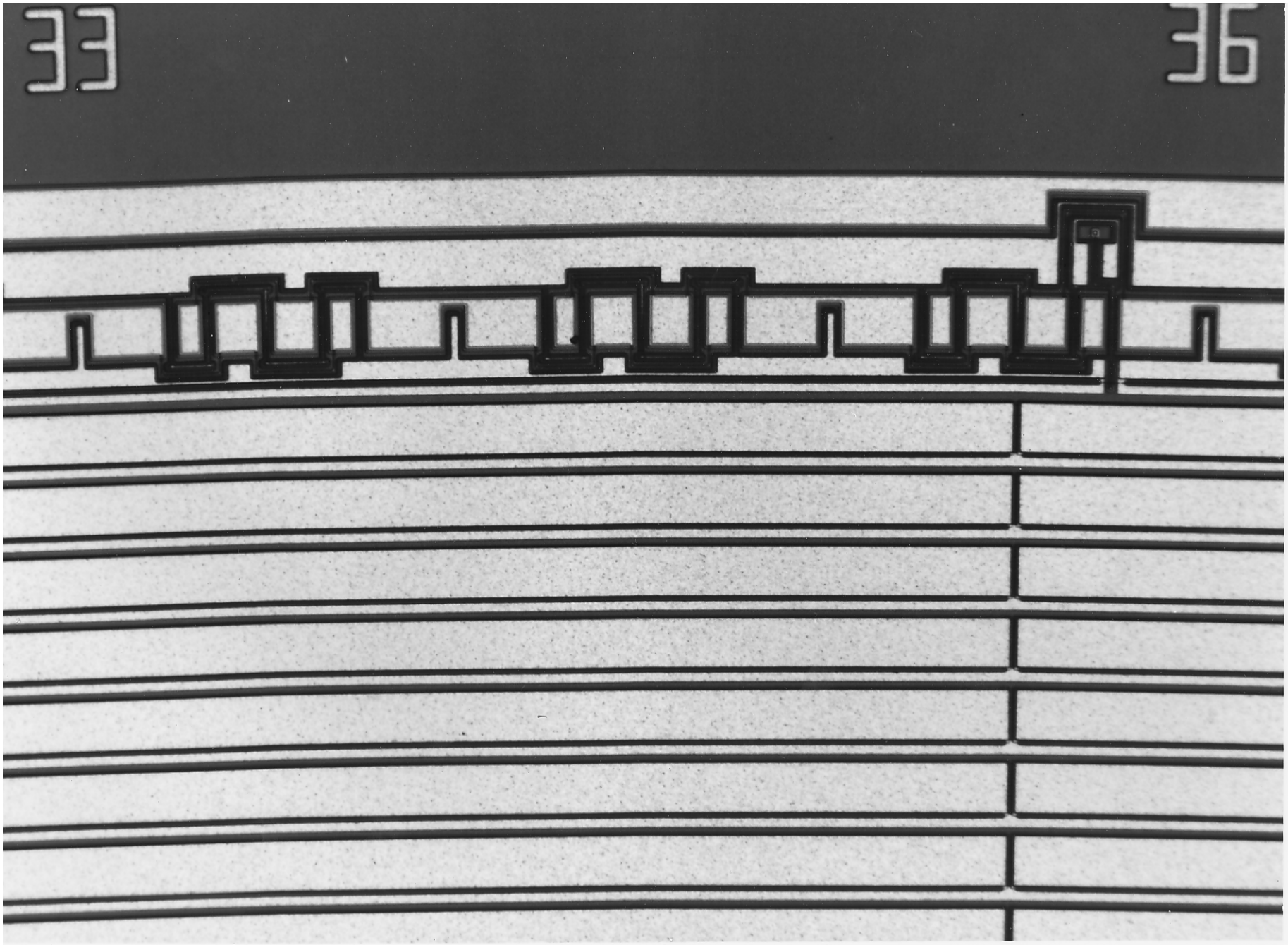
33
36

Innovations in CERES cyl. Det.

- Collection of leakage current generated at the Si-SiO interface at a sink anode
- Interlaced anodes (Nyquist filtering in linear dimension)

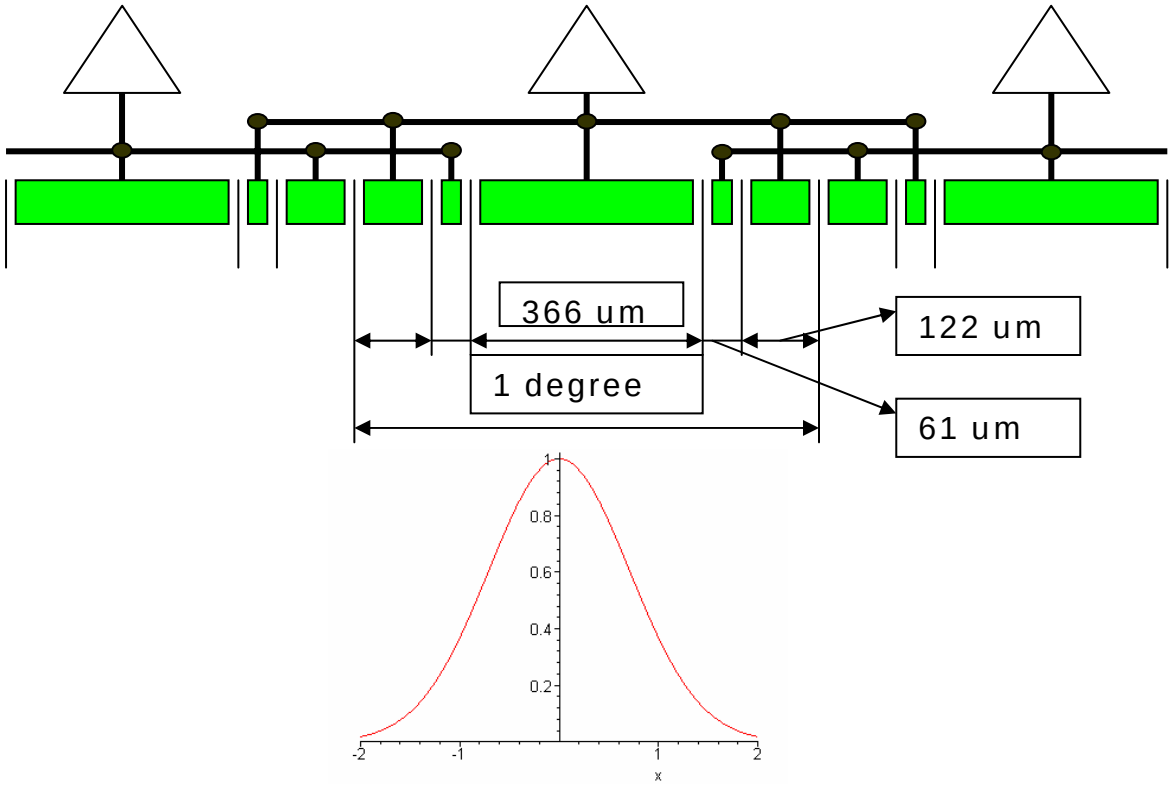

STAR Drift Detector

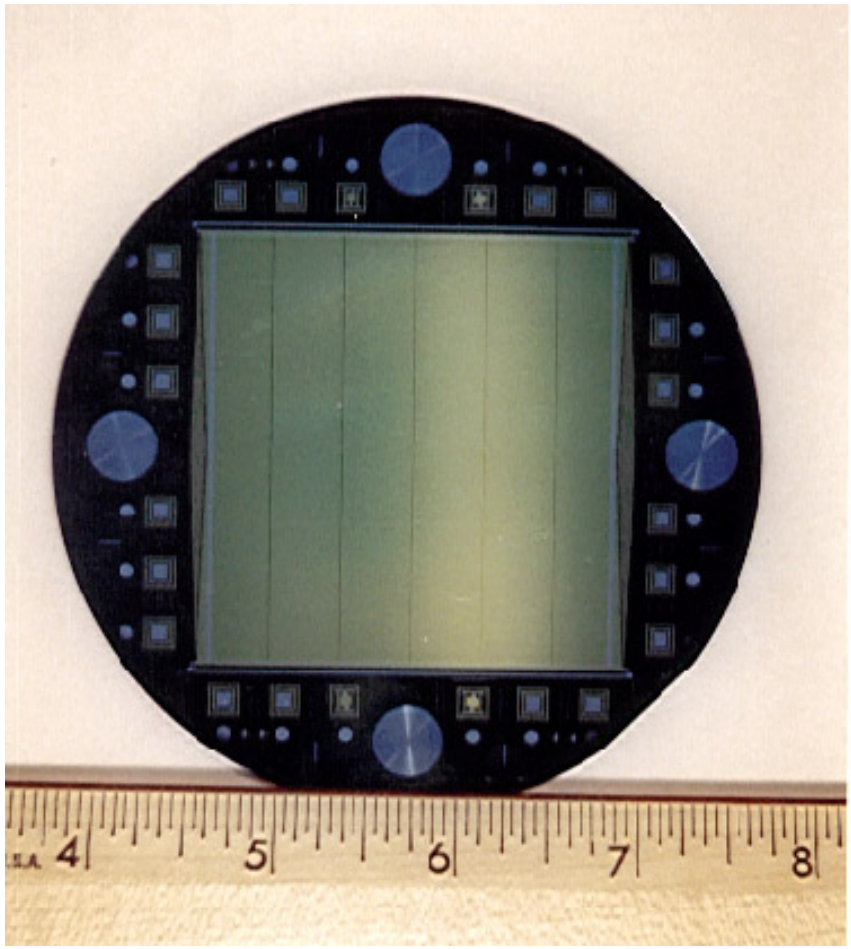

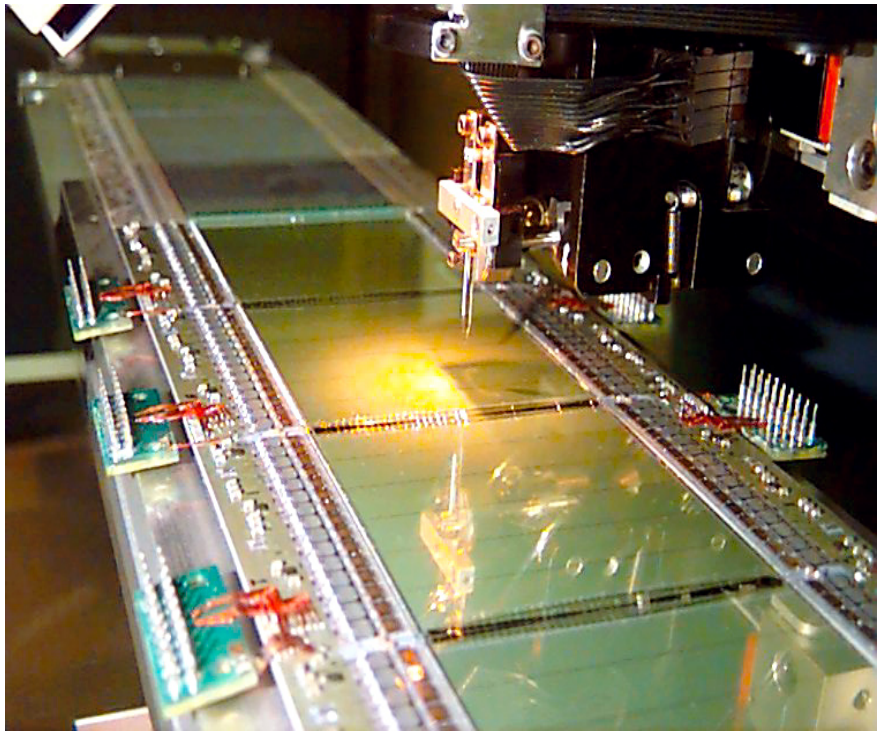

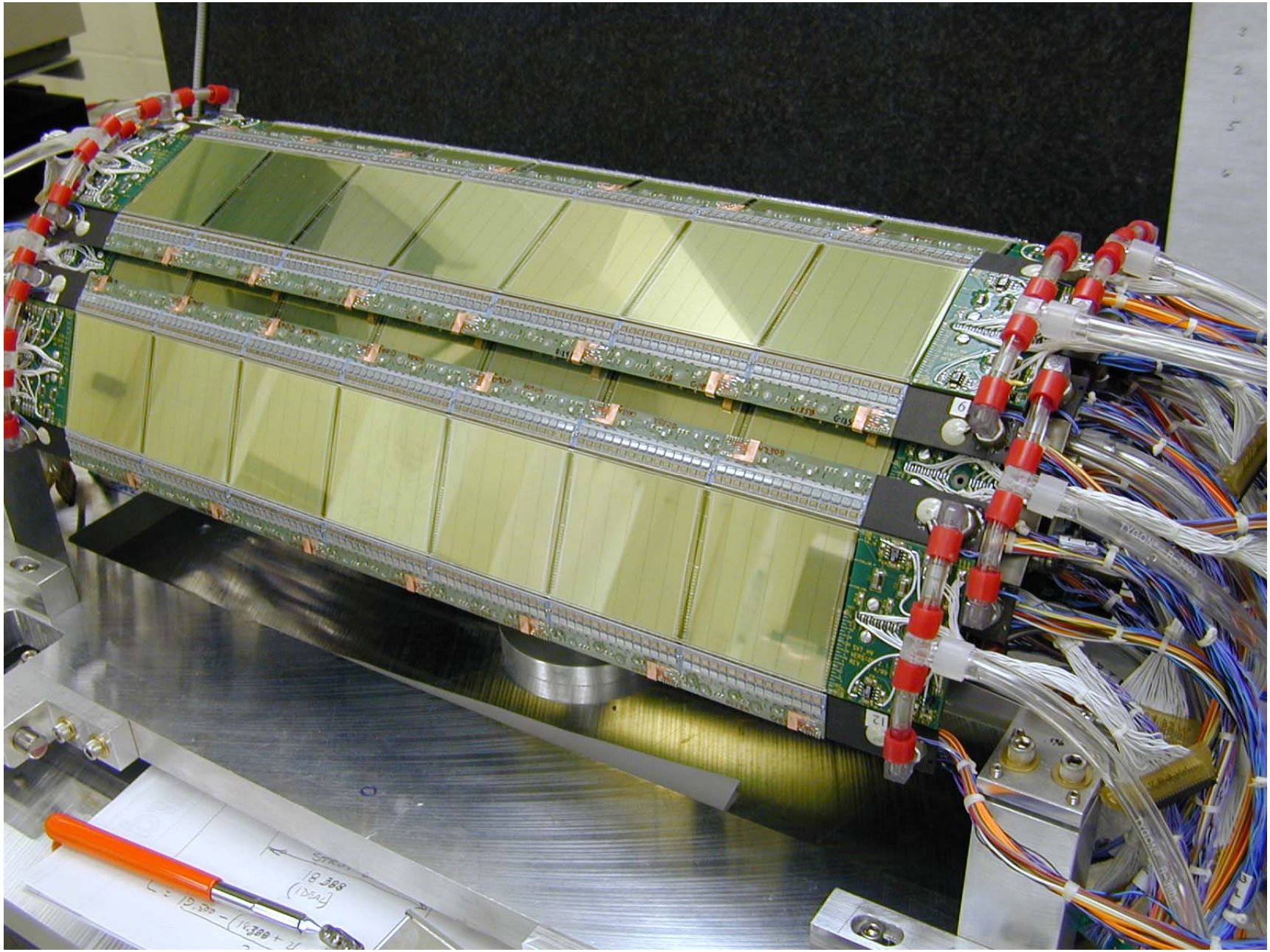

SDD barrels

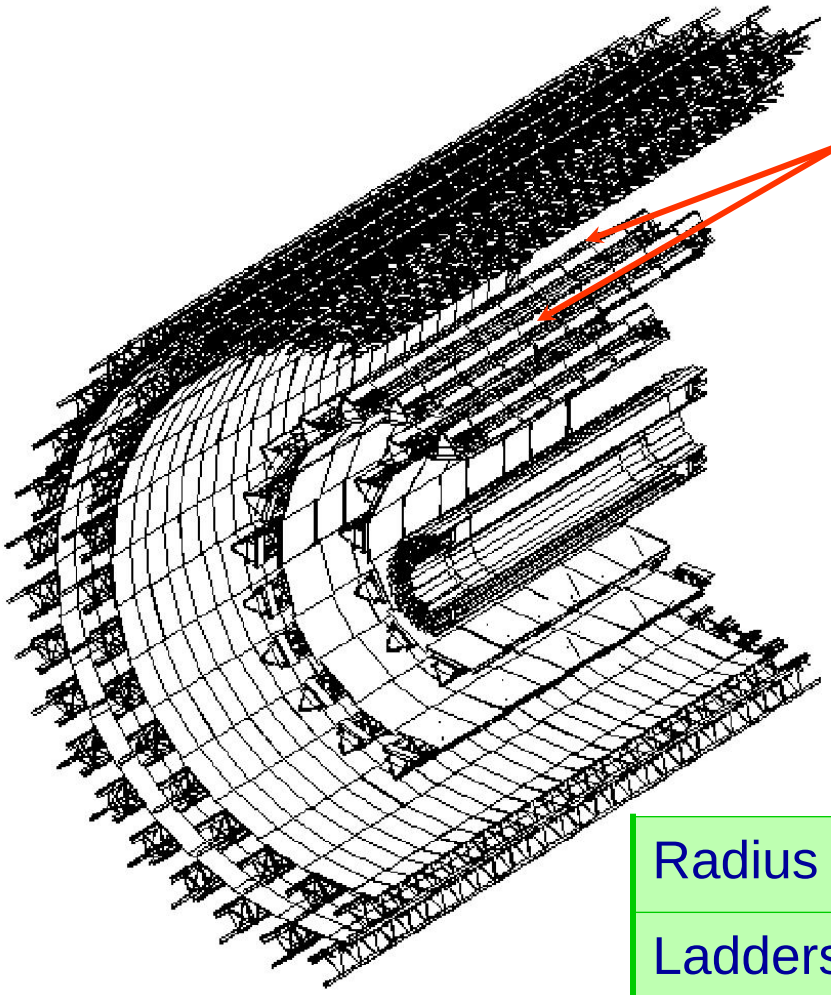

Silicon Drift Detectors

Tot. No. channels 133 •10^3

Tot. No. detectors 260

total area 1.37 m^2

	Layer 3	Layer 4
Radius (mm)	14.9	23.8
Ladders	14	22
SDDs per ladder	6	8

ALICE Silicon Drift Detector

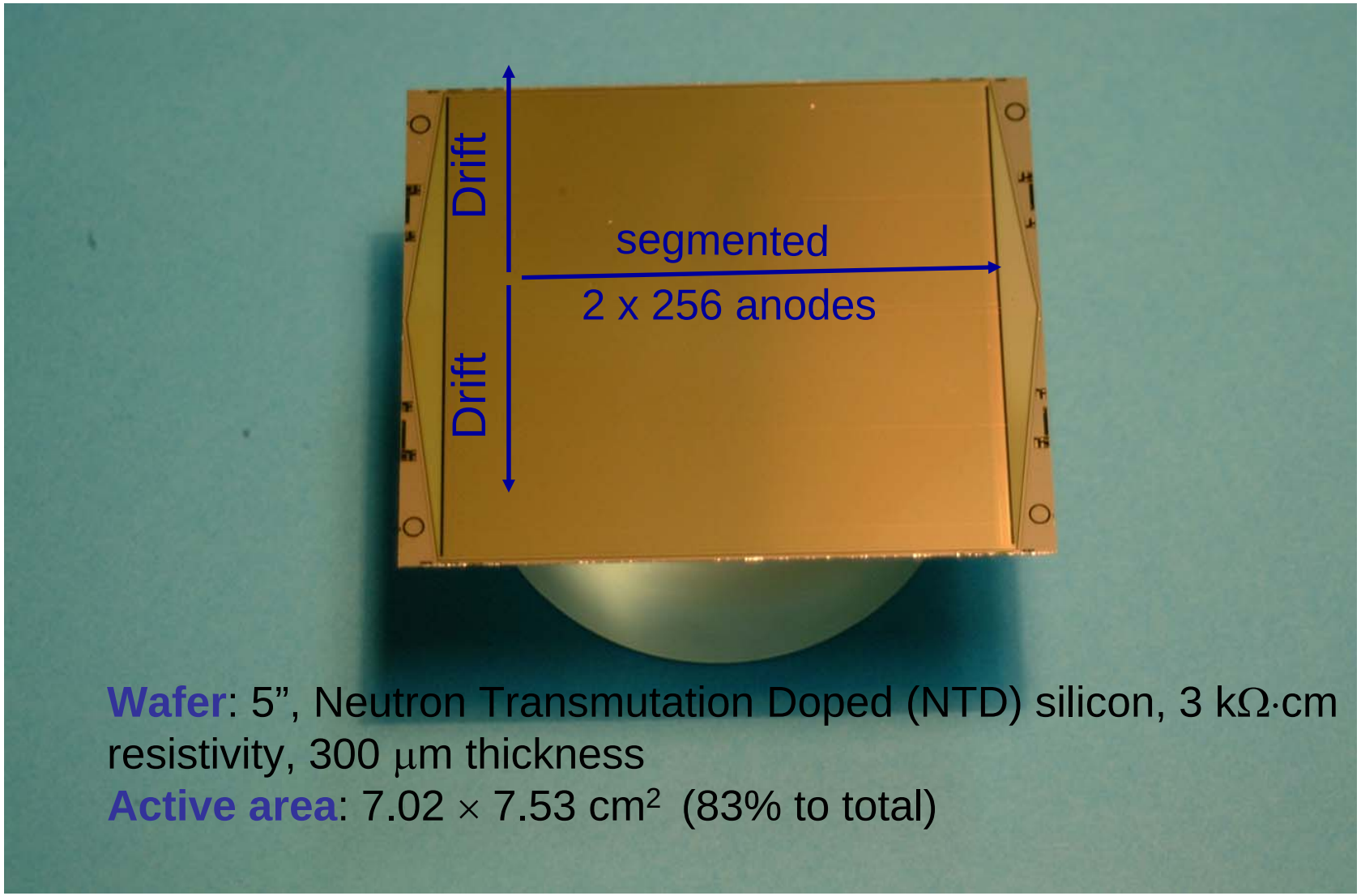

Wafer: 5”, Neutron Transmutation Doped (NTD) silicon, 3 kΩ·cm resistivity, 300 μm thickness

Active area: 7.02 × 7.53 cm^2 (83% to total)

Detector design features

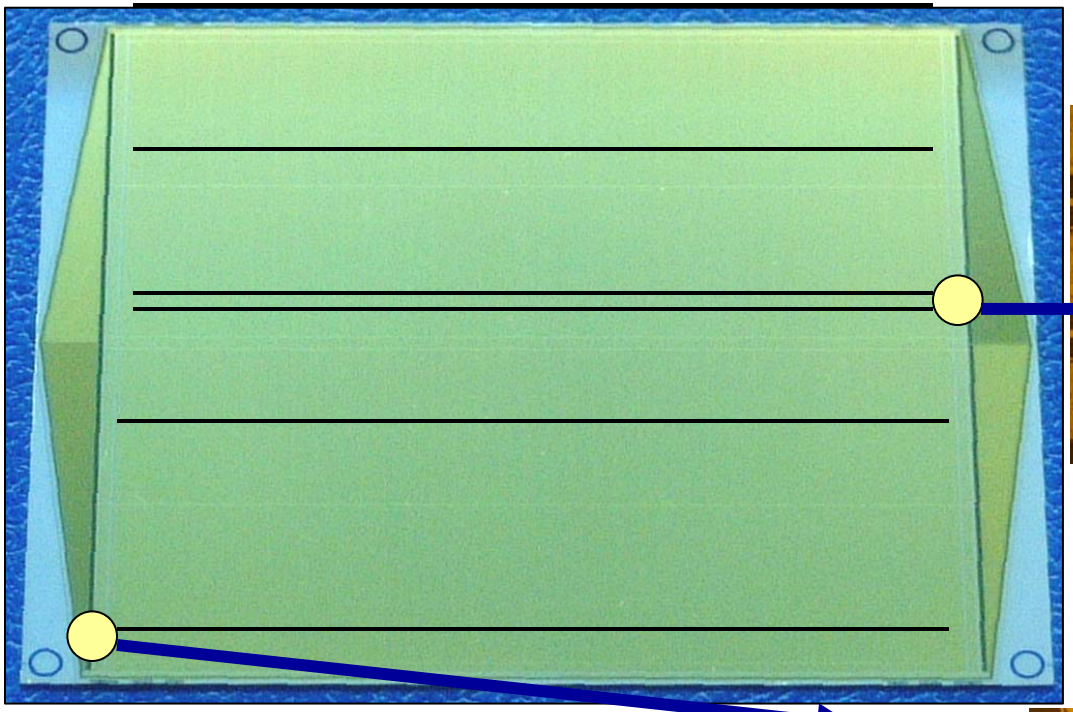

injector lines

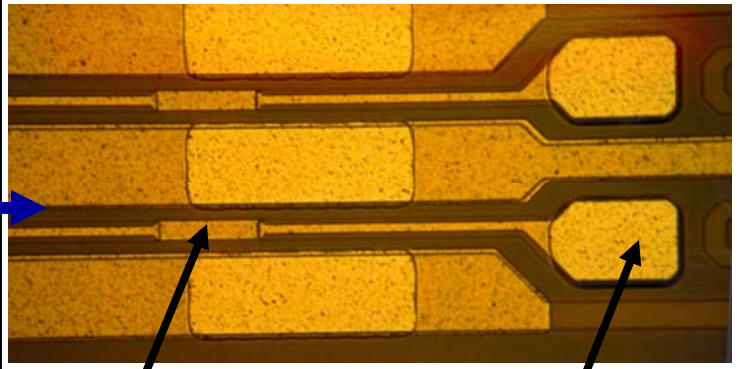

injector line bonding pad

MOS injector (every 8th anode)

Charge collection zone

guard cathodes (32 μm pitch)

292 drift cathodes (120 μm pitch)

implanted HV voltage dividers

256 collection anodes (294 μm pitch)

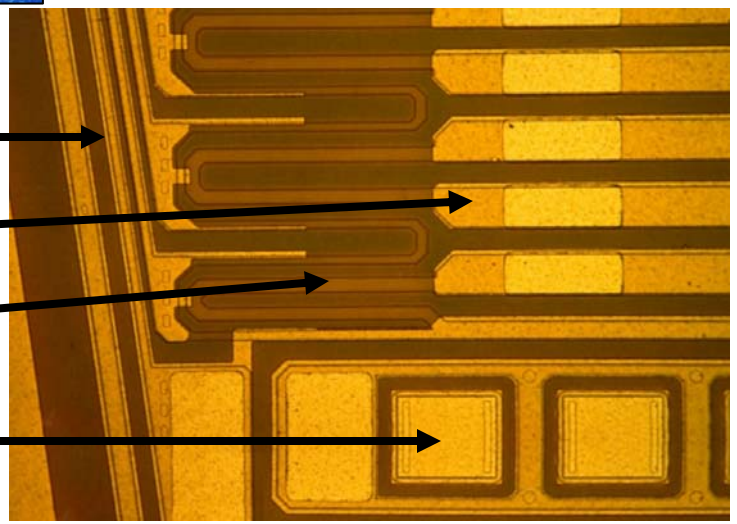

Beam Tests in 2003 – Position resolution

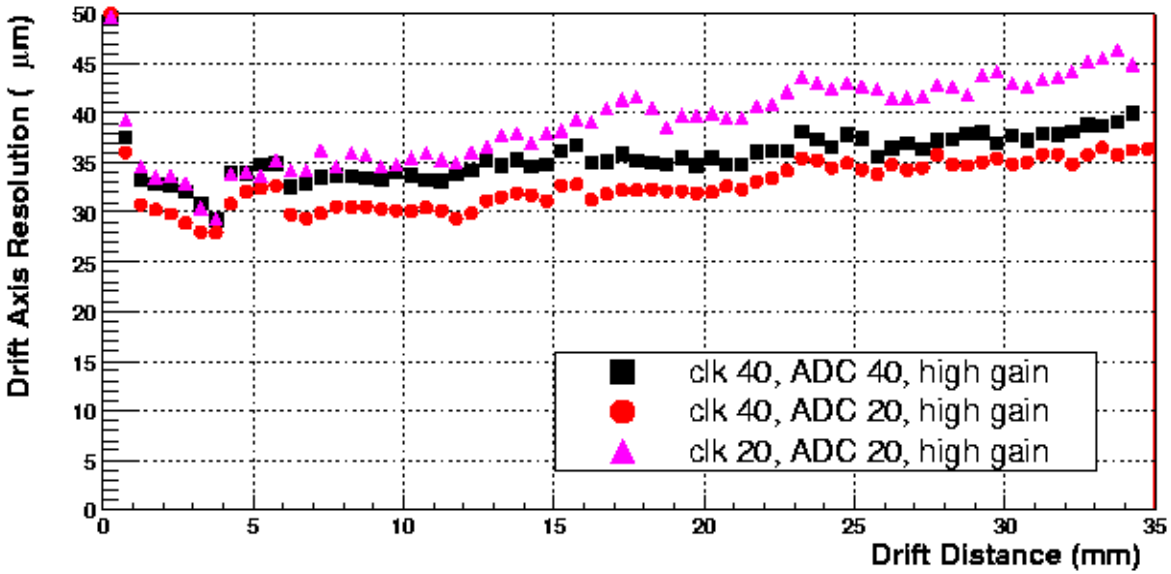

Exhaustive test of the front-end parameters performed in beam test:gain, sampling & ADC frequencies...

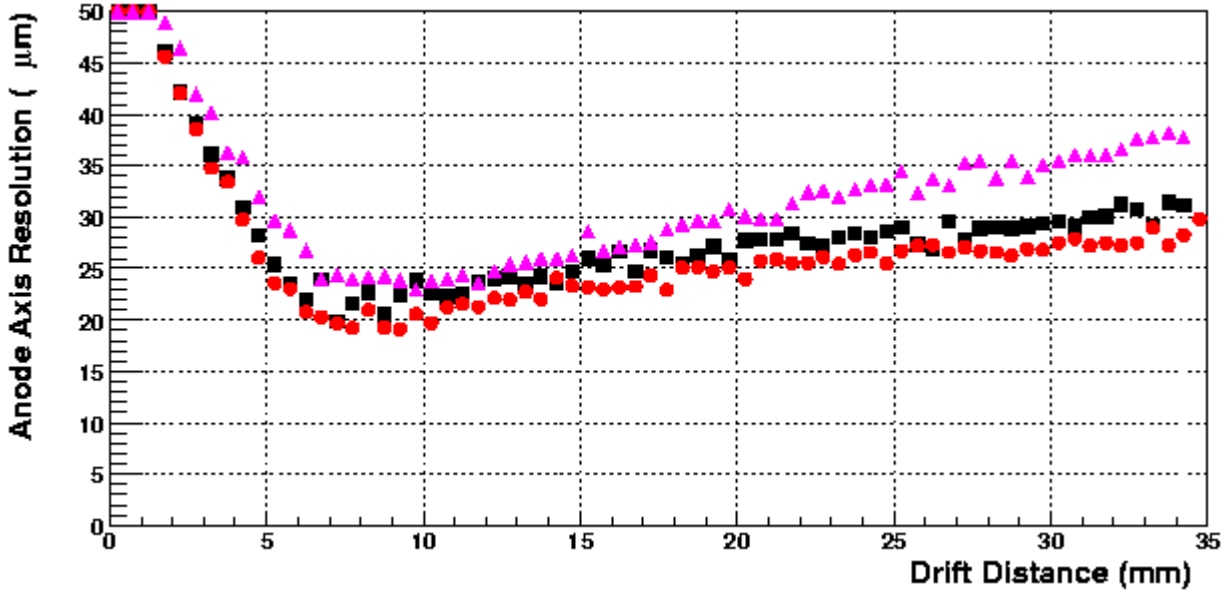

The *Controlled-Drift Detector (CDD)**

(*) Patents:
US 6,249,033
EP0862226

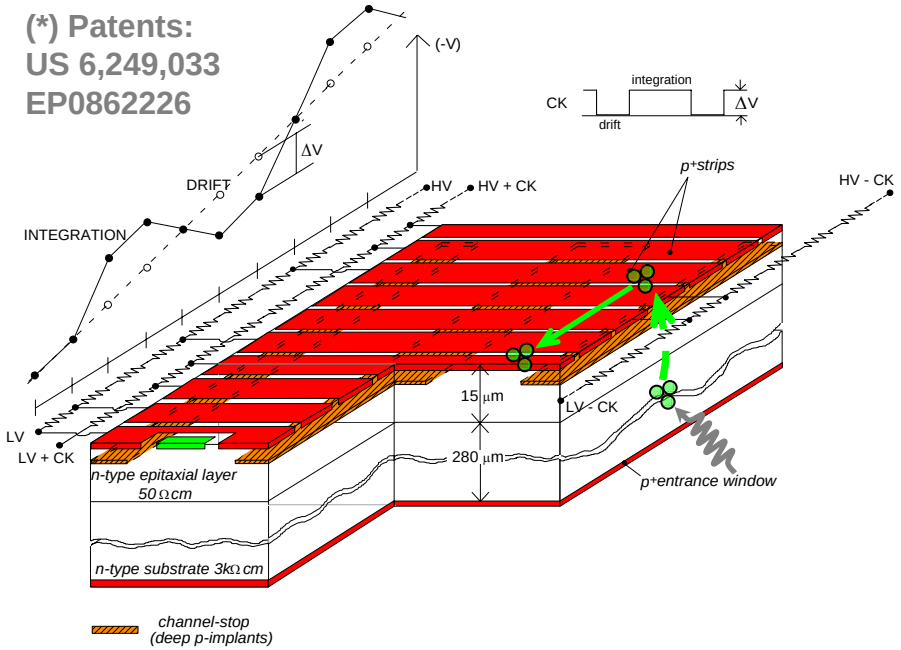

- 2D position sensing (100-200μm)
- low capacitance (~100fF) and integrated JFET⇒ high energy resolution
- low no. of channels (n instead of $n\times n$)
- integrate-readout mode

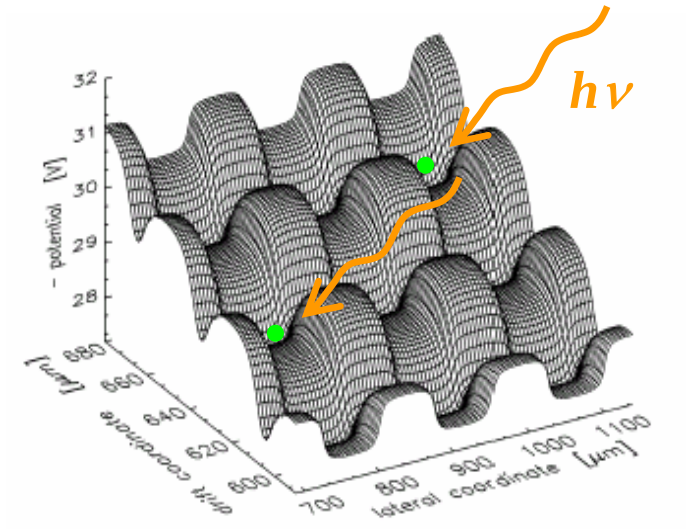

Readout phase

~ 3μs/cm

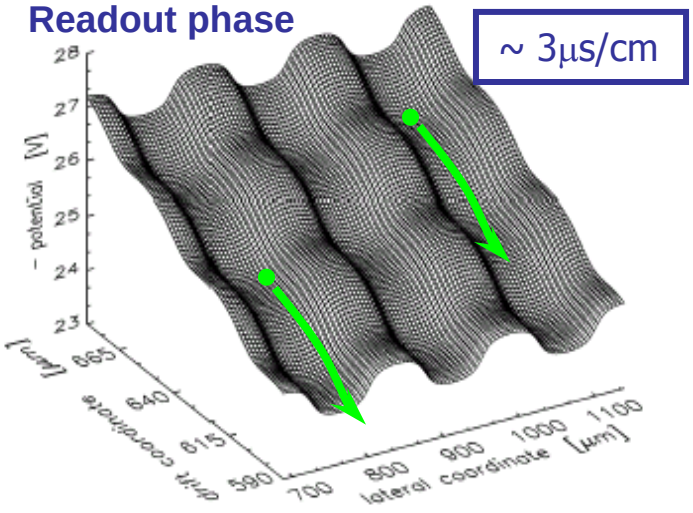

The X-ray position along the drift is obtained from the electrons' drift time

The X-ray energy is obtained from the electron charge collected at the anodes

The BaBar Silicon Vertex Tracker: lessons learned

Giovanni Calderini, INFN Pisa

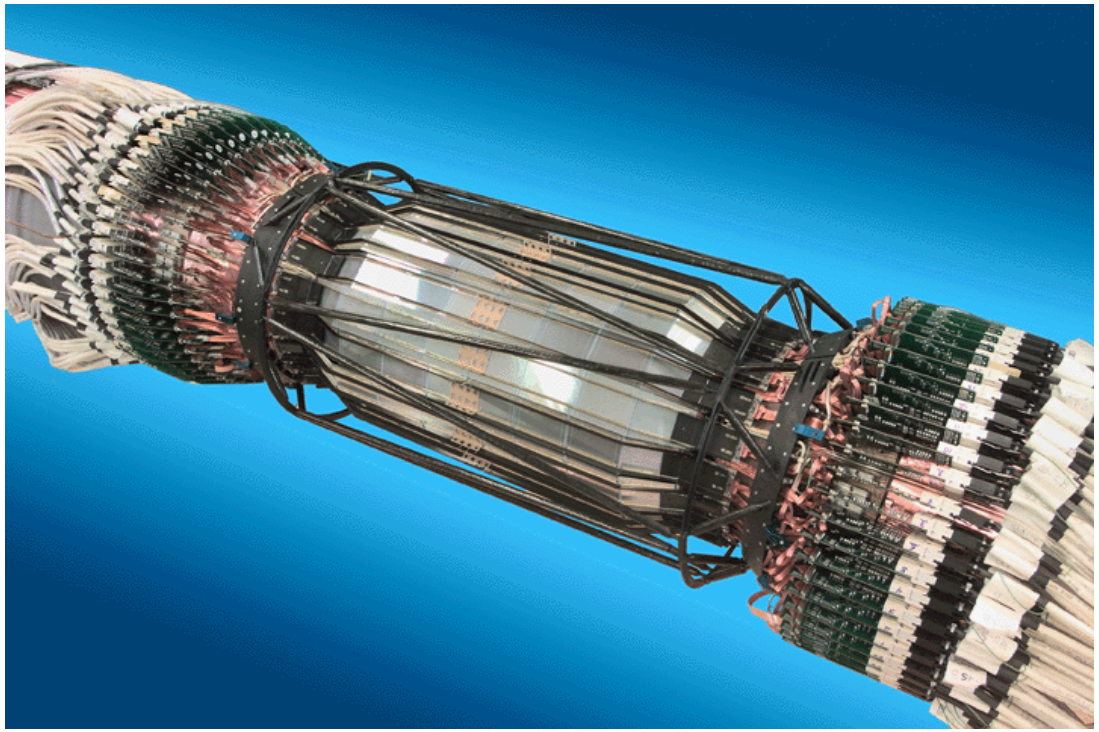

5th Internation Symposium on Semiconductor Tracking Detectors
Hiroshima, Japan

SVT Layout

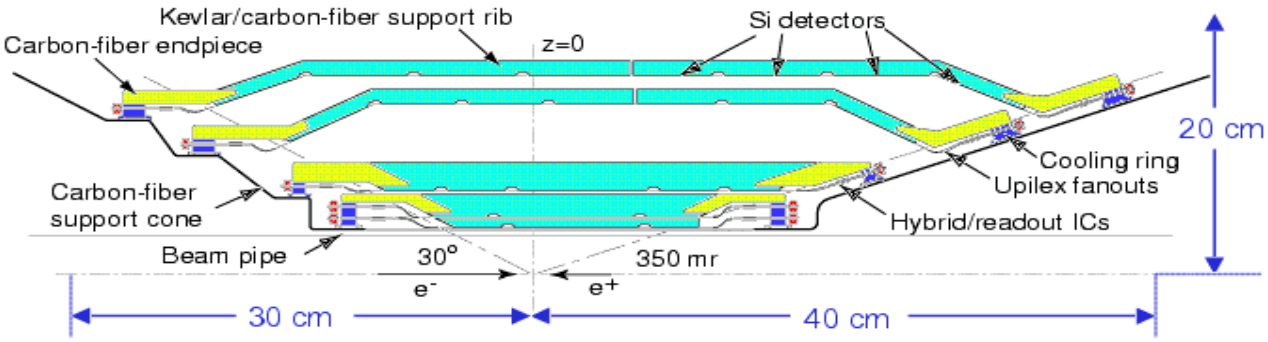

Constraints from the integration with PEP-II:

- Permanent (B1) dipole magnets restrict polar acceptance: $17.2^{o} < \theta < 150^{o}$
- Bunch crossing period: 4.2 ns (almost continuous interactions !)
- Radiation hardness

- Microstrip silicon detector; 5 double-sided layers
- Layer 1-3 (barrel-shaped) for a precise measurement of track impact parameter
- Layer 4-5 (arch shaped) for pattern recognition and low pt tracking
- Resolution dominated by multiple scattering
- 150 k channels, 340 wafers (6 different models)

Integration with PEP-II is a complex technical choice

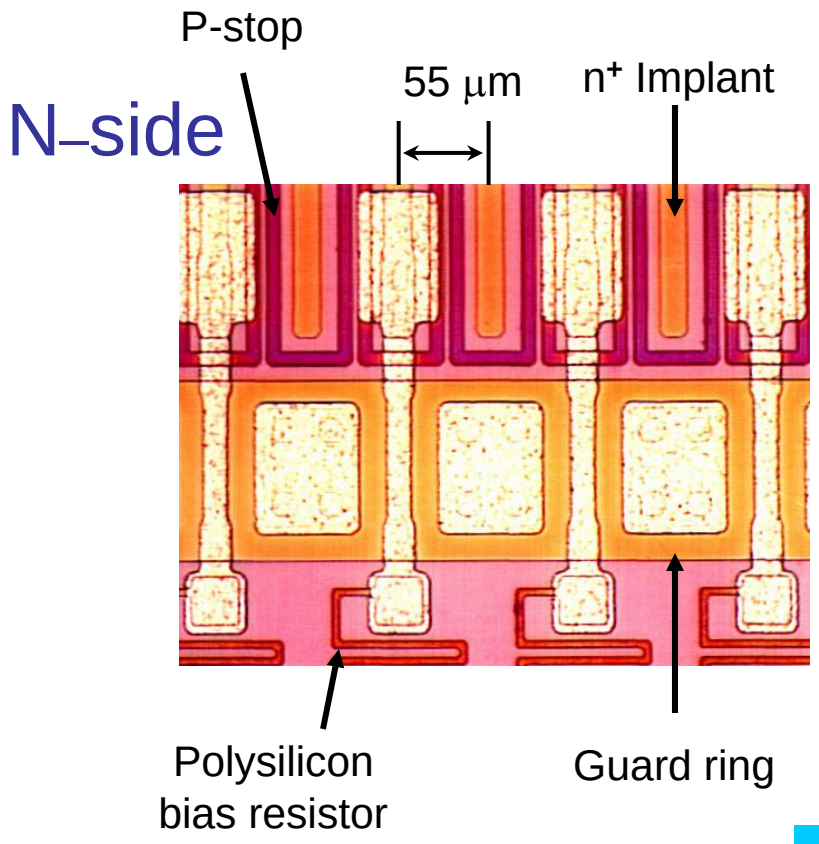

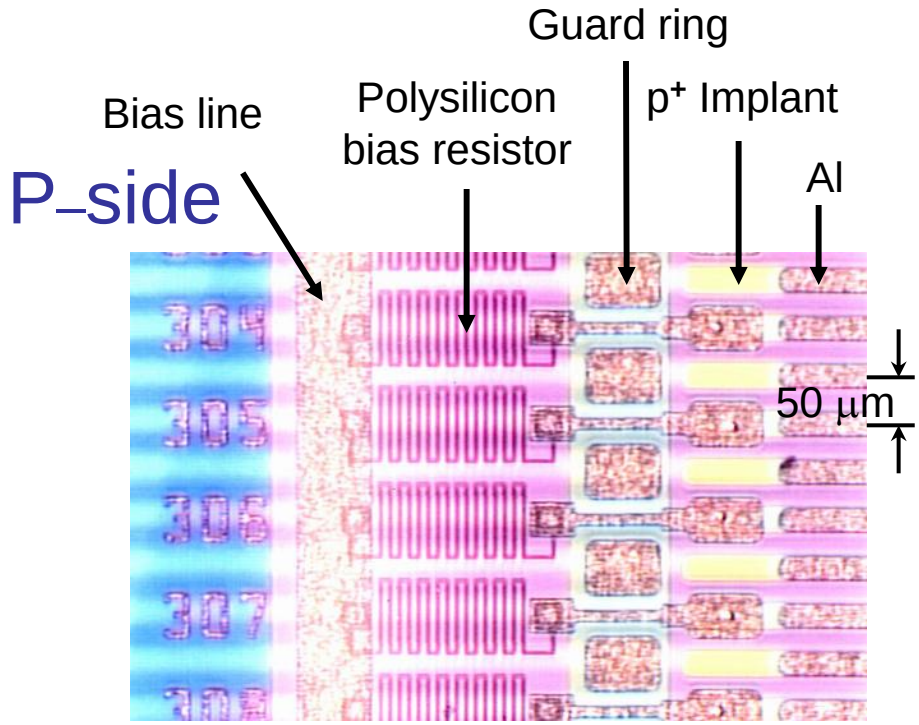

- Double-sided, AC-coupled Si
- Integrated polysilicon bias resistors
- 300 μm n-type (4-8 kΩcm)
- P+ and n+ strips perpendicular to each other

The AToM Chip

(**A** Time **o**ver threshold **M**achine)

- 128 Ch's/chip
- Rad-Hard bulk 0.8 μm CMOS process (HONEYWELL 4")

- Capable of simultaneous:
  - •Acquisition
  - •Digitization
  - •Sparsified Readout

- No common mode noise:
  - •separation analog/digital parts in the chip layout
  - •proper system shielding

- Info from AToM: Timestamp T_0 and TOT
- Internal charge injection
- Digital-based diagnostics

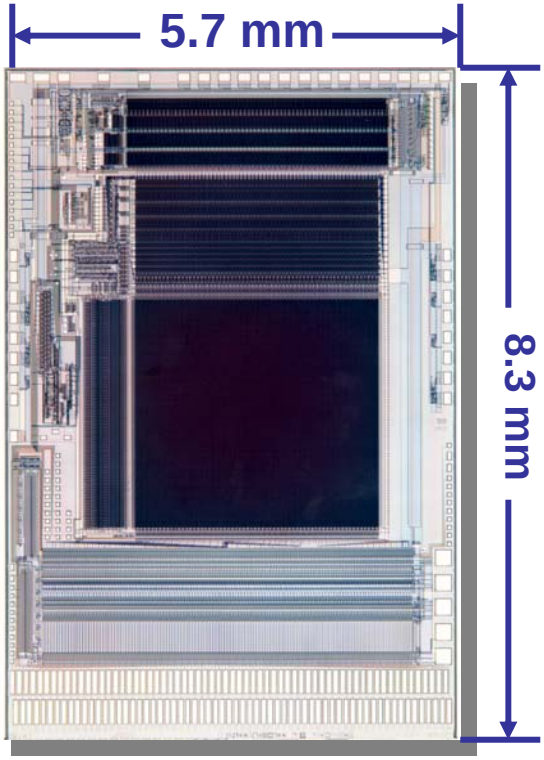

SVT High Density Interconnect

Functions:

- Mounting and cooling for readout ICs.
- Mechanical mounting point for module.

Features:

- AlN substrate.
- Double sided.
- Thermistor for temp. monitor.
- 3 different models.

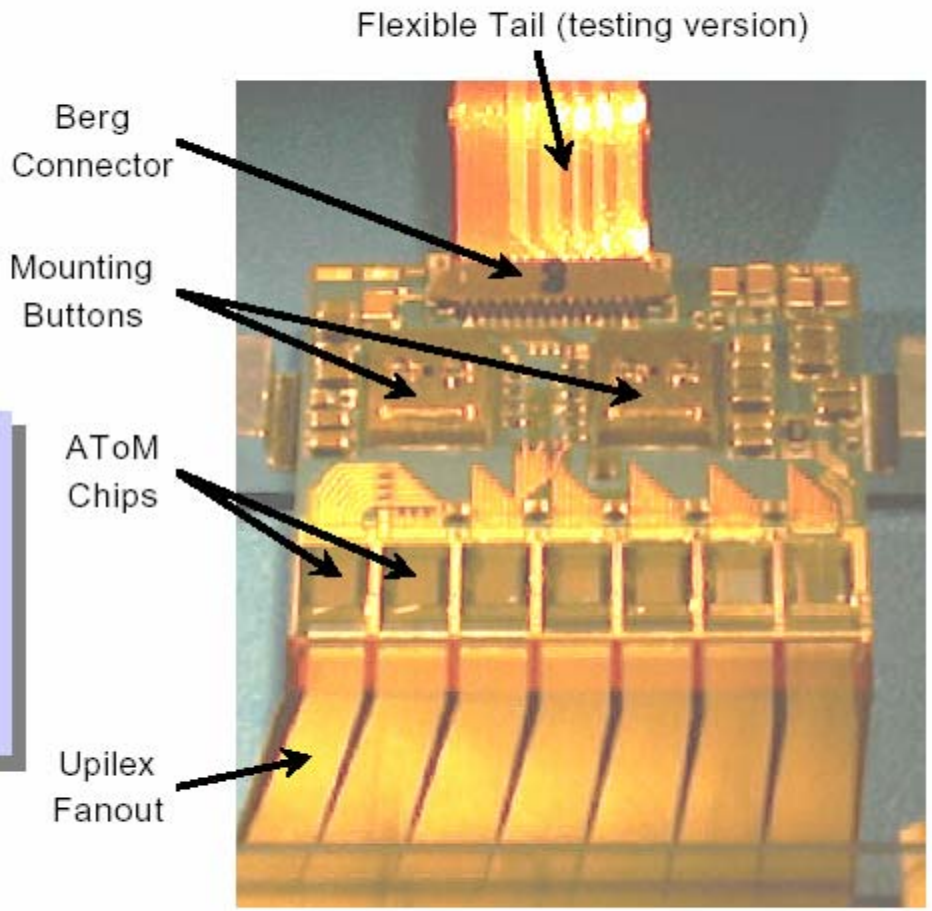

Observed failure modes

(what could we repair and how?)

BaBar SVT not accessible and a shutdown to extract it requires at least four months!
Reliability of every part is critical.
Redundancy whenever possible !

- A) Connectors

  Never careful enough with cables and connectors.

  Connectors on hybrid rather delicate

  Several iterations on insertion tools and procedures.

  Still one of the most critical issues

Redundancy and robustness more important than sophistication.

- Two redundant signal and control paths: used in several modules
- Must carefully balance the pros and cons of permanent vs. breakable connections

Connectors were one of the main sources of failure during and immediately after the installation

Improved insertion procedure during 2002 shutdown
Additional strain reliefs added

At least 3 half modules fixed in this way !

- C) Cooling system: stability

Modest power dissipation: 4mW/ch = 600 W total

Nonetheless cooling issues have been driving several design issues:

- Material of hybrids
  - AlN as a compromise between Al_2O_3 and BeO
- Mechanical structure
  - Integrated cooling lines
- Complexity of interlock system to HV
  - Degree of protection vs. possibility of fake alarms
  - A glitch in the interlock system can trip the power and cost several minutes of data-taking !

General principles

Below atmospheric pressure – can't leak.

And we're happy we did it !!!

Conclusions

The SVT Detector of the BaBar experiment is working very well

Never been replaced since the beginning
Only 3 sections out of 208 not readout
Physics performance as expected

As in any system, some small imperfections: small details in the design that with the present wisdom we would do in a different way

I think at this stage of development of silicon detectors, we should analyze more critically the performance of our systems, and to share experience for the benefit of future designs.

Overview of the SCT

- The SCT forms part of the ATLAS Inner Detector.
- It is constructed using 4088 silicon micro-strip modules
  arranged as 4 barrels in the central region and
  2 x 9 annular wheels in the forward region

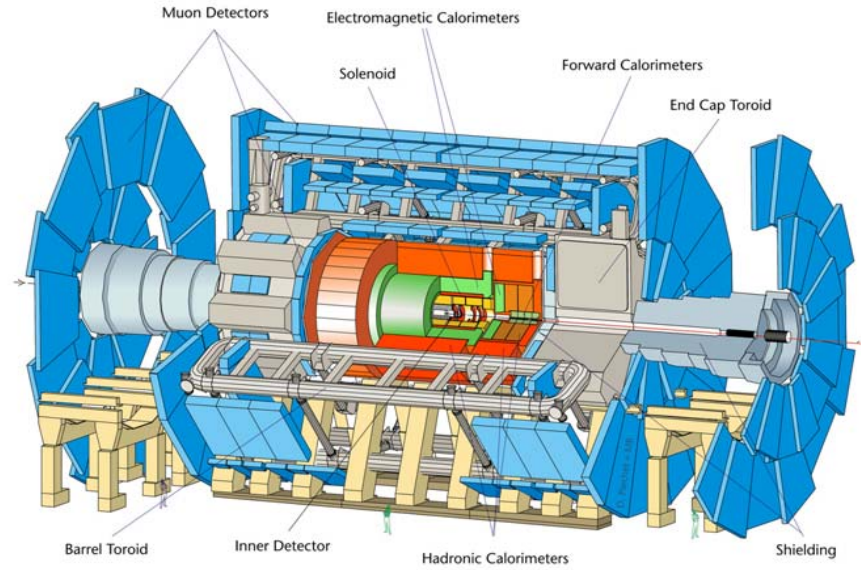

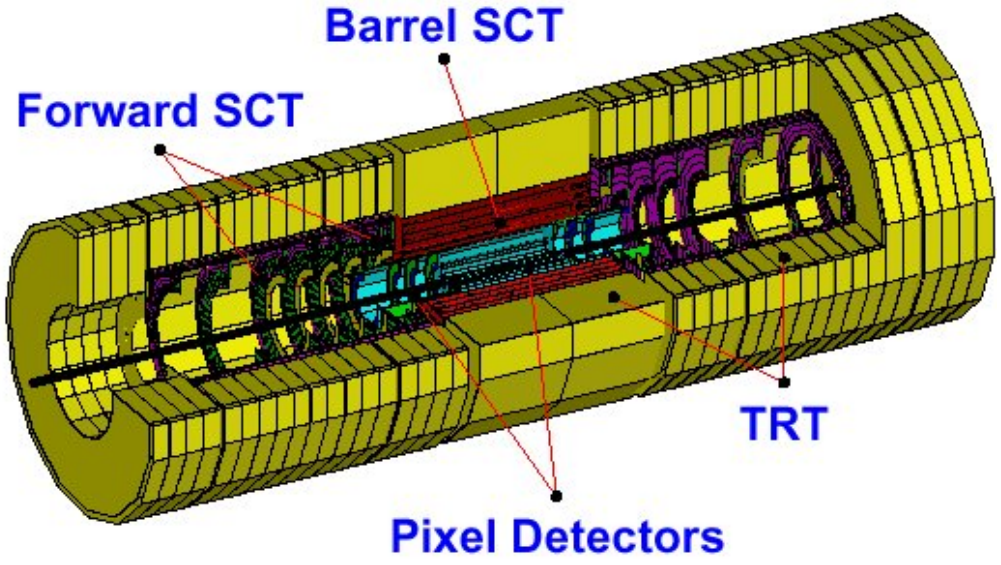

Inner Detector (ID)

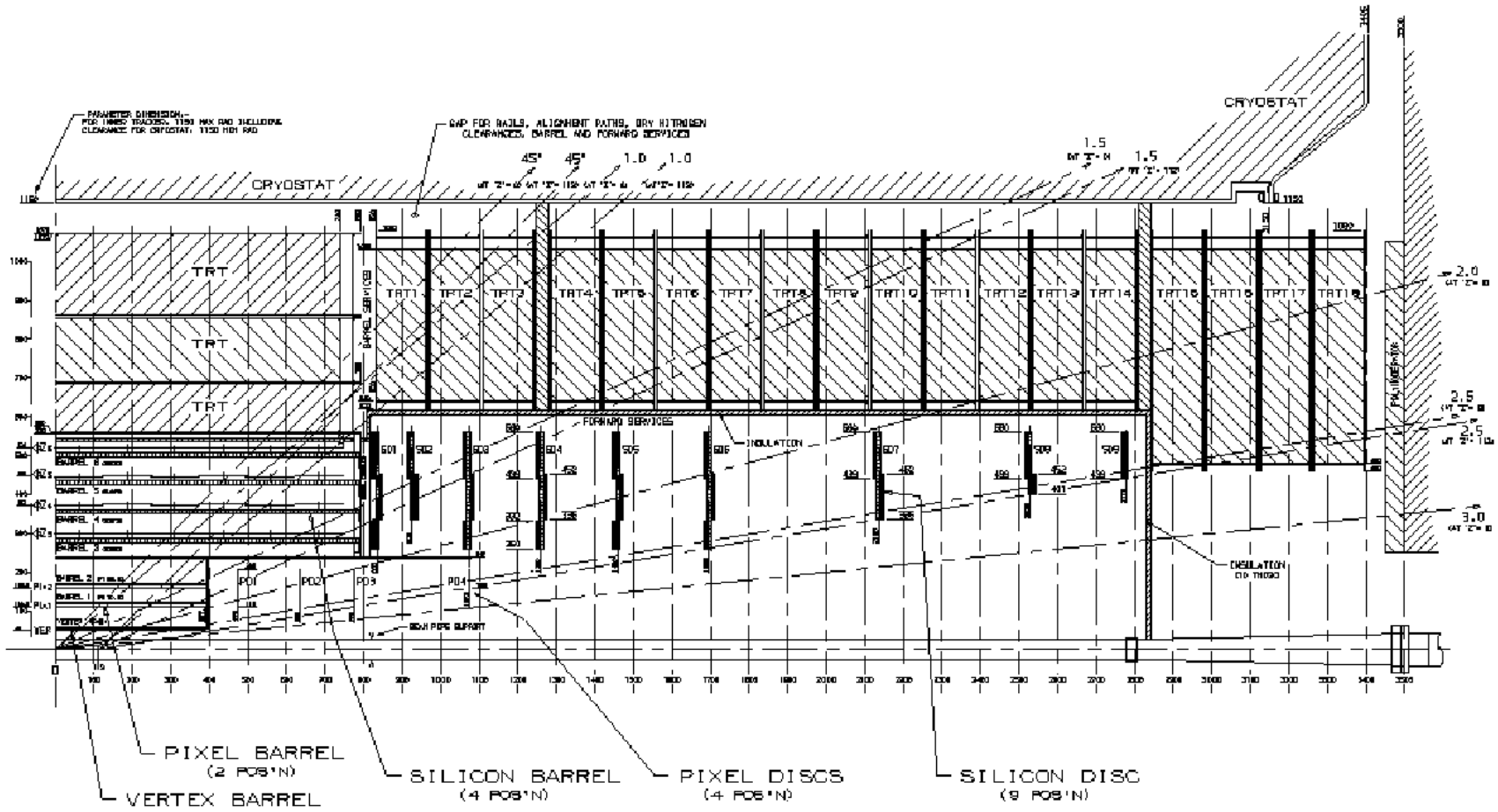

- The modules are arranged to provide 4 space points per track
  $-2.5 < \eta < 2.5$
- Each module measures two coordinates
  - Detector pitch is 80 μm and +-20 mrad stereo

Support structures

- All support structures, cylinders and discs, are produced using a sandwich material constructed with carbon fibre skins and a Korex core in industry
- Cu/Ni cooling pipes, precision mounts for modules, power tapes, opto-fibre harnesses + DCS and are added

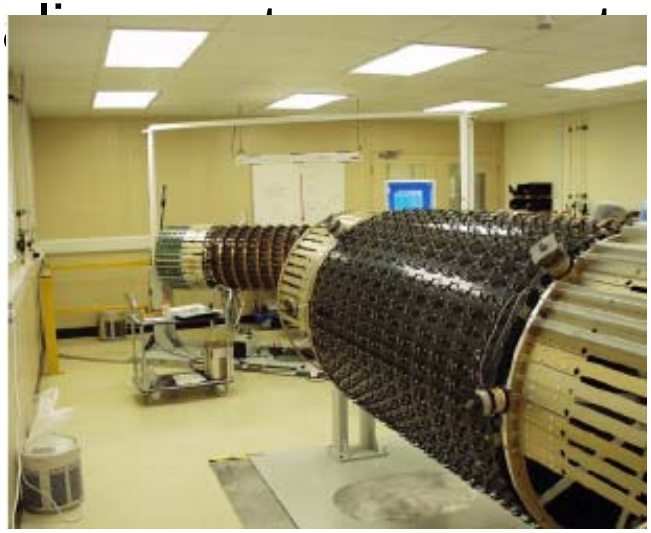

Lessons learned

- The progression from prototyping components to full production can introduce some problems and cause delays
  - e.g. Forward hybrid de-lamination problem
- Do not underestimate the time required to optimise techniques and commission equipment
  - e.g. Module assembly techniques
- Take care in defining specifications
  - Achieving the same quality in multiple sites is not straight forward
- Expect unexpected production problems and allow for the time required to solve them
  - Start with a proper contingency to allow for unexpected problems
  - Rigorous prototyping and QA will minimise unexpected problems

SUMMARY

- The ATLAS SCT is in full production
  - Module production is well advanced (13% forward and ~75% barrel completed)
  - Most of the support structures have been delivered
  - Population with services is underway
  - The macro-assembly of completed barrels and discs is beginning
- Several problems have been solved
  - No show stoppers
- The schedule for completion is very tight but the collaboration is making every effort to achieve it.

The AMS-02 Detector

TRD: e/p separation

TOF: ß and |Z|, sign(Z)

Star tracker: pointing

Magnet: 0.8 T, sign(Z)

Si tracker: p, |Z|, sign(Z)

ACC: anticoincidence system

RICH: ß and |Z|, sign(Z)

ECAL: e/p separation

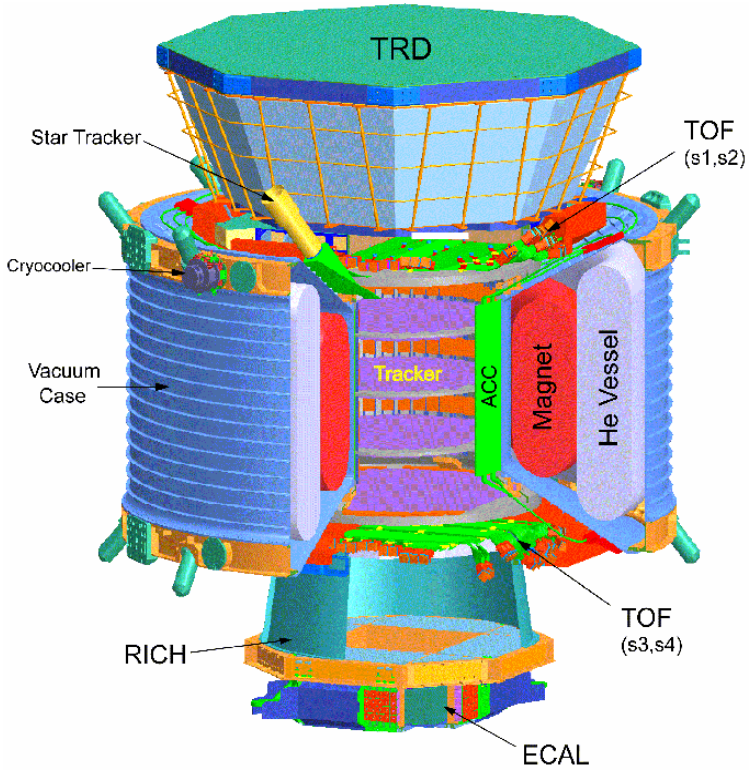

The AMS-02 Tracker

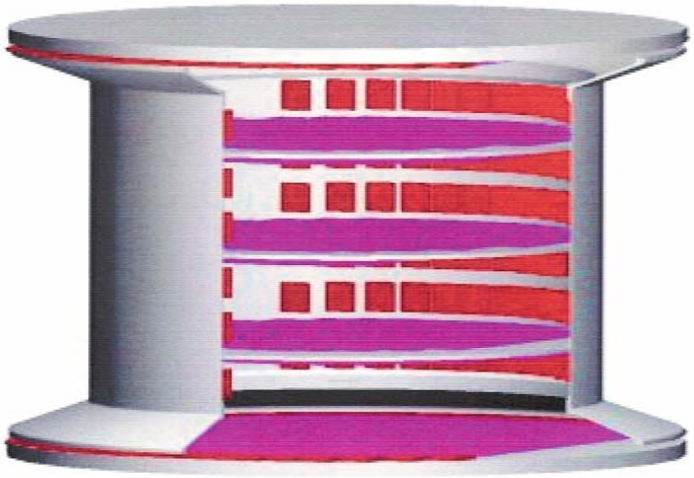

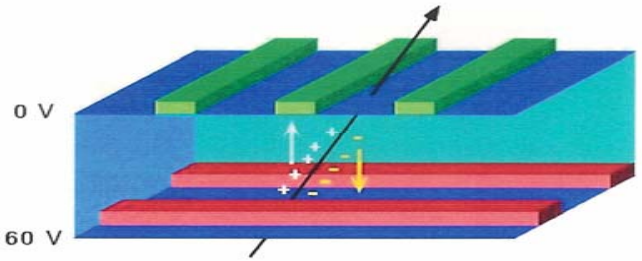

- Localization of charged particle by double sided silicon sensors
- Eight layers (L1 . . . L8) of $\sim 1\text{m}^2$ each on five ultra-light support planes (P1 . . . P5)
- Total of $\sim$2500 double-sided sensors
- Resolution $\sim 10\mu$m in bending direction, $\sim 20\mu$m in non-bending direction

- Measures rigidity p/Z up to a few tens of TeV
- Measures specific energy loss $dE/dx \sim |Z^2|$ for identification of elements
- Measures direction and energy of converted photons

Tracker Thermal Control System

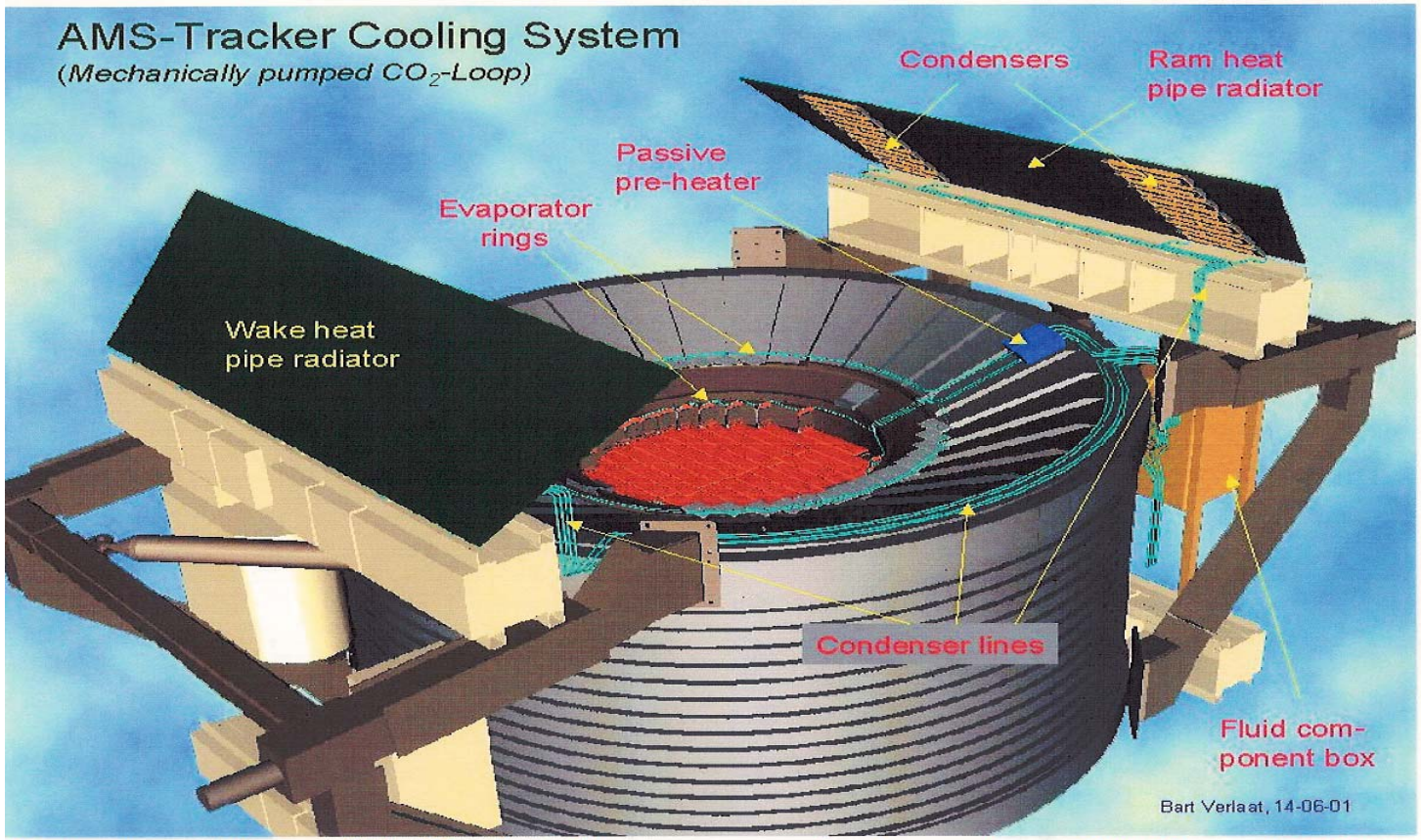

Collaboration with Dutch Aerospace Laboratory NLR and ZSU.

Tracker Performance:
1) spatial resolution

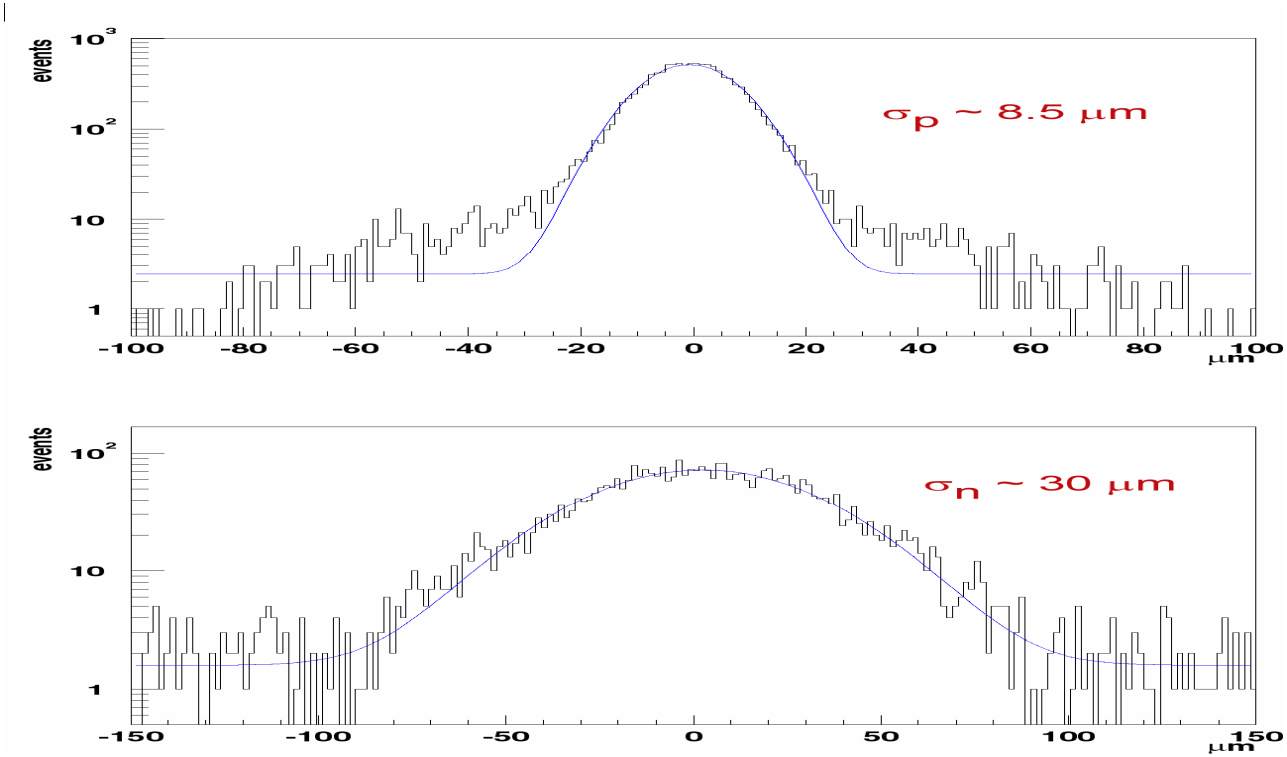

Conclusions

- No major problems encounted with the silicon tracker during AMS-01:

  Electrically and mechanicaly the tracker was unaffected by launch, landing and in orbit operations.

- For AMS-02, the number of independant measurement points and the issue of temperature control needed to be reconsidered.

- The tracker performance on the n-side of the silicon sensors had to be improved.

- In 2005, the new tracker for AMS-02 will be ready for system tests.

Basic Technology: Standard CMOS

CMOS Camera

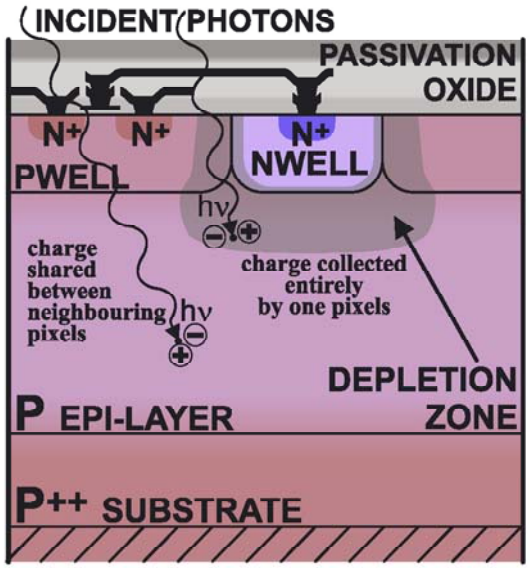

Because of large Capacitance, need Thick DSSDs
-- APS can be VERY Thin

Particle Detector

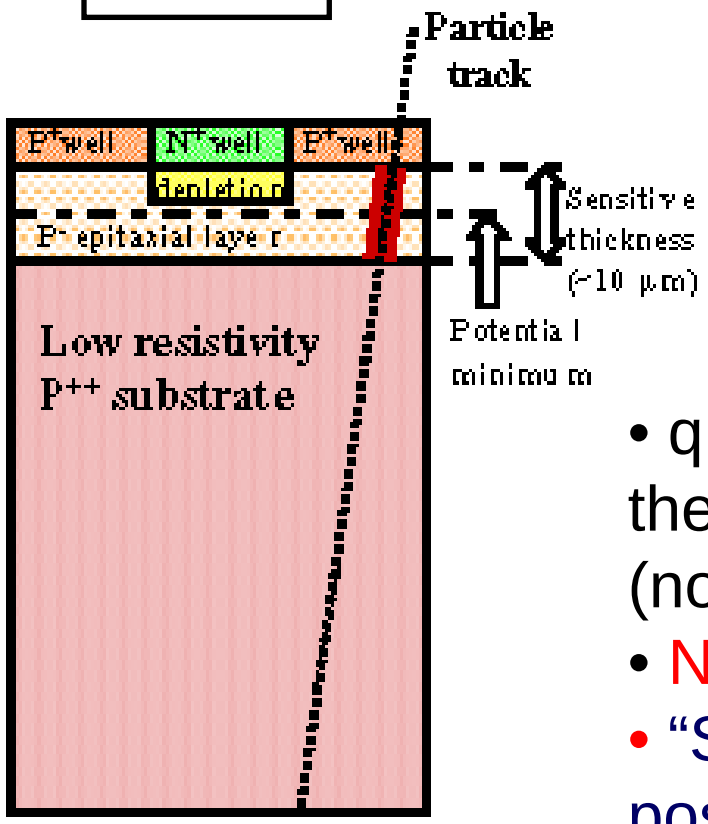

Standard CMOS:

- Low Power
- Excellent Transistors
- Tight Process Control
- Excellent Uniformity
- High volume, low cost
- Large ADC, DSP base

Key Features:

- q collection via thermal diffusion (no HV)
- NO bump bonding
- "System on Chip" possible

Development Efforts

L=10^{34}

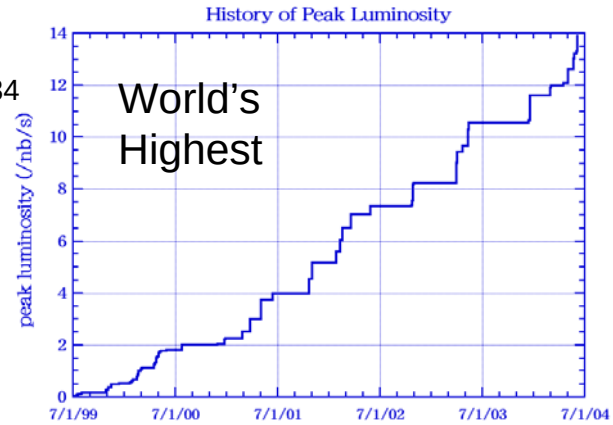

Belle Detector

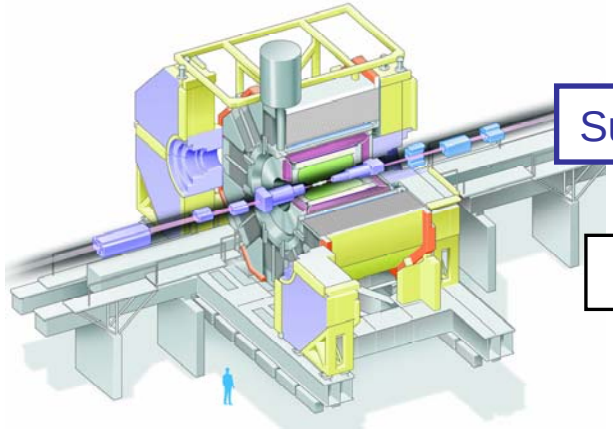

Super-Belle: <=10μs

See T. Tsuboyama's talk

LEPSI,
RAL,
Strassbourg

Linear
Collider

DESY/Hamburg

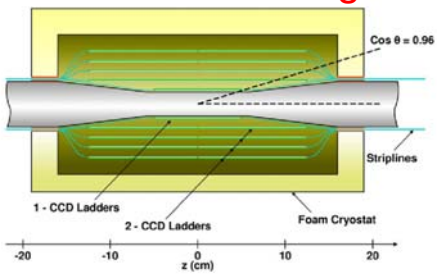

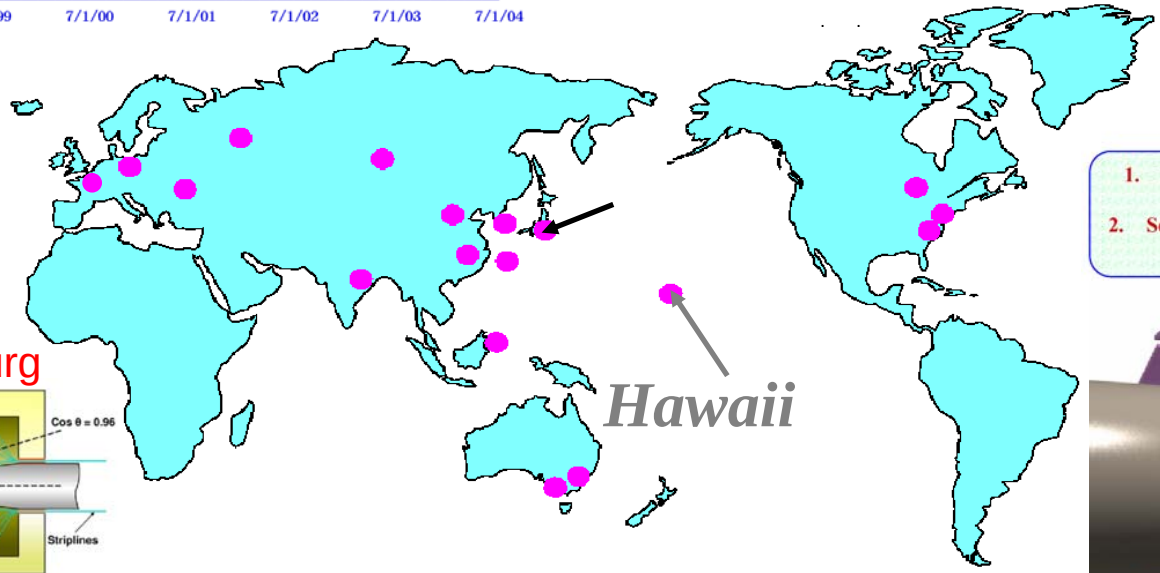

LBNL,
UC Irvine

STAR μvertex detector

1. First upgrade (x4 present luminosity, 2006): 10 – 20 ms readout (integration) time
2. Second upgrade (x40 present luminosity, 2008): 2 – 5 ms readout (integration) time

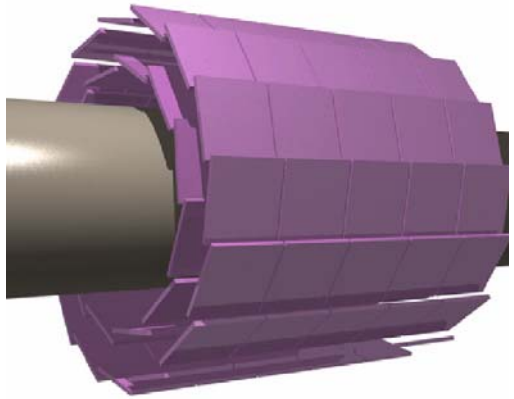

Apologies to those not mentioned:
Easy access will bring others

Operating principles

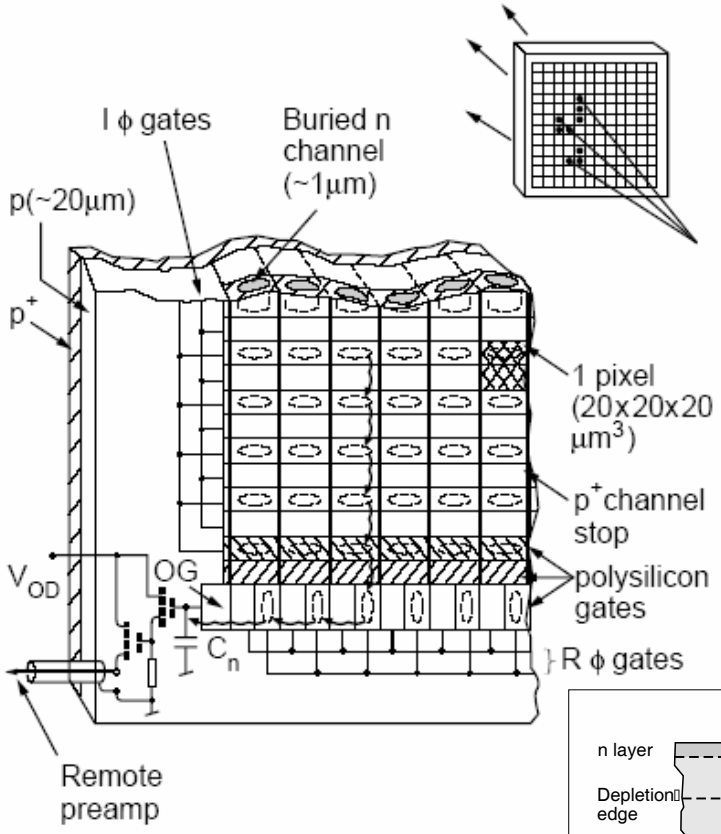

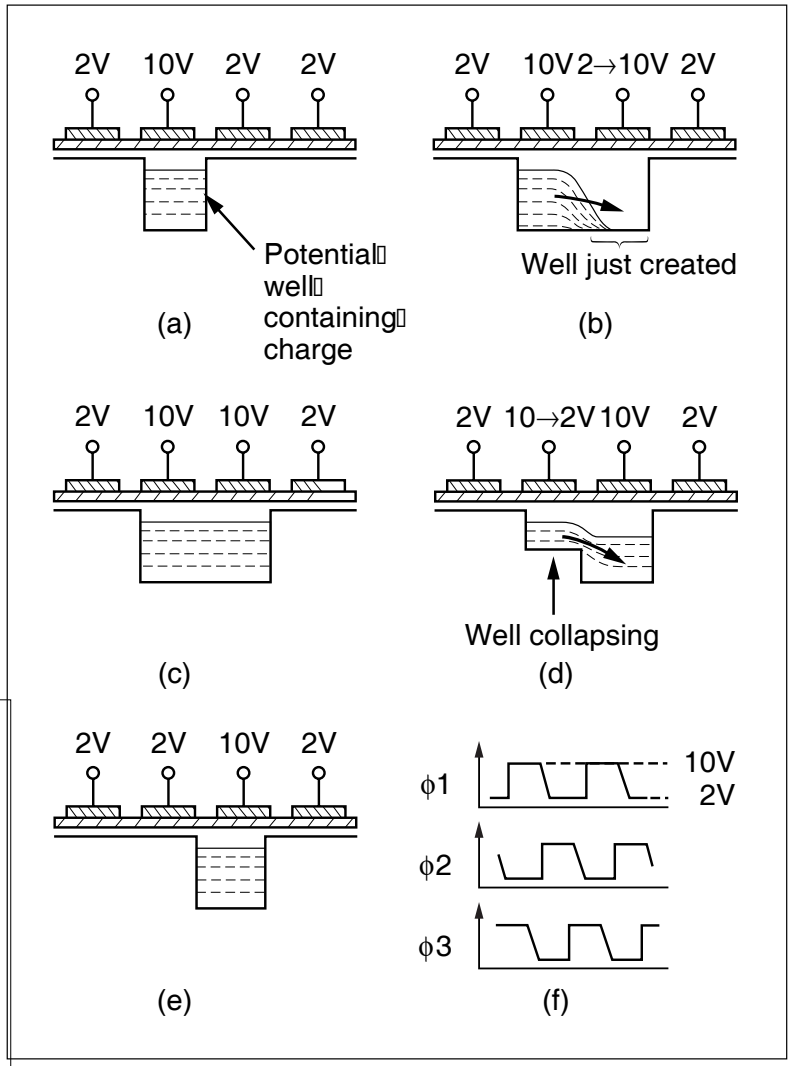

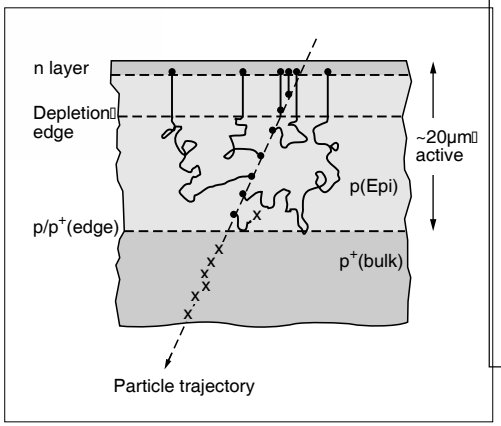

Need good CTI: 10^{-4} produces 25% signal loss after 5 cm charge transport

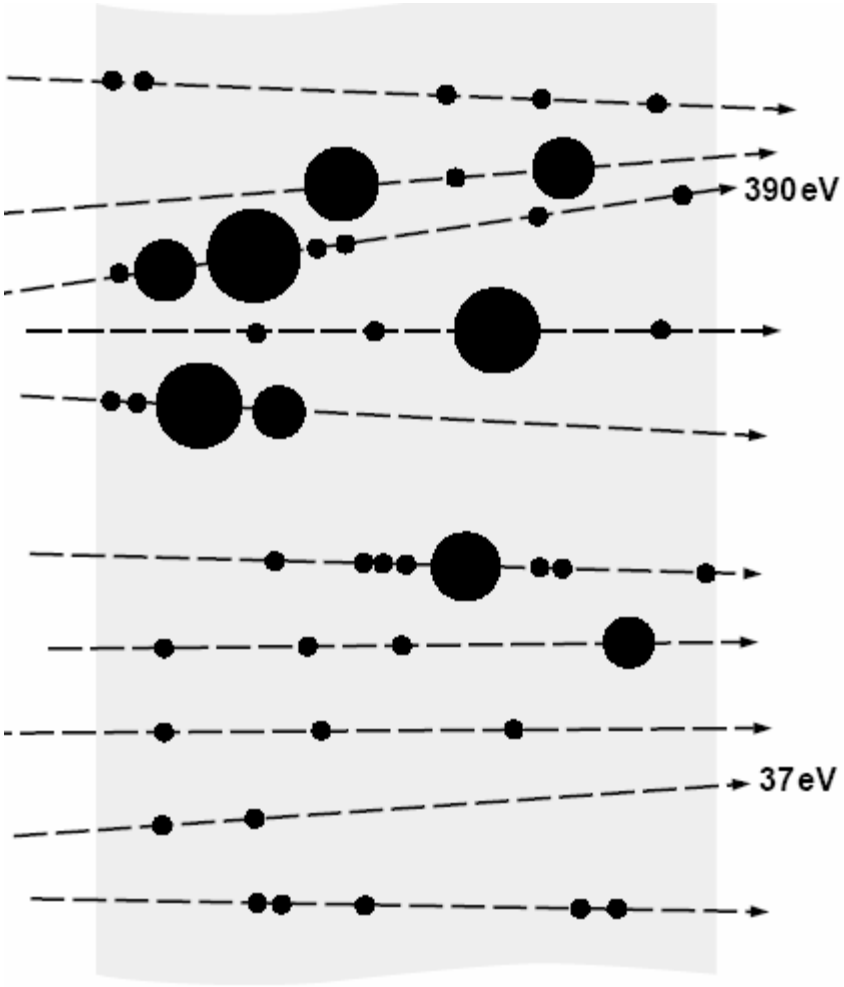

3.2 M-shell plasmons per μm (17 eV)

0.6 L-shell plasmons per μm (120 eV)

0.01 K-shell plasmons per μm (1.5 keV)

~4 primary collisions/μm with wildly fluctuationg energy loss

Final thermalisation yields one e-h pair per 3.6 eV deposited

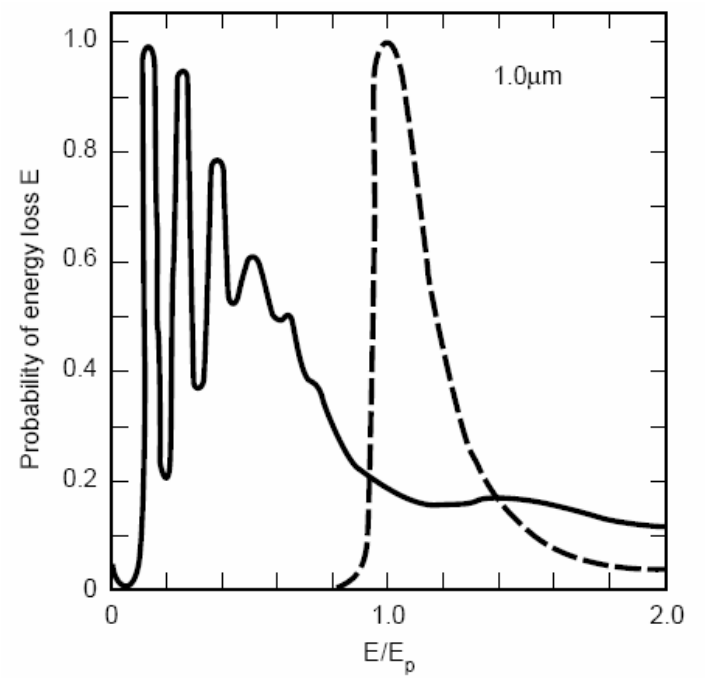
1.0µm
Probability of energy loss E
E/E$_p$
0
0.2
0.4
0.6
0.8
1.0
2.0

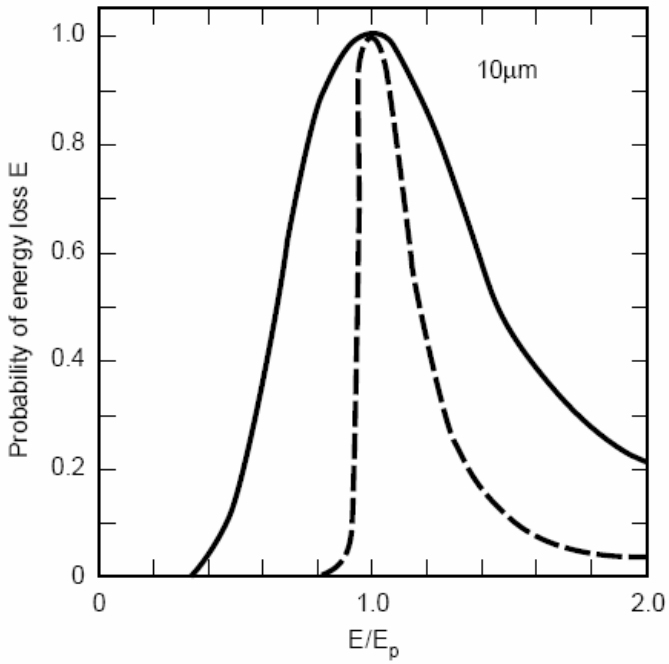
10µm
Probability of energy loss E
E/E$_p$
0
0.2
0.4
0.6
0.8
1.0
2.0

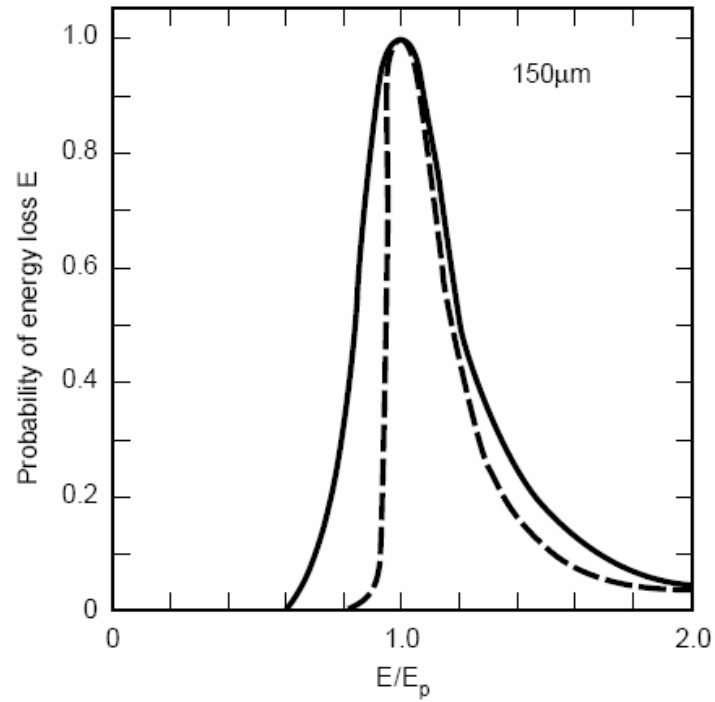
150µm
Probability of energy loss E
E/E$_p$
0
0.2
0.4
0.6
0.8
1.0
2.0

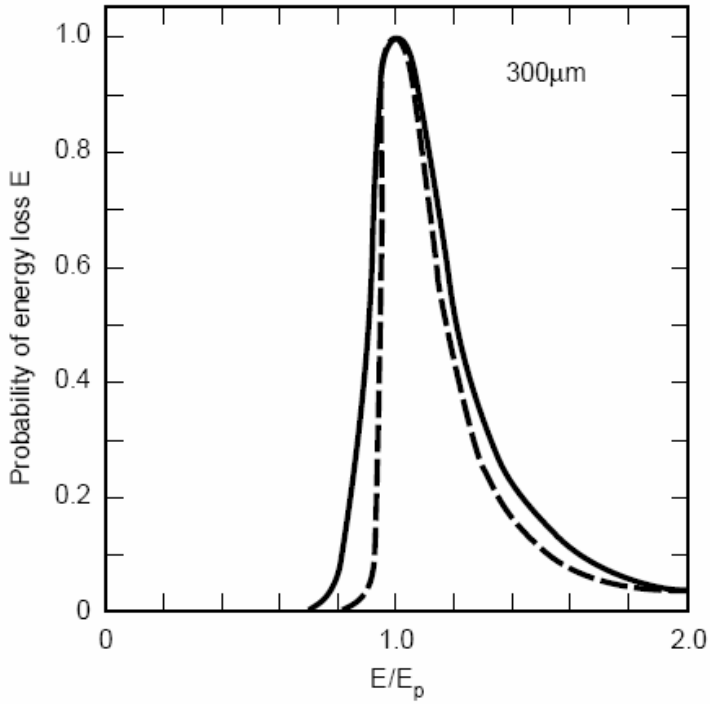
300µm
Probability of energy loss E
E/E$_p$
0
0.2
0.4
0.6
0.8
1.0
2.0

Conclusions

- CCDs have since 20 years been the *only* pixel devices used as sensors in vertex detectors for heavy flavour physics

- This is of course about to change, with ATLAS, CMS, ALICE, BTEV, STAR, …

- The CCD architecture appears to be well matched to the TeV-scale linear collider. The discovery potential of this machine will be orthogonal to the LHC due partly to
  - Ultra-thin and precise gigapixel vertex detector
  - multi-Megavoxel calorimeter allowing sophisticated energy flow

Status of radiation-hard materials for tracking detectors at SLHC

Property	Si	Diamond	Diamond	4H SiC
Material Quality	Cz, FZ, epi	Polycrystalline	single crystal	epitaxial
E_g [eV]	1.12	5.5	5.5	3.3
$E_{breakdown}$ [V/cm]	$3 \cdot 10^5$	10^7	10^7	$2.2 \cdot 10^6$
μ_e [cm^2/Vs]	1450	1800	>1800	800
μ_h [cm^2/Vs]	450	1200	>1200	115
v_{sat} [cm/s]	$0.8 \cdot 10^7$	$2.2 \cdot 10^7$	$2.2 \cdot 10^7$	$2 \cdot 10^7$
Z	14	6	6	14/6
ε_r	11.9	5.7	5.7	9.7
e-h energy [eV]	3.6	13	13	7.6
Density [g/cm3]	2.33	3.515	3.515	3.22
Displacem. [eV]	13-20	43	43	25
e-h/μm for mips	89	36	36	55
Max initial ccd [μm]	>500	280	550	40 (= thickness)
Max wafer ϕ tested	6”	6”	6mm	2”
Producer	Several	Element-Six	Element-Six	Cree-Alenia, IKZ
Max f luence[cm^{-2}]	7×10^{15} 24GeV p	2×10^{15} n, π, p	Not reported	10^{16} in progress
CERN R&Ds	RD50, RD39	RD42	RD42	RD50

See H. Kagan Talk

See Kinoshita Talk

Radiation Induced Microscopic Damage in Silicon

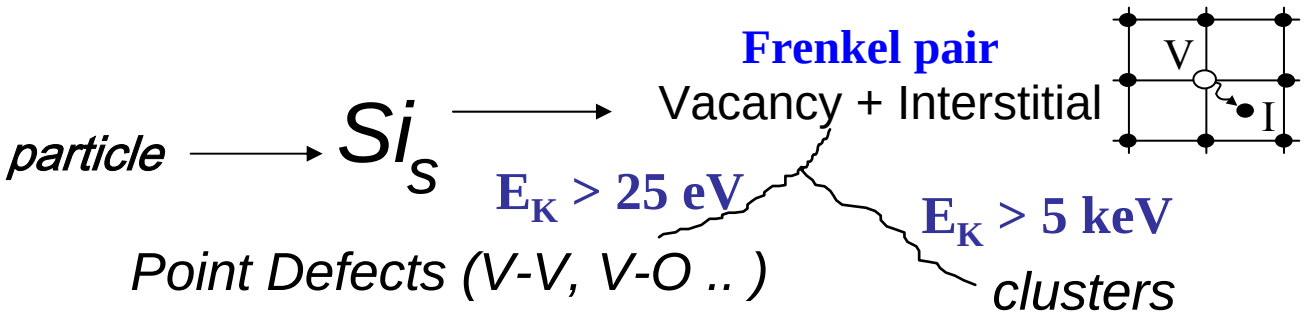

Influence of defects on the material and device properties

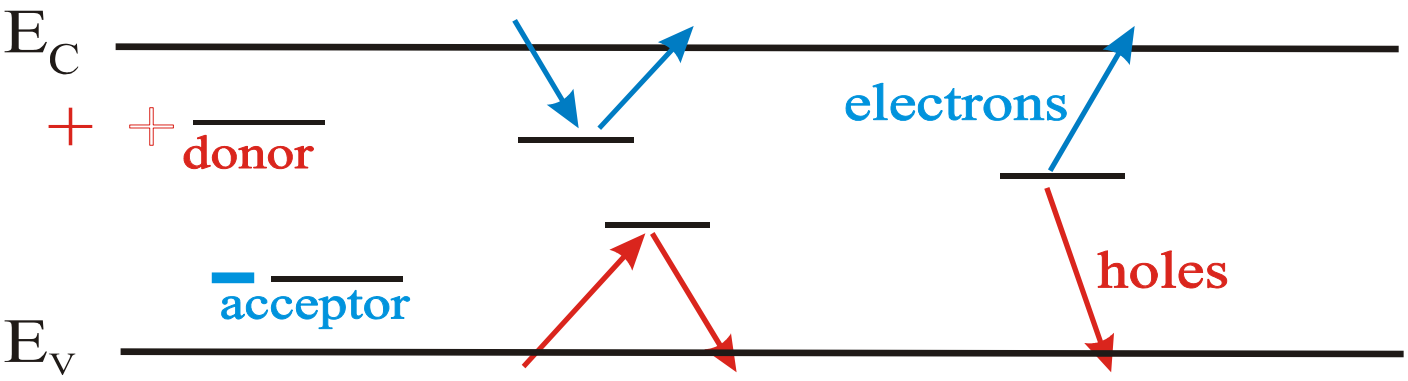

charged defects
⇒ **N_{eff} , V_{dep}**
e.g. donors in upper and acceptors in lower half of band gap

Trapping (e and h)
⇒ **CCE**
shallow defects do not contribute at room temperature due to fast detrapping

generation
⇒ **leakage current**
Levels close to midgap most effective

Leakage Current

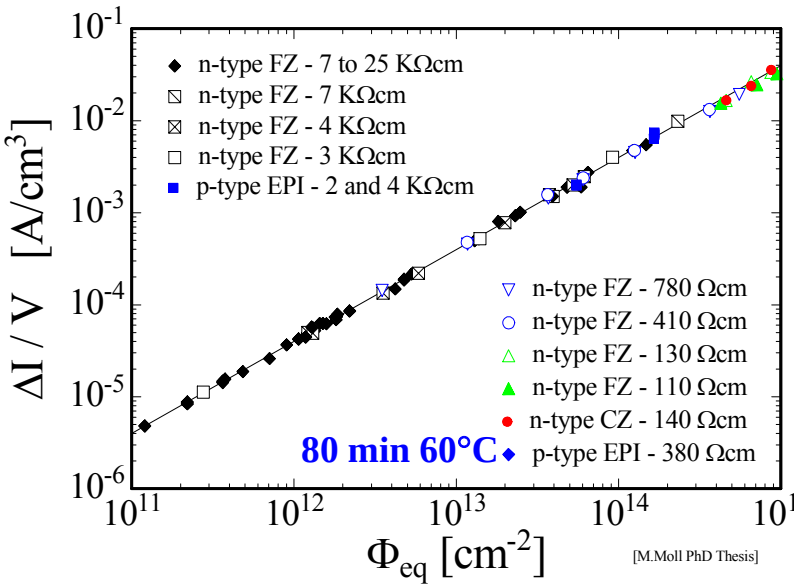

V_{dep}, N_{eff}

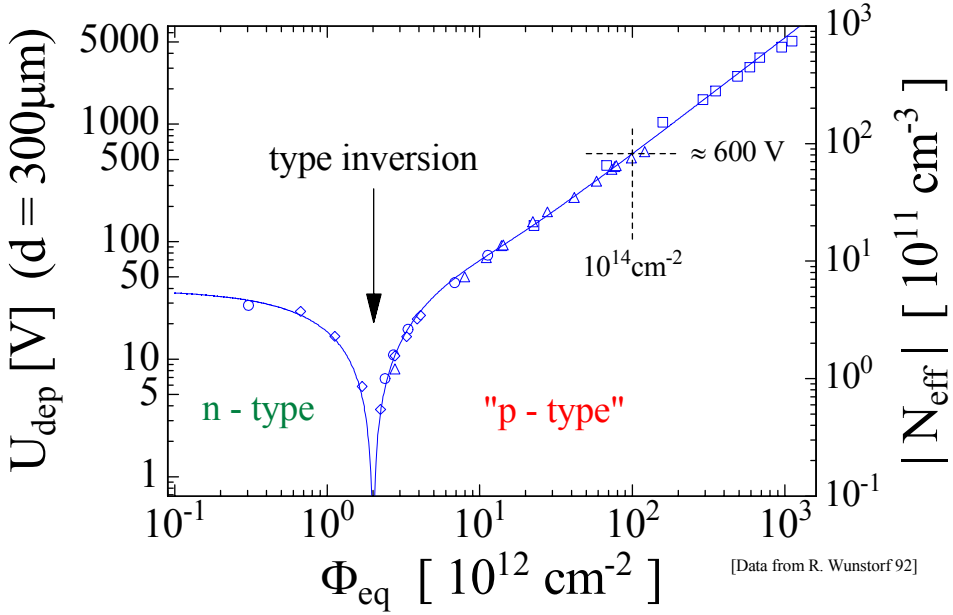

- **Damage parameter α (slope)**

$$\alpha = \frac{\Delta I}{V \cdot \Phi_{eq}}$$

- **α independent of Φ_{eq} and material kind**

M. Moll, Thesis

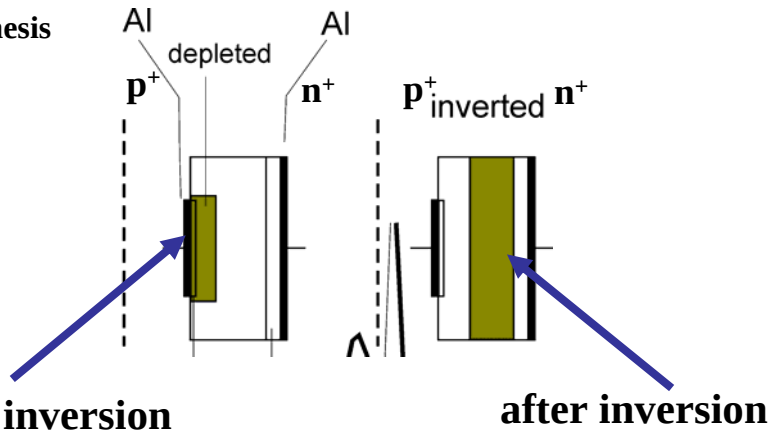

Cz-Si as Detector Material

- High resistivity Cz-Si previously not available because lack of commercial applications

- Available in large diameters (up to 300mm) and in large quantities if necessary

- Oxygen content can be adjusted by crystal pulling speed within the range from few ppma above the O solid solubility in Si

- Homogenous impurity distribution in crystal can be achieved if a magnetic field is applied during the growth

- N and P-type high resistivity Cz-Si available

Thermal Donor generation (experimental results)

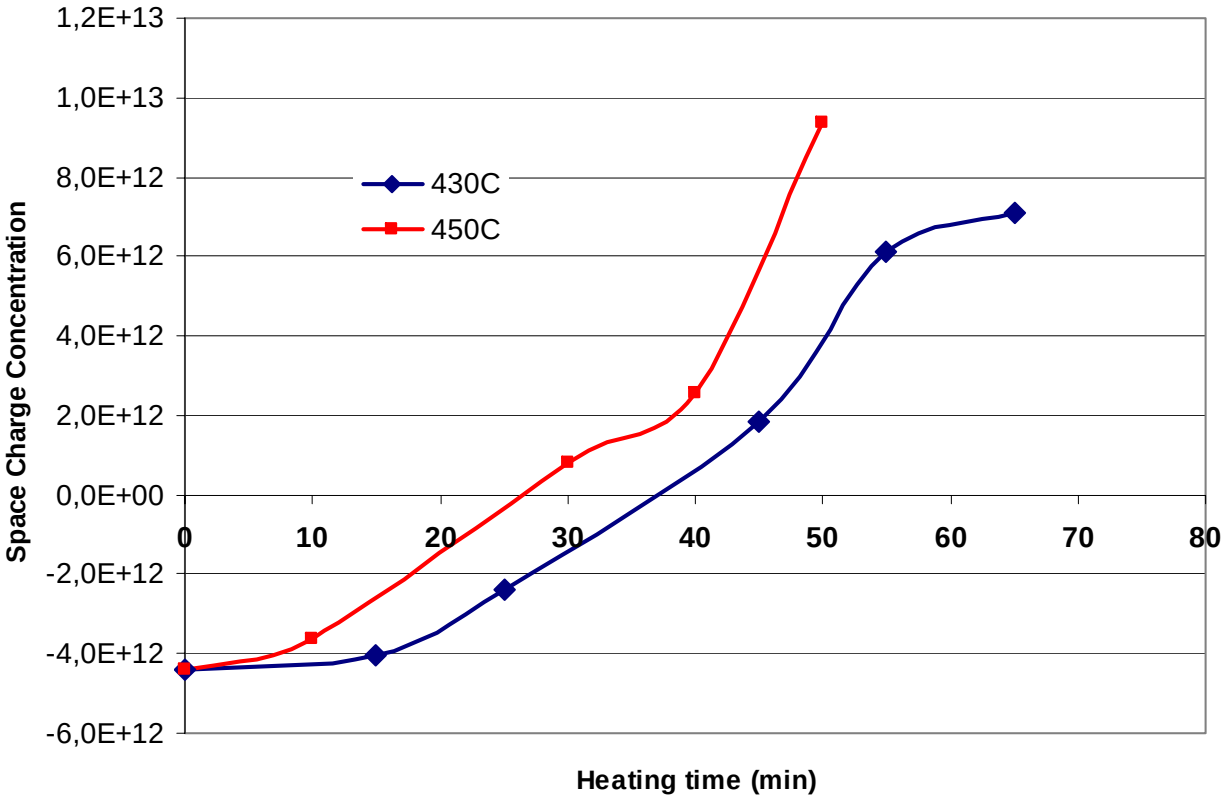

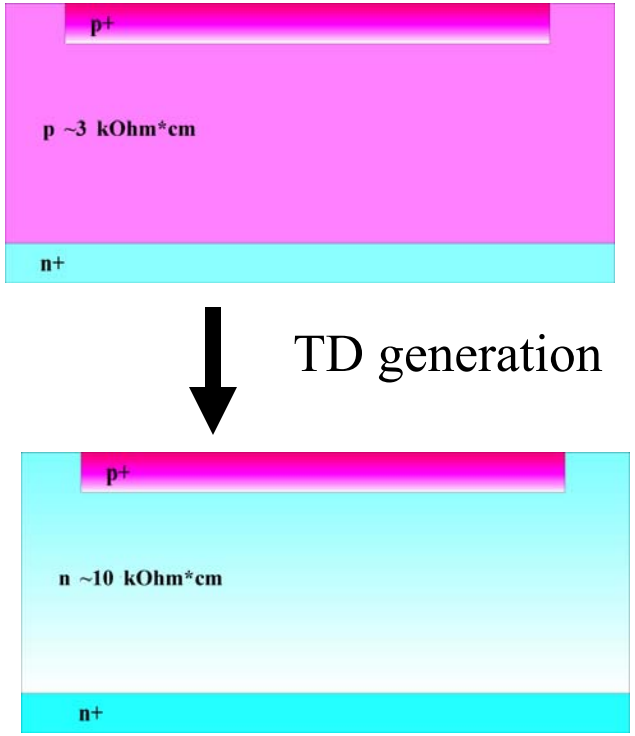

Thermal Donor generation

$$N_{TD} = \left(\frac{a}{b}\right) C_{io}^{\chi} \frac{1}{\left|N_d - N_A\right|^2} \left\{1 - e^{-bD_i C_{io} t}\right\}$$

$$D_i = 0{,}13\, e^{-\frac{E_A}{kT}}$$

$$2{,}4 \leq \chi \leq 2{,}6$$

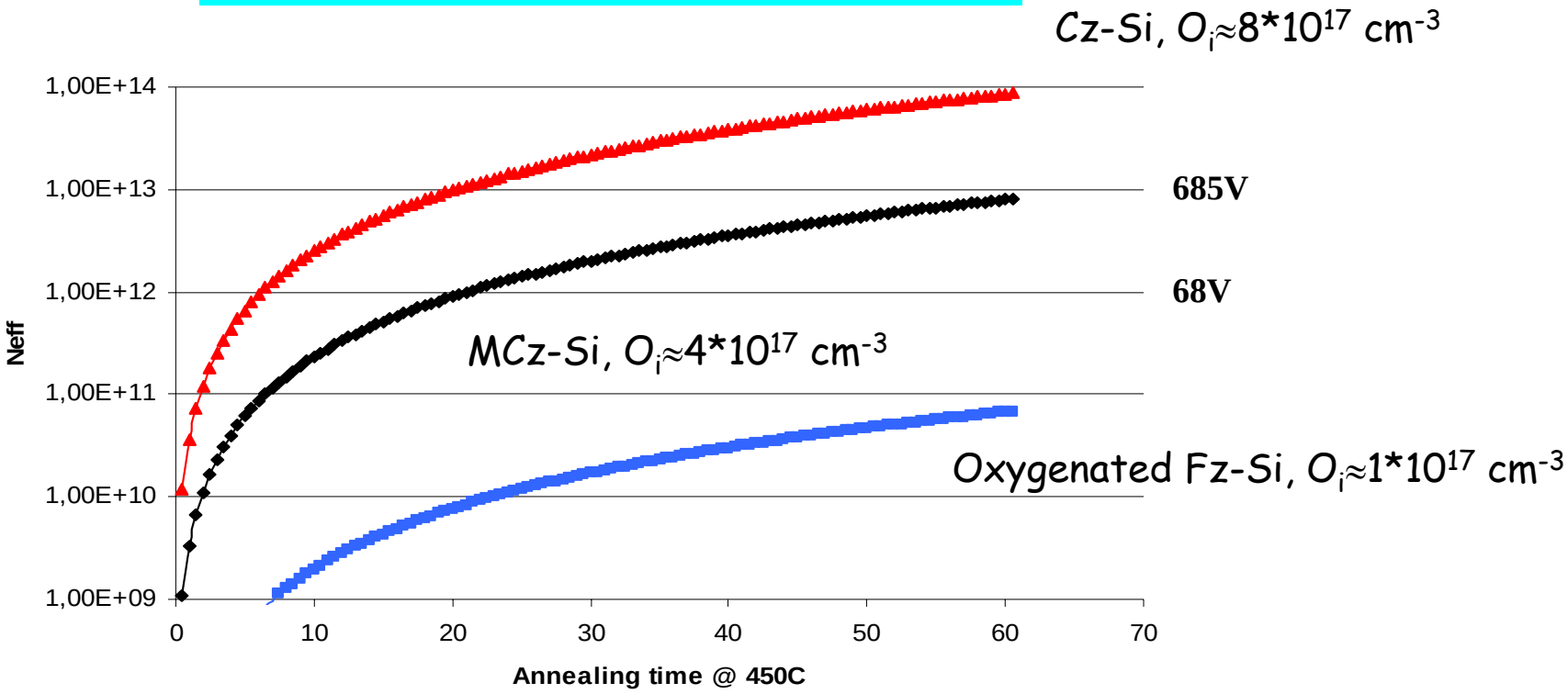

Conclusions

- We have demonstrated first full-sized particle detectors ever made of Cz-Si
- Cz-Si shows very promimsing radiation hardness properties in proton beams
- High O content $p^+/n^-/n^+$ detectors can be processed with p-type boron doped Cz-Si wafers by inverting p $\rightarrow$ n with TD's
- It is low temperature, low cost process >> feasible solution for large scale experiments
- Resistivity range is very wide in p $\rightarrow$ n TD-process 500Ωcm < σ < ~10 kΩcm
- O content should be within some limits (3ppma < O_i < 6ppma). Magnetic field may be required in crystal growth.

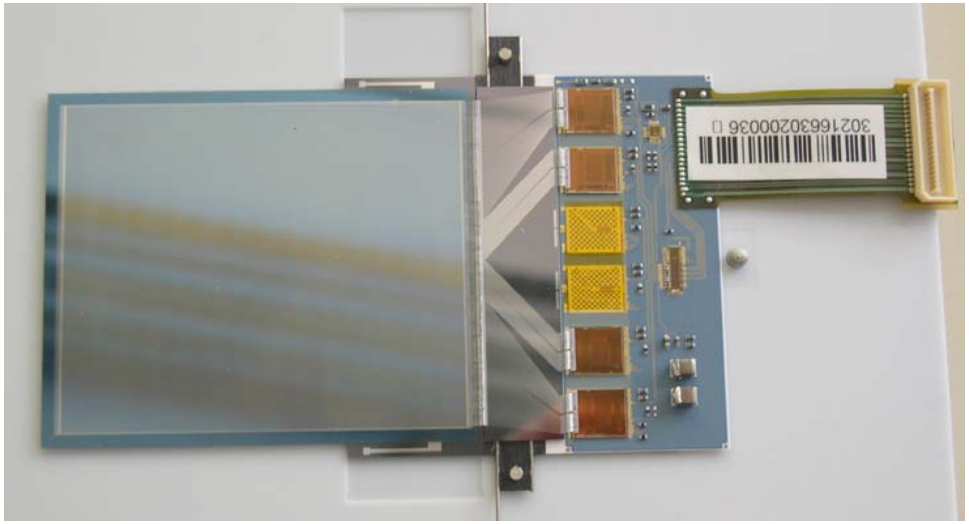

SiC Properties

Silicon carbide (SiC) is expected to be applied to high-power and high-frequency devices.

- Bandgap
  - × 2~3
- Break-down field
  - × one order
- Saturation velocity of electron
  - × 2
- Thermal conductivity
  - × 3
- High operation temperature
  - 500-600℃(Si:150℃)
- Radiation tolerance
  - × 1~2 order （MOSFET, γ rav）

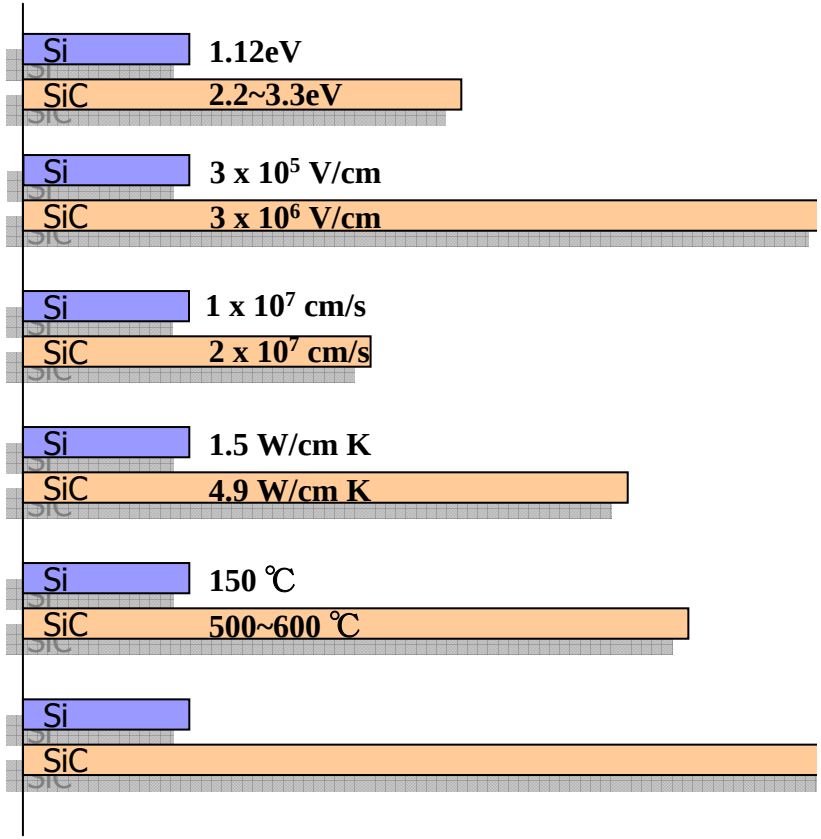

Summary

- We have evaluated electrical characteristics and detector performance for alpha particle before and after irradiations (γ, β).
  - I-V characteristics
    - Forward — η is no significant difference
    - Reverse — Leakage current increase
  - C-V characteristics
    - N_{eff} — Neff decrease
  - CCE
    - CCE-V — η is changed so as to Neff
    - Life time — τ is no significant difference
  - The results of measurement for irradiated Si indicate that SiC has the possibility of radiation hardness as compared with Si.

The SCT Module

- Built with 2 pairs of identical single-sided silicon sensors
  - 768 AC-coupled p-strips on n-type silicon
  - 80 μm strips pitch
  - Glued back to back
    - with 40 mrad stereo angle
    - on a mechanical core of Thermal Pyrolitic Graphite (TPG)
- Each pair of sensors wire bonded to form long strips of 126 mm

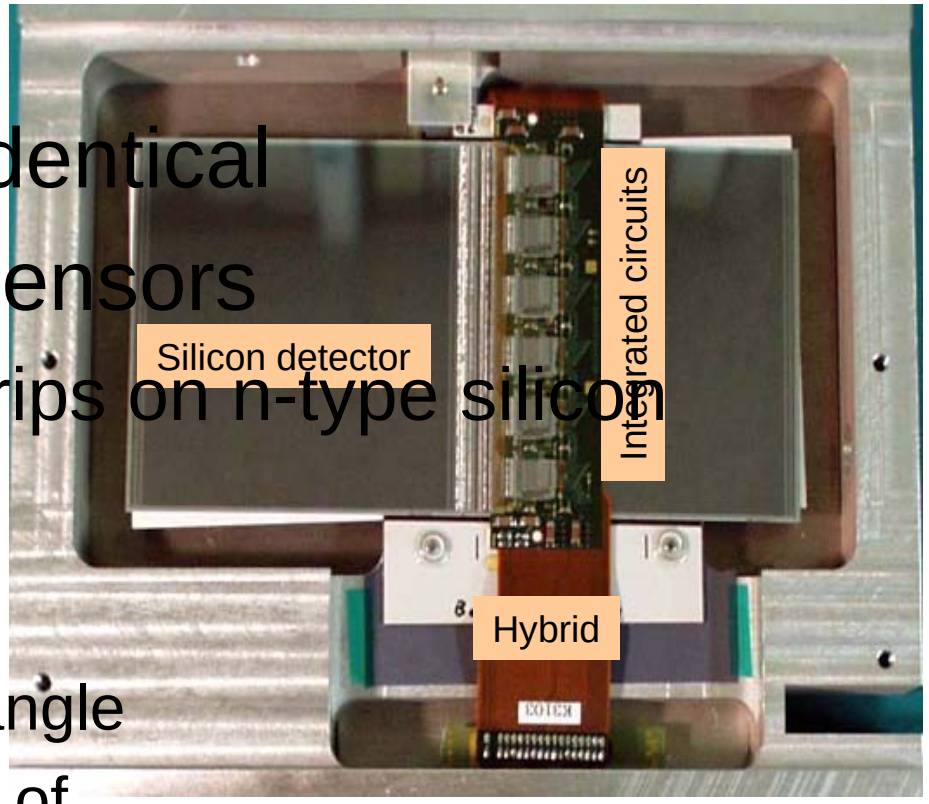

The ATLAS SCT Readout Electronics

- Handled by ASICS realized in the radiation hard DMILL technology (ABCD3T)
- Custom IC designed by the ATLAS-SCT design team (W. Dabrowski et al.)
- 128-channel analog front-end consisting of amplifiers and comparators
- Digital readout circuit (pipeline)
- Operating at the LHC bunch crossing frequency (40 MHz)
- Utilizes the “binary” scheme
  - Signals from the silicon detector are amplified and then compared to a threshold
  - Only the result of this comparison (hit or no-hit logic)

The Wafer production testing and IC grading

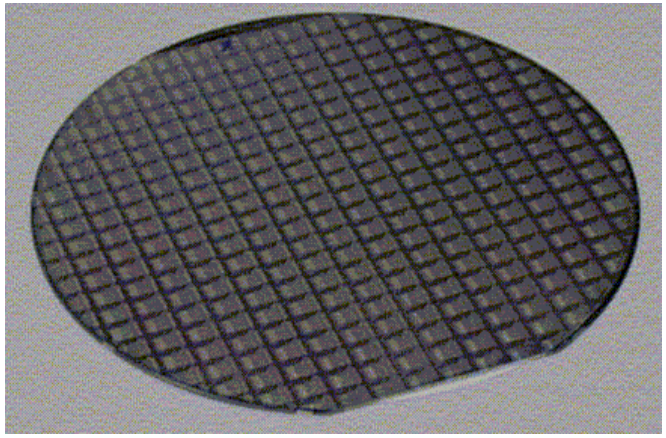

- 6 inch wafer (fabricated by AT France)
- 256 IC’s
- Wafer testing shared between SCIPP
- Design and implementation of a sophisticated tester
  - verify the analog front-end performance (gain & noise)
  - digital functions (control register, addressing, communication, pipeline, and output buffer)
  - the power consumption

SCT Hybrid Testing

- An extensive suite of both hardware and software has been developed to facilitate hybrid and module testing.
- The readout system is based on custom designed VME boards including Low Voltage and High Voltage boards developed specifically for SCT production testing.
- Two automated series of tests have been designed to simplify the testing procedure:
  - ***Characterization Sequence*** aimed to perform a full characterization of a hybrid or a module for both digital and analog performance

Conclusion

- By developing diagnostic tools during SCT module production we were able to reduce the rate of ASIC replacements on hybrids with defective ASICs and increase the number of working modules.

- The studies have demonstrated the importance of the capability to adjust the FE parameters and the importance of

the bench beam tests

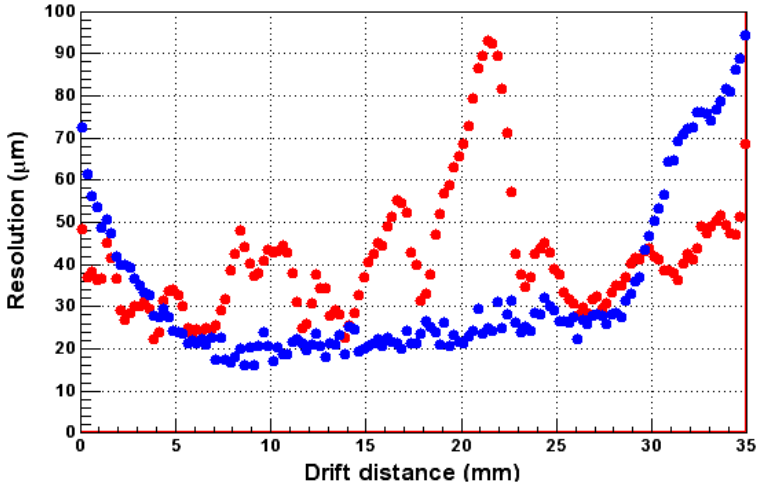

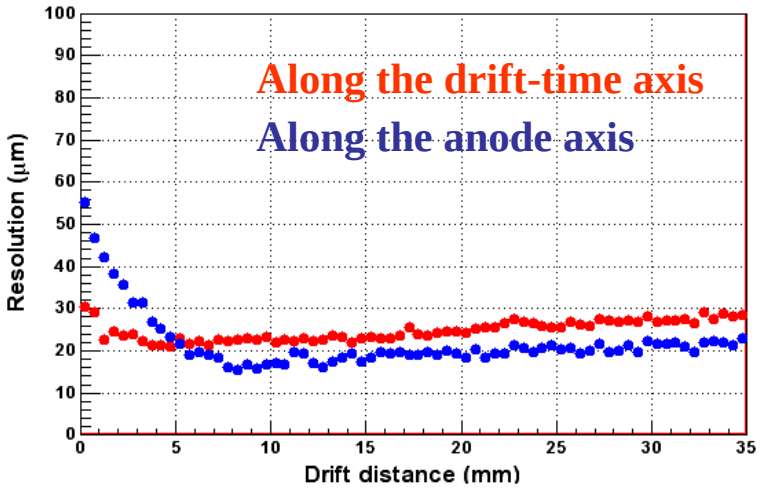

the bench beam tests

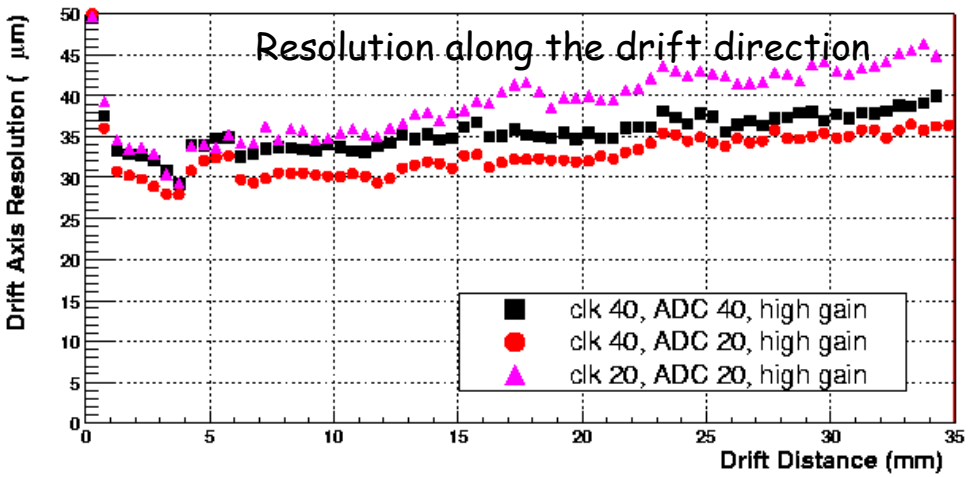

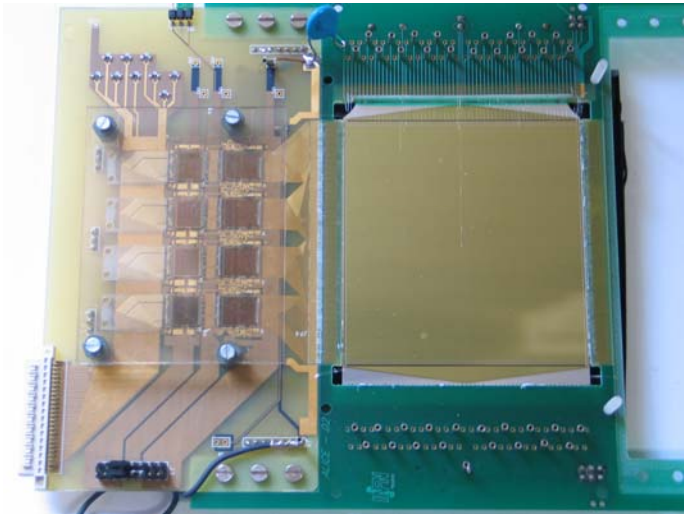

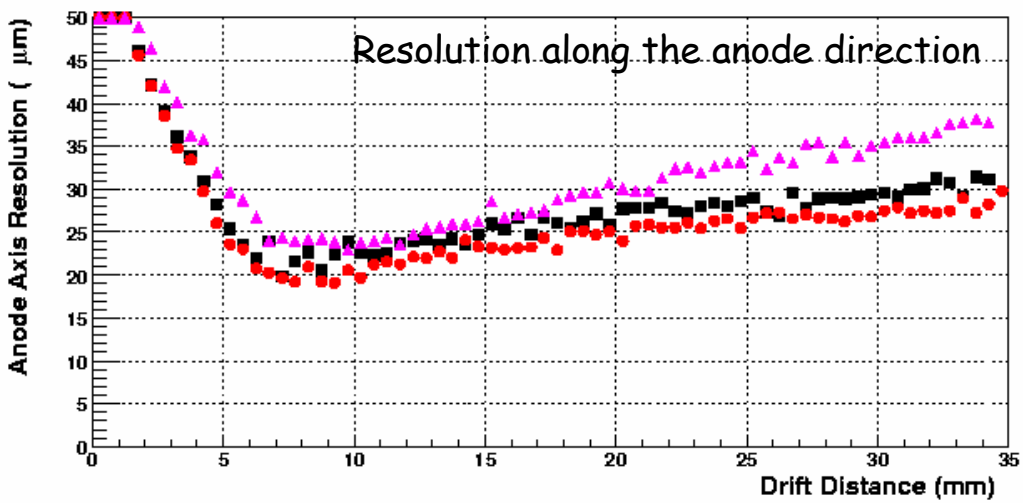

BUMP BONDING + CMOS PROCESSOR

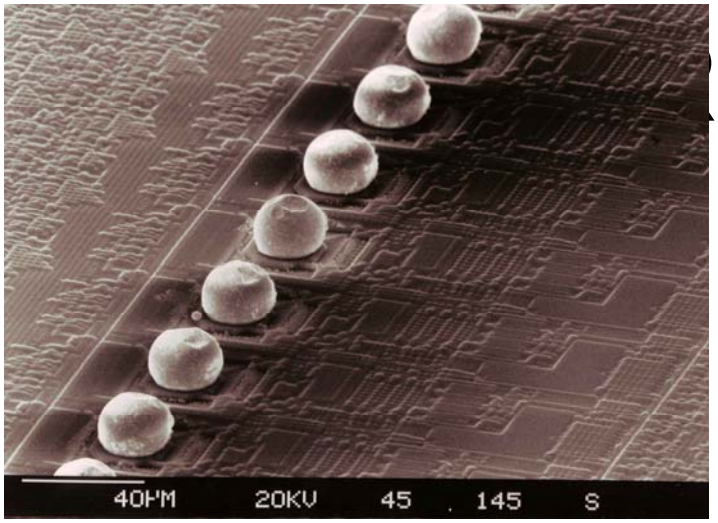

SPECIAL FEATURES

GLOBAL ADJUSTMENT for COMPARATOR
TESTING / MASKING of EACH PIXEL
DELAY 6 ns rms DIGITAL TUNING in EACH PIXEL
DARK CURRENT COMPENSATION / COLUMN

LHC1 CHIP CERN 1996
16 COLUMNS x 256 ROWS
pixel 50μm x 500 μm

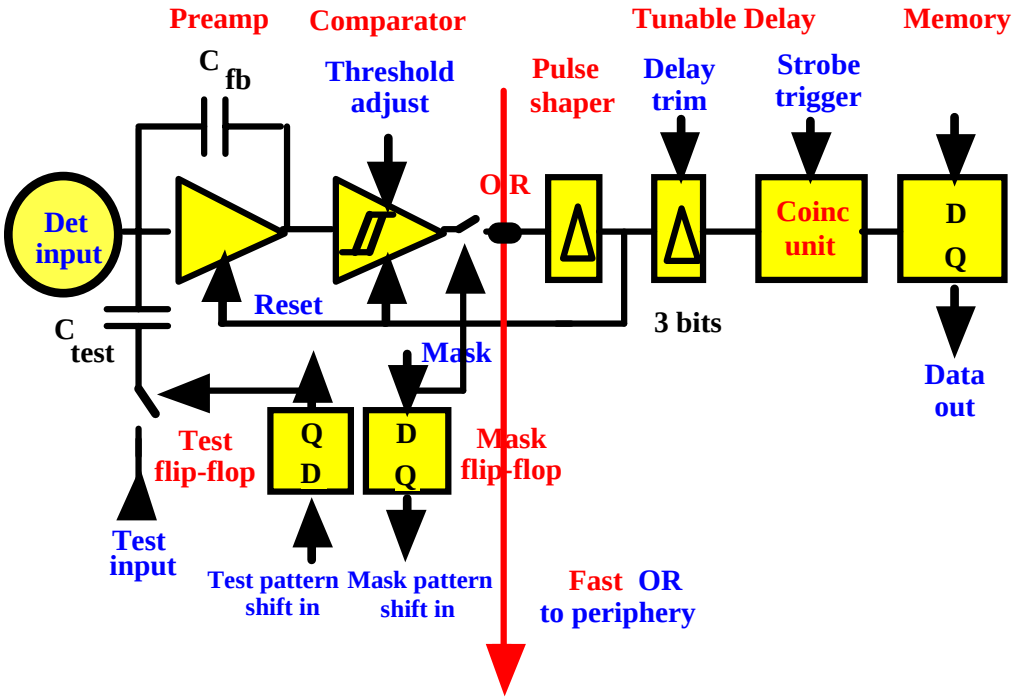

PRESENTED in HIROSHIMA 1996

SYSTEM INTEGRATION

- CAN BE USED for IMAGING

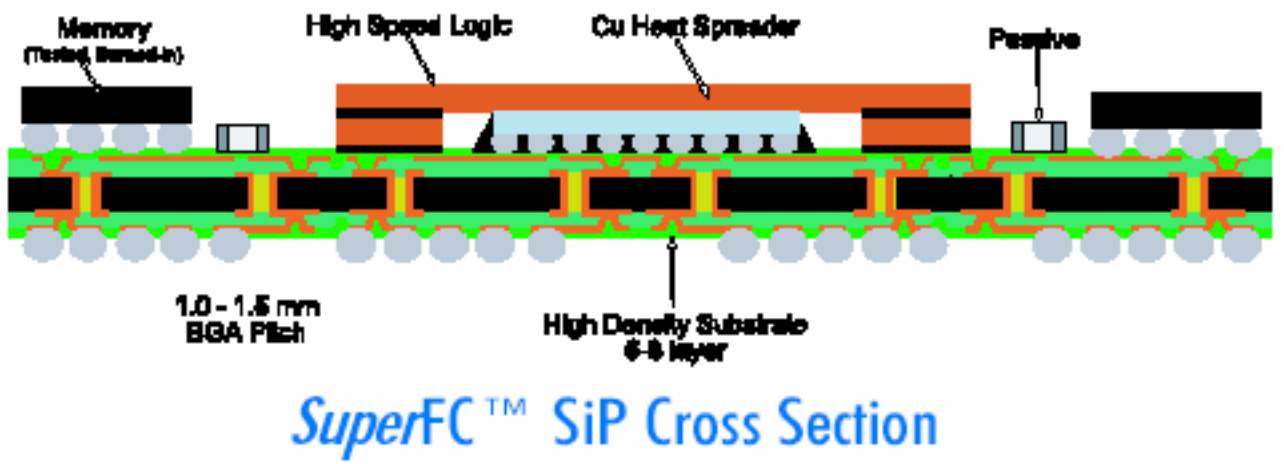

3D ELECTRONICS : IMEC

- **THINNING of WAFERS**
- **INSERTION of Epoxy or Silicon Interposer LAYERS**
- **3D connectivity (8 chips shown)**
- **already in production (e.g. Bluetooth)**
- **typical cost: ~ 10 $ per package in volume production**

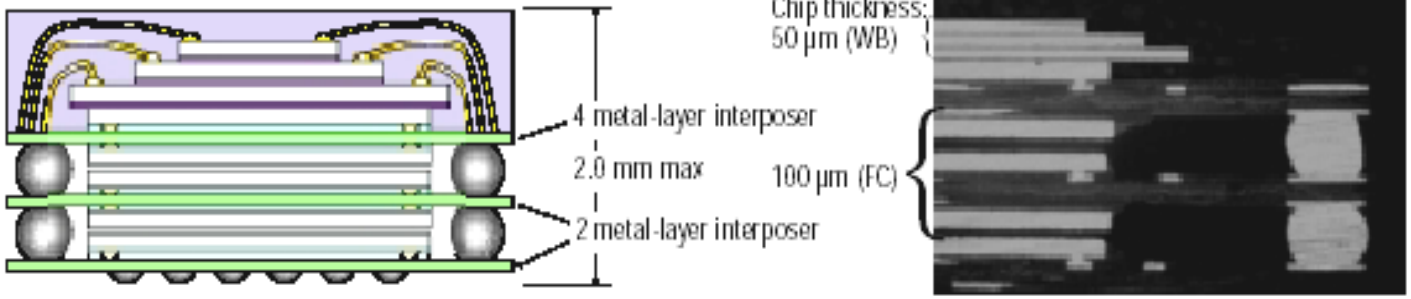

HIGH DENSITY BONDING

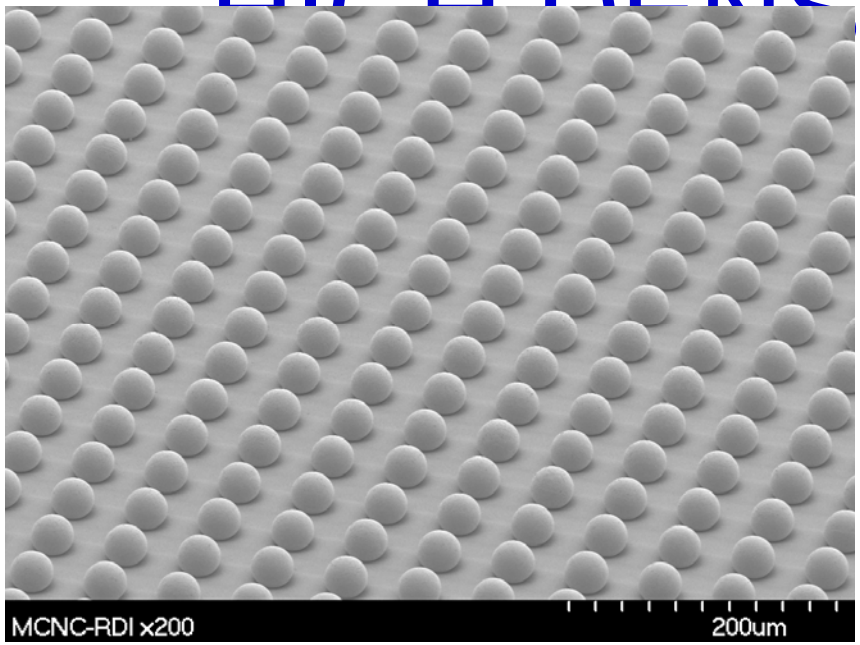

BUMP DEPOSITION
& SEM PHOTOS
COURTESY MCNC-RDI DURHAM NC

PITCH 55 µm x 55 µm

HIGH RESISTIVITY
Si SENSOR MATRIX
CANBERRA SEMICONDUCTOR

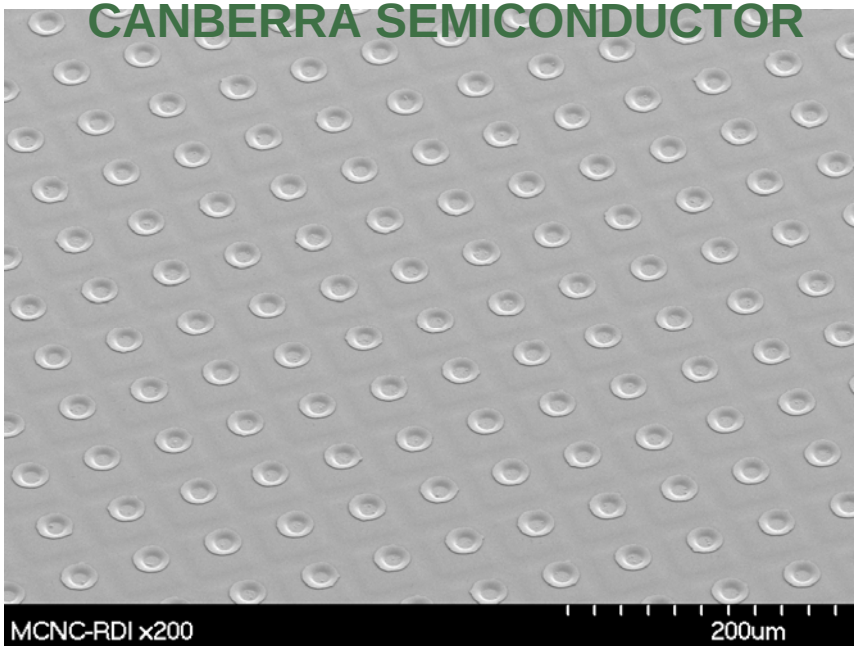

0.25 µm CMOS CHIP
CERN 2001
CAMPBELL & LLOPART
256 COLUMNS x 256 ROWS
pixel 55µm x 55 µm

INDUSTRIAL BUMP BONDING

- BECOMING MAINSTREAM

AMKOR

with UNITIVE

PITCH 200 µm

Flip Chip CABGA Cross Section

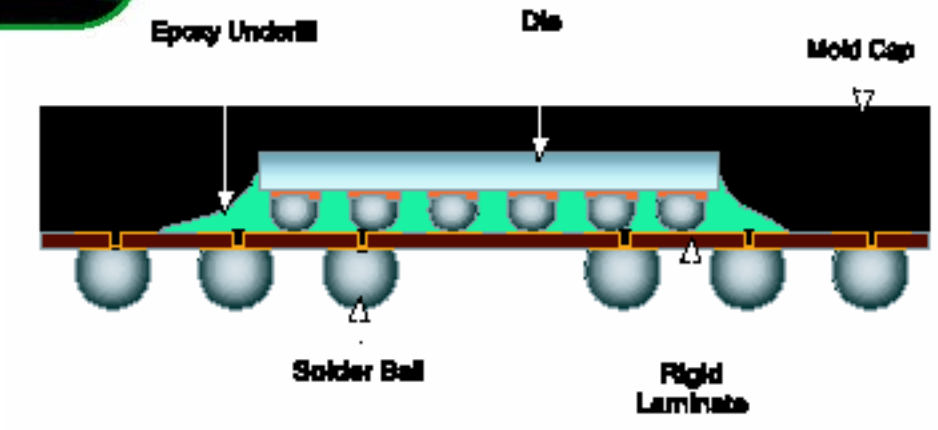

INTERPOSERS

MULTILAYER CHIP PACKAGE

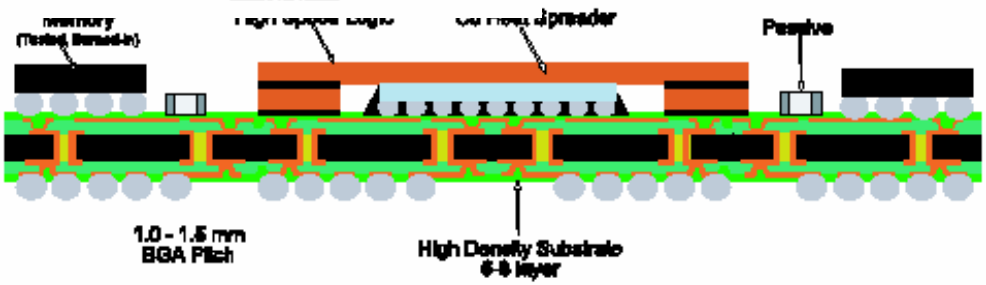

*Super*FC™ SiP Cross Section

INTEGRATED CHIP ASSEMBLIES

- Ravi Mahajan, Johanna Swan, Nasser Grayeli
  INTEL
- Assembly Technology Development
- Technology Manufacturing Group Technology

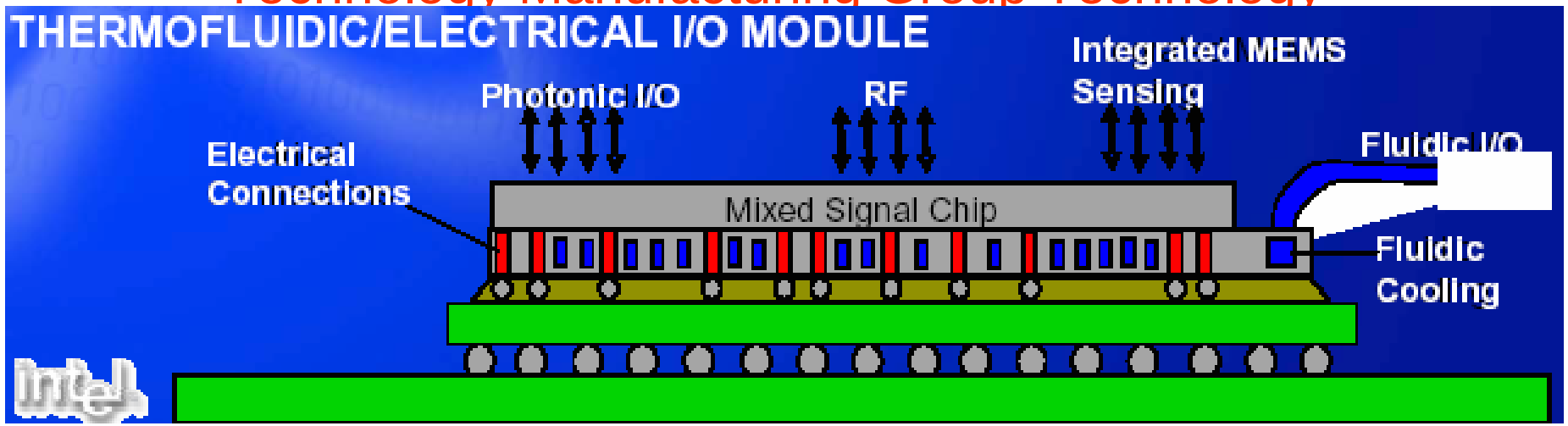

NEW PACKAGING TECHNOLOGIES

CONNECTIONS beyond BUMP-BONDING

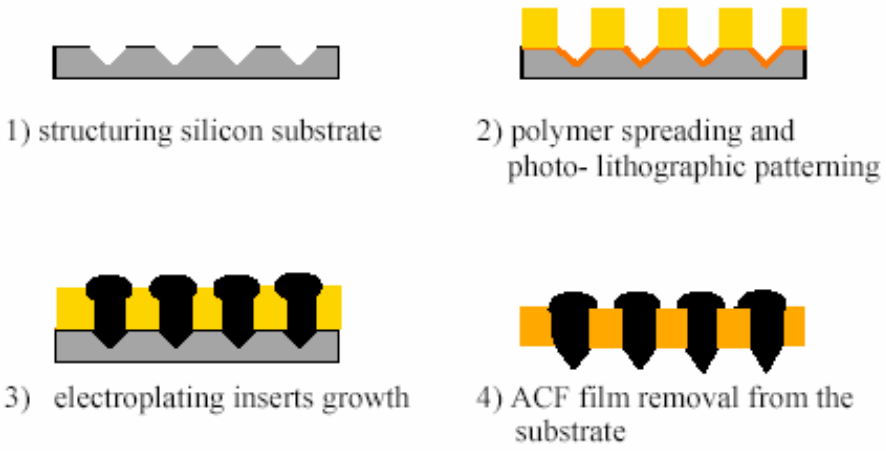

Figure 2 : Manufacturing process of the Z-axis A

Z-AXIS PINS
CEA-LETI Gasse et al.

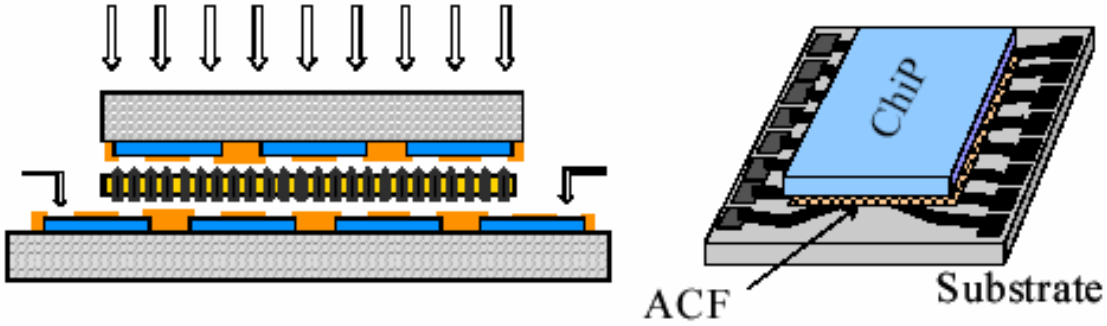

Figures 4 : Cross section of bump-less Flip-Chip bonding

PITCH 10 µm -30 µm

TRACK VECTOR DETECTOR

- 3D MULTILAYER ASSEMBLY

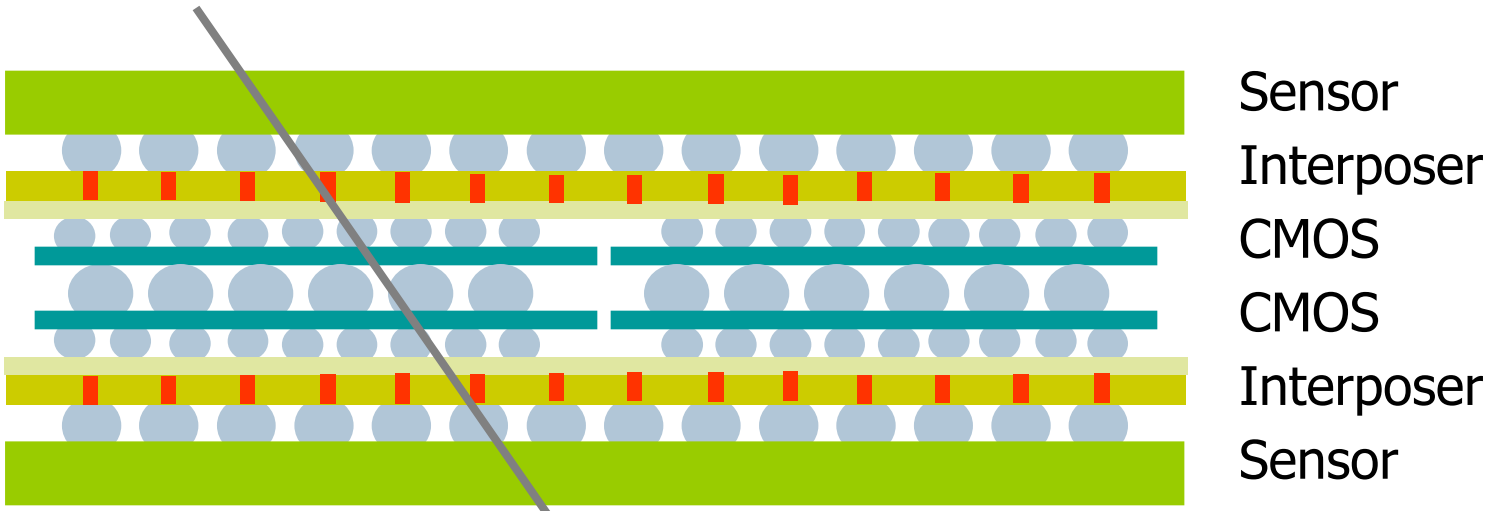

PROVIDES X , Y , Θ_X , Θ_Y

intersecting position + angular direction

AMBITIOUS MULTI-LAYER

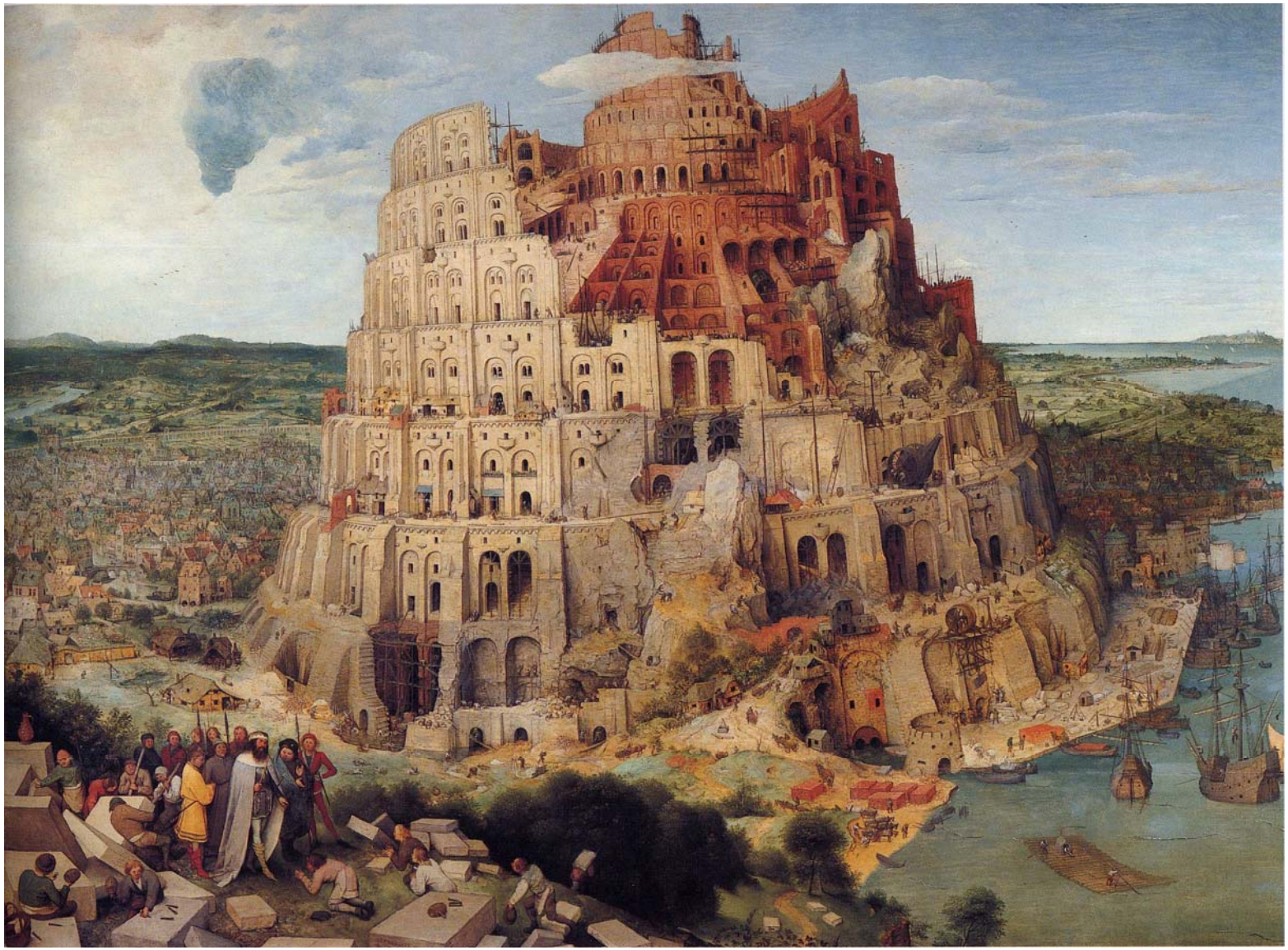

Gamma-ray Large Area Space Telescope

GLAST Mission

- **High-energy gamma-ray observatory with 2 instruments:**
  - **Large Area Telescope (LAT)**
  - **Gamma-ray Burst Monitor (GBM)**
- **Launch vehicle: Delta-2 class**
- **Orbit: 550 km, 28.5^{o} inclination**
- **Lifetime: 5 years (minimum)**

GLAST Gamma-Ray Observatory:

- **LAT ~20 MeV - 300 GeV**
- **GBM 20 keV to 20 MeV**
- **Spacecraft bus (Spectrum Astro)**

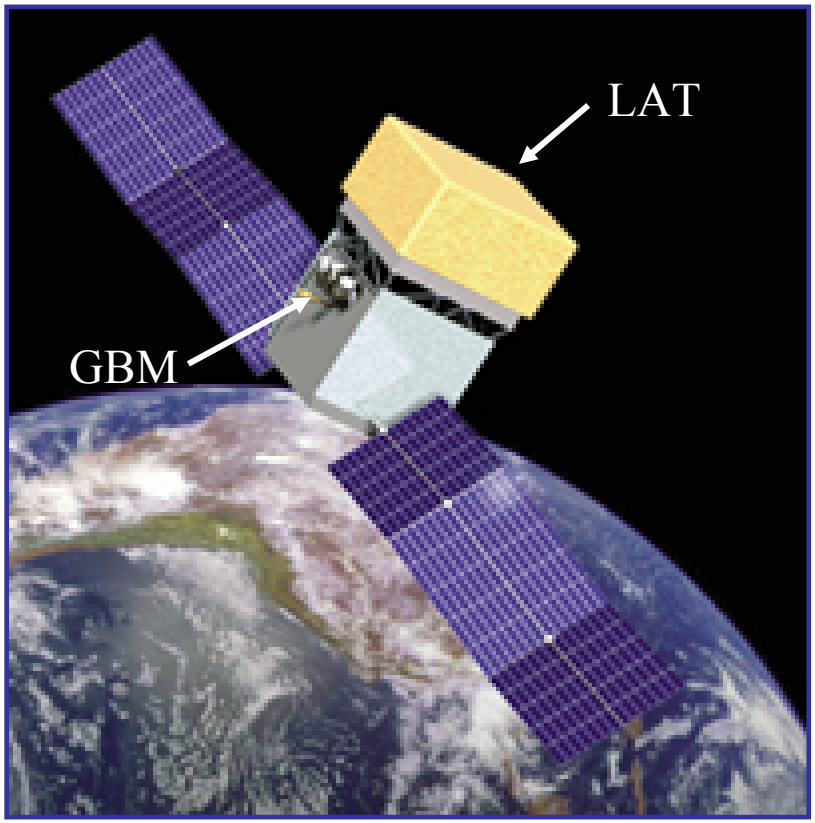

GLAST LAT Overview

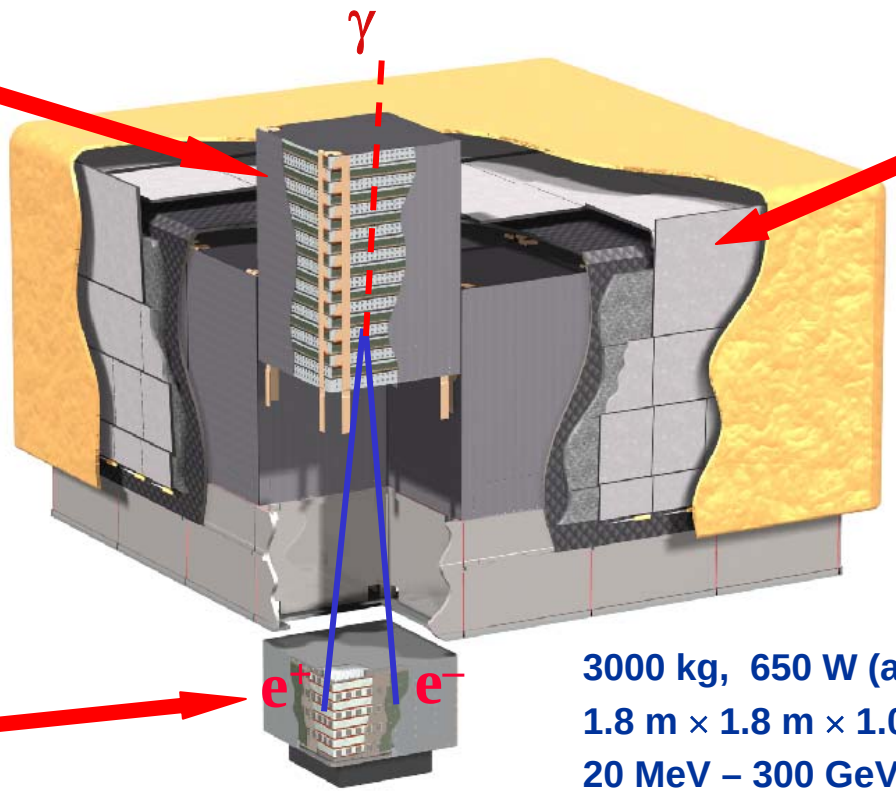

Si Tracker

8.8×10^5 channels, <160 Watts per 16 tower units

16 tungsten layers,

36 SSD layers per one tower

Strip pitch = 228 μm

Self triggering

ACD

Segmented scintillator tiles

0.9997 efficiency

Minimal self veto

CsI Calorimeter

Hodoscopic array

8.4 X_0 8 × 12 bars

2.0 × 2.7 × 33.6 cm

- ⇒ **cosmic-ray rejection**
- ⇒ **shower leakage correction**

3000 kg, 650 W (allocation)

1.8 m × 1.8 m × 1.0 m

20 MeV – 300 GeV

Mega-channel particle-physics detector *in orbit:*

⇒ Low power (<650 W)!

⇒ Extensive data reduction on orbit!

⇒ No maintenance!

Overview of Silicon Tracker (TKR)

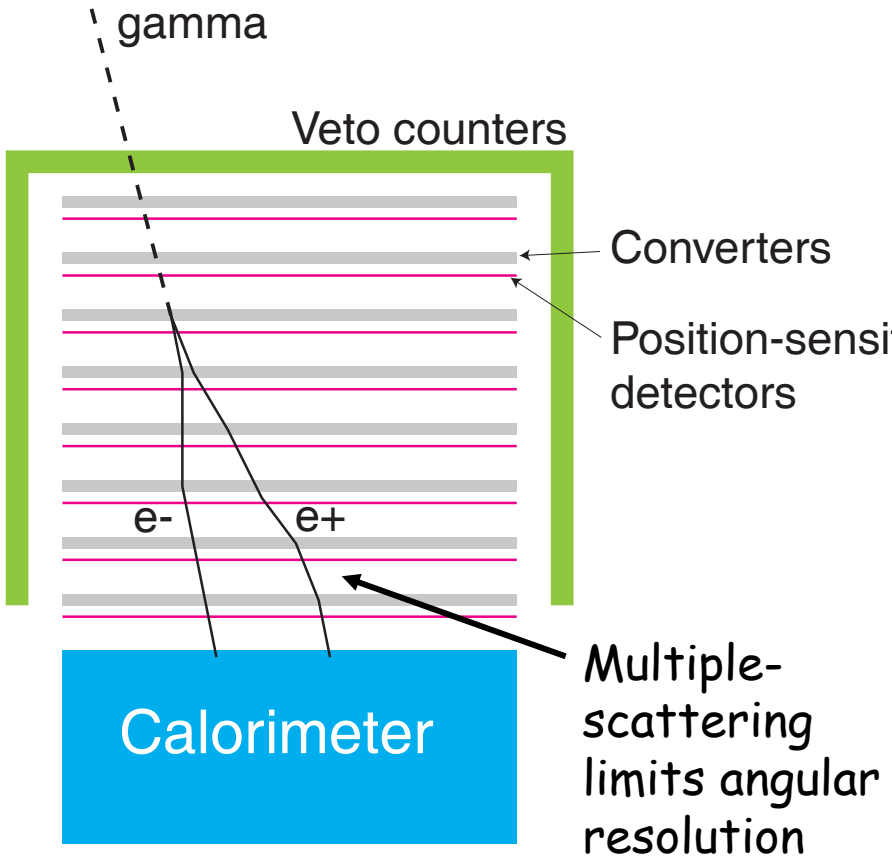

- Pair-conversion telescope
- Advantage of silicon tracker, comparing with EGRET spark chamber
  - Self trigger
  - High density optimal packing of converters and detectors enabled.
  - Fine strip pitch
    - > fine track

Front-end Electronics MCM (Multi-chip Module)

- Two custom ASICs implemented by Agilent 0.5μm process
  - GTFE: 64-channel amplifier-discrim 24/layer
  - GTRC: read-out controller, 2/layer
- Power consumption
  - Analog: 1.5V and 2.5V lines,

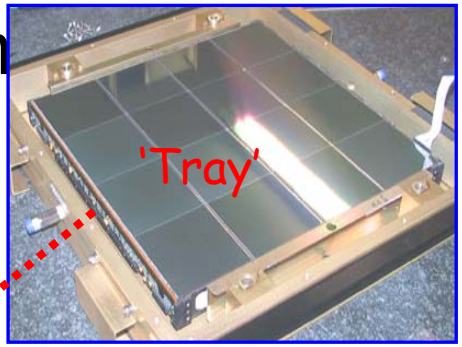

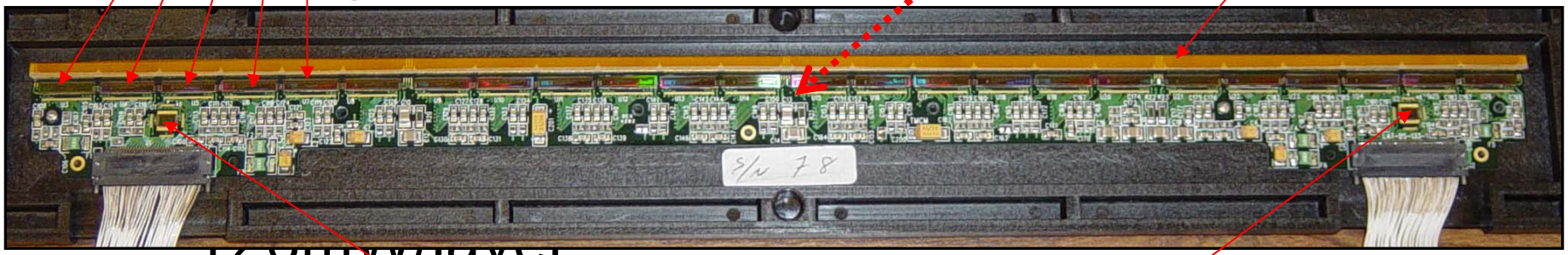

EM (Engineering Model) Mini

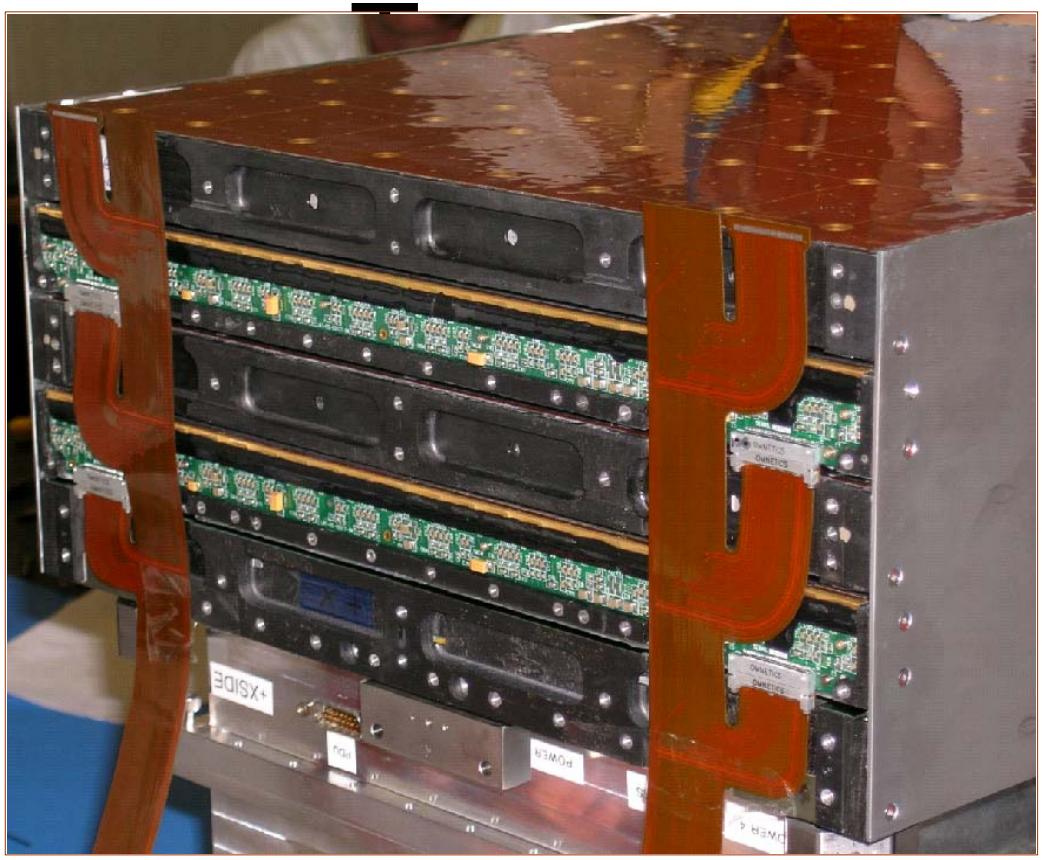

- 6 SSD layers (3 x and 3 y) and 3 tungsten-converter layers:

  minimum configuration to test trigger condition

Summary (Current Status)

- To launch in early 2007, productions and tests of flight TKR towers are now going.
  - Fabrication of front-end electronics MCM (Teledyne LA in USA)
  - Burn-in tests of MCM (SLAC in USA)
  - Kapton flex-circuit cable fabrication (UCSC, SLAC, in USA)
  - Tray assembly and test (in Italy)
  - Composite tray panels (in Italy)
  - Sidewall fabrication (in Italy)
  - Tower assembly and test (in Italy)